

Genome Wide assessment of Early Osseointegration in Implant-Adherent Cells

Ghadeer N. Thalji

A dissertation submitted to the faculty of the University of North Carolina at Chapel Hill in partial fulfillment of the requirements for the degree of Doctor of Philosophy in the School of Dentistry
(Oral Biology)

Chapel Hill
2012

Approved by

Lyndon F. Cooper, DDS, PhD

Eric T. Everett, PhD

Gustavo Mendonça, DDS, MS, PhD

Salvador Nares DDS, PhD

Clark M. Stanford, DDS, PhD

© 2012
Ghadeer N. Thalji
ALL RIGHTS RESERVED

ABSTRACT

GHADEER N. THALJI: Genome wide assessment of early osseointegration in implant-adherent cells
(Under the direction of Professor Lyndon F. Cooper)

Objectives: To determine the molecular processes involved in osseointegration.

Materials and methods: A structured literature review concerning in vitro and in vivo molecular assessment of osseointegration was performed. A rat and a human model were then used to identify the early molecular processes involved in osseointegration associated with a micro roughened and nanosurface superimposed featured implants. In the rat model, 32 titanium implants with surface topographies exhibiting a micro roughened (AT-II) and nanosurface superimposed featured implants (AT-I) were placed in the tibiae of 8 rats and subsequently harvested at 2 and 4 days after placement. Whereas in the human model, four titanium mini-implants with either a moderately roughened surface (TiOblast) or super-imposed nanoscale topography (Osseospeed) were placed in edentulous sites of eleven systemically healthy subjects and subsequently removed after 3 and 7 days. Total RNA was isolated from cells adherent to retrieved implants. A whole genome microarray using the Affymetrix 1.1 ST Array platform was used to describe the gene expression profiles that were differentially regulated by the implant surfaces.

Results: The literature review provided evidence that particular topographic cues can be specifically integrated among the many extracellular signals received by the cell in its signal transduction network. In the rat model, functionally relevant categories related to ossification, skeletal system development, osteoblast differentiation, bone development and biomineral tissue development were upregulated and more prominent at AT-I compared to AT-II. In the human model, there were no

significant differences when comparing the two-implant surfaces at each time point. However, the microarray identified several genes that were differentially regulated at day 7 vs. day 3 for both implant surfaces. Functionally relevant categories related to the extracellular matrix, collagen fibril organization and angiogenesis were upregulated at both surfaces. Abundant upregulation of several differential markers of alternative activated macrophages was also observed. The biological processes involved with the inflammatory/immune response gene expression were concomitantly downregulated.

Conclusions: The presence of micro-roughened and nanosurface features modulated in vivo bone response. This work confirms previous evaluations and further implicates modulation of the inflammatory/immune responses as a factor affecting the accrual of bone mass shortly after implant placement.

ACKNOWLEDGEMENTS

I would like to express my deepest gratitude to my advisor, Dr. Lyndon Cooper, for his excellent guidance, caring and encouragement. I feel I was very fortunate to be mentored by him throughout my prosthodontics residency training, as well as my PhD education.

I would like to thank my committee members, Dr. Salvador Nares, Dr. Eric T. Everett, Dr. Clark M. Stanford and Dr. Gustavo Mendonça for their valuable and constructive criticism that have contributed to my completion of my dissertation.

I would like to thank Mrs. Lisa Cooper for her kindness and making me feel like one of her family in a foreign country. Her thoughtfulness will long be remembered.

I would also like to thank my parents, my sisters; Abeer, Nour, Huda and Hala and my brothers; Bader and Musa for all their love, understanding and support all along.

Last, but by no means least, I thank my friends at UNC School of Dentistry for their friendship and encouragement throughout.

TABLE OF CONTENTS

I. List of tables.....	viii
II. List of figures.....	x
III. List of abbreviations and symbols	viii
VI. Introduction.....	1
V. Chapter 1: Molecular Assessment of Osseointegration <i>In Vitro</i> ; A review of current literature.....	5
A. Abstract.....	5
B. Introduction.....	6
C. Materials and Methods.....	7
D. Results.....	8
E. Conclusions.....	16
F. References.....	39
VI. Chapter 2: Molecular Assessment of Osseointegration <i>In Vivo</i> ; A review of current literature.....	61
A. Abstract.....	61
B. Introduction.....	62
C. Materials and Methods.....	64
D. Results.....	65

E. Discussion.....	66
F. Conclusions.....	73
G. References.....	82
VII. Chapter 3: Comparative Molecular Assessment of Early Osseointegration in Implant-Adherent Cells. Rat model.....	89
A. Abstract.....	89
B. Introduction.....	91
C. Materials and Methods.....	92
D. Results.....	95
E. Discussion.....	98
F. Conclusions.....	101
G. References.....	116
VIII. Chapter 4: Early molecular assessment of osseointegration in humans.....	120
A. Abstract.....	120
B. Introduction.....	122
C. Materials and Methods.....	124
D. Results.....	126
E. Discussion.....	128
F. Conclusions.....	133
G. References.....	147

LIST OF TABLES

Table 1.1 Surface modification and coatings examined in the in-vitro studies.....	17
Table 1.2 Cell culture models used at different implant surfaces.....	22
Table 1.3 Genes examined in in-vitro culture models with different implant surfaces along with their functional gene ontology annotation.....	24
Table 1.4 Technique used in in-vitro culture models for molecular assessment of osseointegration with different implant surfaces.....	34
Table 1.5 Genome wide expression profiling in in-vitro culture models for molecular assessment of osseointegration.....	36
Table 2.1 In vivo models used for molecular assessment of osseointegration.....	76
Table 2.2 Methods used to assess gene expression adjacent to different implant surfaces in in-vivo models.....	76
Table 2.3 Molecular assessment of osseointegration in in-vivo models along with Gene Ontology classification.....	77
Table 2.4 Wide genome expression profiling studies in vivo.....	81
Table 3.1 Surface roughness values as determined by optical interferometry.....	102
Table 3.2 Quantitative chemical surface composition	103
Table 3.3 Number of genes differentially expressed at AT-I, AT-II (Day 4 vs. Day 2).....	103
Table 3.4 List of the top 35 differentially regulated genes at AT-I (Day4 vs. Day2).....	104
Table 3.5 List of the top 35 differentially regulated genes at AT-II (day4 vs. day2).....	105
Table 3.6 List of top 25 differentially expressed genes at AT-I (Day 4 vs. day2) with their fold regulation in AT-I, AT-II.	106
Table 3.7 Top 25 downregulated genes at AT-I.	107
Table 3.8 Top 25 downregulated genes at AT-II.	108
Table 3.9 The validation of the array data was carried out by qRT-PCR of select number of transcripts for equal number of AT-I and AT-II samples	109
Table 3.10 Top 60 GO terms for differentially regulated genes at AT-I (Day 4 vs Day2)	110
Table 3.11 Top 60 GO terms for the differentially regulated genes at AT-II satisfying the criteria of fold upregulation >2 and p-value <0.05.	112
Table 3.12 Top 25 GO terms for downregulated genes at AT-I (Day 4 vs Day 2).	114
Table 3.13 GO terms related to downregulated genes at AT-II. 21 terms satisfied p < 0.05 and fold downregulation >2.....	115
Table 4.1 Number of genes differentially expressed (Day 7 vs. Day 3)	135

Table 4.2 List of top 35 differentially upregulated genes at OS (Day 7 vs. day3) with their fold regulation and p-value in OS and TiO.	136
Table 4.3 List of top 35 differentially downregulated genes at OS (Day 7 vs. day3) with their fold regulation and p-value in OS and TiO.	138
Table 4.4 Top 30 GO terms for differentially upregulated genes at both surfaces (Day 7 vs. Day3).....	140
Table 4.5 List of differentially expressed genes in the functional categories related to ECM and collagen fibril organization, blood vessel development, ossification and osteoclastogenesis.	142
Table 4.6 List of genes differentially expressed relevant to alternative activation of macrophages pathway...	145
Table 4.7 Top 30 downregulated genes at both surfaces.	146

LIST OF FIGURES

Figure 1.1 Topography-dependent signaling and phenotype.....	38
Figure 2.1 Histological result of osseointegration and the process(es) that lead to it.....	74
Figure 2.2 An in-vivo evaluation model of implant adherent cells.....	75
Figure 3.1 Scanning electron microscopic (SEM) evaluation of tested implant surfaces.....	102

LIST OF ABBREVIATIONS AND SYMBOLS

ANOVA	analysis of variance
BMP	bone morphogenic proteins
Ca	calcium
Cr	chromium
Co	cobalt
cDNA	complimentary deoxyribonucleic acid
COX	cyclooxygenase
Cp Ti	commercially pure
ELISA	enzyme-linked immunosorbent assay
ECM	extracellular matrix
FC	fold change
GO	gene ontology
GAPDH	glyceraldehyde 3-phosphate dehydrogenase
GAG	glycosaminoglycans
hMSC	human mesenchymal cells
HUVEC	human umbilical vein endothelial cells
HCL	hydrochloric acid
HF	hydrofluoric acid
H ₂ O ₂	hydrogen peroxide
HA	hydroxyapatite
ID	identification
ISQ	implant stability quotient
IL	interleukin
Fe	iron
Mg	magnesium
Mn	manganese
mRNA	messenger ribonucleic acid

Mod	modified
Mo	Molybdenum
MAO	monoamine oxidation
Ni	nickel
Nb	niobium
NS	not significant
OS	osseospeed
P	phosphate
PMMA	polymethylmethacrylate
qRT-PCR	quantitative real-time polymerase chain reaction
RhoA	Ras homolog gene family, member A
RBM	rat bone marrow cells
RT-PCR	real-time polymerase chain reaction
RANKL	receptor activator of nuclear factor kappa-B ligand
SEM	scanning electron microscopy
SBF	serum blood fluid
Si	silicon
Ag	silver
SMO	smooth
Sst	stainless steel
Sa	surface roughness
TRAP	tartrate resistant acid phosphatase
Sn	tin
Ti	titanium
TiO	TiOBlast
TiO ₂	titanium oxide
TNF	tumor necrosis factor
UNC	University of North Carolina at Chapel Hill

UV	ultraviolet
Wt	weight
XPS	X-ray photoelectron spectroscopy
Zn	zinc
Zr	zirconium
α	alpha
β	beta
γ	gamma
μ	micro

Introduction

Current tooth replacement strategies typically consider the alloplastic integrated replacement of missing teeth using endosseous dental implants as a primary choice among available modes of therapy. The success of contemporary dental implants is largely attributed to the process of osseointegration. Osseointegration is defined as a direct structural and functional connection between ordered living bone and the surface of a load-carrying implant [1]. Despite the high success rates achieved, implant failures that mandate implant removal do occur. Factors attributing to implant failures include local and systemic conditions such as reduced bone volume, reduced bone density, periodontitis, and impaired wound healing (e.g., diabetes, smoking, osteoporosis, radiation therapy, chemotherapy) [2-6]. Efforts to enhance osseointegration of dental implants allowing for faster prosthetic rehabilitation and improved success rates in clinically challenging situations, included modifications to the physical and chemical properties of the implants surfaces.

It is well demonstrated that implants with moderately rough surfaces (average height deviation of 1-2 μ m) enhance the rate and quality of osseointegration with greater bone-to-implant contact and higher resistance to torque removal [7-11]. Human clinical investigations have provided histomorphometric data indicating the importance of surface topography for improvement of osseointegration. At the histological level, pair-wise comparisons of machined implant surfaces with etched or grit-blasted surfaces revealed marked increases in bone-to-implant contact for the rough surface implants. The majority of the studies focusing on this comparison involved implants placed in the posterior regions of the maxilla and mandible (presumed type III or IV bone) and represented healing periods of greater than 3 months duration [12-15].

In contrast to micron-features of alloplastic materials, bone is composed of constituent nanofeatures [16]. Nanostructured materials are those with features less than 100nm in at least one dimension [17]. In the dynamic research field of implants, a multitude of biomaterial modification approaches with nanoscale features have been pursued. Typically applied techniques include lithography, ionic implantation, anodization, acid etching, alkali treatment, peroxidation and sol-gel deposition [18]. Various reports support that embellishment of the micron-rough surface with nanoscale features further enhances osteoblast differentiation [19-21], which could also promote stability and increase interfacial biomechanical locking with bone [22-24].

Precisely how this is achieved has not been clearly delineated. Only recently has the molecular basis of osseointegration been considered. A comprehensive understanding of the molecular and cellular processes relevant to peri-implant healing is critical for achieving therapeutically relevant targets to positively influence implant osseointegration.

The scope of work presented in this dissertation included a comprehensive structured literature review of current molecular data in vitro and in vivo and genome-wide evaluation of nanoscale topography influences on osseointegration in a rodent model and in man.

References

1. Branemark PI, Hansson BO, Adell R, Breine U, Lindstrom J, Hallen O, Ohman A. Osseointegrated implants in the treatment of the edentulous jaw. Experience from a 10-year period. *Scand J Plast Reconstr Surg Suppl* 1977;16:1-132.
2. Alsaadi G, Quirynen M, Komarek A, van Steenberghe D. Impact of local and systemic factors on the incidence of oral implant failures, up to abutment connection. *J Clin Periodontol* 2007;34:610-617.
3. Anner R, Grossmann Y, Anner Y, Levin L. Smoking, diabetes mellitus, periodontitis, and supportive periodontal treatment as factors associated with dental implant survival: a long-term retrospective evaluation of patients followed for up to 10 years. *Implant Dent* 2010;19:57-64.
4. Nevins ML, Karimbux NY, Weber HP, Giannobile WV, Fiorellini JP. Wound healing around endosseous implants in experimental diabetes. *Int J Oral Maxillofac Implants* 1998;13:620-629.
5. Takeshita F, Murai K, Iyama S, Ayukawa Y, Suetsugu T. Uncontrolled diabetes hinders bone formation around titanium implants in rat tibiae. A light and fluorescence microscopy, and image processing study. *J Periodontol* 1998;69:314-320.
6. van Steenberghe D, Jacobs R, Desnyder M, Maffei G, Quirynen M. The relative impact of local and endogenous patient-related factors on implant failure up to the abutment stage. *Clin Oral Implants Res* 2002;13:617-622.
7. Cochran DL, Schenk RK, Lussi A, Higginbottom FL, Buser D. Bone response to unloaded and loaded titanium implants with a sandblasted and acid-etched surface: a histometric study in the canine mandible. *J Biomed Mater Res* 1998;40:1-11.
8. Wennerberg A, Albrektsson T, Andersson B, Krol JJ. A histomorphometric and removal torque study of screw-shaped titanium implants with three different surface topographies. *Clin Oral Implants Res* 1995;6:24-30.
9. Wennerberg A, Hallgren C, Johansson C, Danelli S. A histomorphometric evaluation of screw-shaped implants each prepared with two surface roughnesses. *Clin Oral Implants Res* 1998;9:11-19.
10. Buser D, Schenk RK, Steinemann S, Fiorellini JP, Fox CH, Stich H. Influence of surface characteristics on bone integration of titanium implants. A histomorphometric study in miniature pigs. *J Biomed Mater Res* 1991;25:889-902.
11. Gotfredsen K, Wennerberg A, Johansson C, Skovgaard LT, Hjorting-Hansen E. Anchorage of TiO₂-blasted, HA-coated, and machined implants: an experimental study with rabbits. *J Biomed Mater Res* 1995;29:1223-1231.
12. Degidi M, Perrotti V, Piattelli A, Iezzi G. Mineralized bone-implant contact and implant stability quotient in 16 human implants retrieved after early healing periods: a histologic and histomorphometric evaluation. *Int J Oral Maxillofac Implants* 2010;25:45-48.
13. Ivanoff CJ, Widmark G, Johansson C, Wennerberg A. Histologic evaluation of bone response to oxidized and turned titanium micro-implants in human jawbone. *Int J Oral Maxillofac Implants* 2003;18:341-348.
14. Ivanoff CJ, Hallgren C, Widmark G, Sennerby L, Wennerberg A. Histologic evaluation of the bone integration of TiO₂ blasted and turned titanium microimplants in humans. *Clin Oral Implants Res* 2001;12:128-134.
15. Trisi P, Rao W, Rebaudi A. A histometric comparison of smooth and rough titanium implants in human low-density jawbone. *Int J Oral Maxillofac Implants* 1999;14:689-698.*
16. Bozec L, Horton MA. Skeletal tissues as nanomaterials. *J Mater Sci Mater Med* 2006;17:1043-1048.

17. Balasundaram G, Webster TJ. Nanotechnology and biomaterials for orthopedic medical applications. *Nanomedicine (Lond)* 2006;1:169-176.
18. Mendonca G, Mendonca DB, Aragao FJ, Cooper LF. Advancing dental implant surface technology--from micron- to nanotopography. *Biomaterials* 2008;29:3822-3835.
19. Valencia S, Gretzer C, Cooper LF. Surface nanofeature effects on titanium-adherent human mesenchymal stem cells. *Int J Oral Maxillofac Implants* 2009;24:38-46.
20. Cooper LF, Zhou Y, Takebe J, Guo J, Abron A, Holmen A, Ellingsen JE. Fluoride modification effects on osteoblast behavior and bone formation at TiO₂ grit-blasted c.p. titanium endosseous implants. *Biomaterials* 2006;27:926-936.
21. Dalby MJ, Gadegaard N, Curtis AS, Oreffo RO. Nanotopographical control of human osteoprogenitor differentiation. *Curr Stem Cell Res Ther* 2007;2:129-38.
22. Ellingsen JE, Johansson CB, Wennerberg A, Holmen A. Improved retention and bone-to-implant contact with fluoride-modified titanium implants. *Int J Oral Maxillofac Implants* 2004;19:659-666.
23. Berglundh T, Abrahamsson I, Albouy JP, Lindhe J. Bone healing at implants with a fluoride-modified surface: an experimental study in dogs. *Clin Oral Implants Res* 2007;18:147-152.
24. Meirelles L, Currie F, Jacobsson M, Albrektsson T, Wennerberg A. The effect of chemical and nanotopographical modifications on the early stages of osseointegration. *Int J Oral Maxillofac Implants* 2008;23:641-647.
25. Johansson CB, Gretzer C, Jimbo R, Mattisson I, Ahlberg E. Enhanced implant integration with hierarchically structured implants: a pilot study in rabbits. *Clin Oral Implants Res* 2011.

Chapter 1

Molecular Assessment of Osseointegration *In Vitro*; A review of current literature

Abstract:

This paper represents the results of a structured review of the literature concerning in vitro molecular assessment of osseointegration at the level of cell – surface topography interactions. A search of the electronic databases was performed up to and including November, 2010. 320 articles met the inclusion criteria. Characteristics of the included in-vitro reports were model systems used, genes examined, techniques used for molecular assessment of the osseointegration process, and wide gene expression profiling studies. There exists a growing body of in vitro evidence to support a role for surface topography in the direct influence of cellular phenotypes as related to the process of osseointegration. Most recently, functional or mechanistic studies have provided evidence that particular topographic cues can be specifically integrated among the many extracellular signals received by the cell in its signal transduction network. Such investigations begin to define linkages between the character of the implant surface and adherent cellular responses, including cells from extravasated blood (e.g., platelets) and of the immune system (e.g., monocytes). In vitro studies involving cell culture on endosseous implant related biomaterials offer important and beneficial insight into the clinical control of the implant/bone interface.

Introduction:

The dental implant surface represents one of the key factors affecting osseointegration success. Earliest studies indicated that implant surfaces could dramatically influence the possible formation of a direct bone to implant contact [1], despite the recognized influence of surgical technique and loading conditions [2]. In the influential report of Buser et al (1991), comparison of experimental implant surfaces bearing different surface topography ranging from electropolished to electropolished and plasma sprayed hydroxyapatite-coated surfaces revealed that increasing surface roughness resulted in increased bone-to implant contact [3]. The efforts of Wennerberg and co-workers also systematically revealed that compared to machined cpTitanium surfaces, increasing surface roughness improved both bone-to-implant contact and physical interaction with bone (removal torque) [4-8]. In summary reviews, it was concluded that numerous investigations demonstrated that smooth ($S(a) < 0.5$ micron) and minimally rough ($S(a) 0.5 - 1.0$ micron) surfaces showed less strong bone responses than rougher surfaces [7,9].

The current literature involving *in vivo* studies of surface topography effects on osseointegration at the molecular level further supports both histomorphometric and biomechanical data of improved osseointegration [8,10]. These studies demonstrate that surface topography is, in part, responsible for changes in the interfacial tissue responses to the endosseous implant that lead to greater bone to implant contact. These changes are manifest by a) greater bone-to-implant contact and b) increased biomechanical interlocking with bone in animal and human studies.

Human clinical investigations have provided histomorphometric data indicating the importance of surface topography for improvement of osseointegration. At the histological level, pair-wise comparisons of machined implant surfaces with etched or grit-blasted surfaces revealed marked increases in bone-to-implant contact for the rough surface implants. The majority of the studies focusing on this comparison involved implants placed in the posterior regions of the maxilla and mandible (presumed type III or IV bone) and represented healing periods of greater than 3 months duration [11-14]. Implants with altered topography, indicated partly by increased $S(a)$ values, supported greater bone accumulation at the interface. It is assumed that the surface topographic changes of the surface represent alloplastic cues that promote tissue changes leading to increased bone accrual at the implant surface.

Several *in vivo studies* at the molecular level indicate that surface topography influences adjacent cellular functions including the process of bone matrix biosynthesis and mineralization [15]. Most recent investigations focusing on mRNA expression profiles within cells adjacent to tissue at implants or cells adherent on implant surfaces. The findings include increased expression of mRNAs involved in the regulation of cell proliferation, angiogenesis, osteoinduction and osteogenesis [16].

The complexity of wound healing is self evident in the many changes in gene expression observed in gene profiling studies such as those recently published regarding osseointegration. For example, examination of gene expression events at 4, 7 and 14 days in tissues surrounding SLActive surface implants in the retromolar area of 9 human volunteers revealed thousands of differentially significant genes that increased and decreased with time [17]. The biological processes identified at day 4 prominently involved the cell cycle, the immune response and inflammatory gene regulation, phagocytosis and macrophage activation. These prominent changes suggested the induction of fundamental wound healing events. At day 14, gene expression events representing skeletal development, ossification and cellular differentiation were prominently revealed. The complexity of these processes requires detailed analysis and model systems that permit the testing of hypotheses to confirm what descriptive analyses have suggested.

In vitro studies that pursue aspects of osseointegration, particularly cellular responses to implant surface topography, provide insight into the role that the implant surface plays in modulating cellular responses during the complex process of osseointegration. It is the aim of this review to assess the knowledge that has been gained to date from molecular biological evaluations of cellular responses to endosseous dental implant surface topography.

Materials and methods:

For the literature to be included in this review, the following eligibility criteria were used: *in vitro* reports assessing the molecular process of osseointegration, and articles published only in English. Studies related to wear particles, letters to the editor and reviews were excluded. Articles limited to assessment of Alkaline phosphatase activity were excluded. Articles limited to biological coatings were excluded in this review.

Search Strategy: A thorough search was performed up to and including November, 2010 through the following databases: PubMed (1948 to November, 2010), using the following terms: (titanium[tw] OR zirconium[tw] OR dental implant*[tw]) AND (gene expression[MeSH Terms] OR gene expression[tw] OR differentiation[tw] OR rna[MeSH Terms] OR rna[tw] OR messenger rna[tw] OR mrna[tw]), EMBASE via OVID (1947 to November, 2010) using: (Titanium.mp. or zirconium.mp. or tooth implantation/ or dental implant*.mp. and gene expression.mp. or exp gene expression/ or exp DIFFERENTIATION/ or differentiation.mp. or ena.mp. or exp RNA/ or messenger rna.mp.[mp=title, abstract, subject headings, heading words, drug trade name, original title, device manufacturer, drug manufacturer] or mrna.mp.[mp=title, abstract, subject headings, heading words, drug trade name, original title, device manufacturer, drug manufacturer], and BIOSIS Previews via ISI Web of Science (1969 to November, 2010), ISI Citation via ISI Web of Science (1955 to November, 2010) using the following words: Topic=((titanium OR zirconium OR "dental implant*") AND ("gene expression" OR differentiation OR rna OR rna OR "messenger rna" OR mrna)). Titles and abstracts were screened for possible inclusion in the review. The full text of the articles judged to be relevant by the title and abstract was read and independently evaluated against the eligibility criteria. In addition, a hand search of the reference lists of original studies that were found to be relevant was conducted.

Results:

320 articles met the inclusion criteria. Characteristics of the included in-vitro reports including surfaces examined, model systems used, genes examined, techniques used for molecular assessment of the osseointegration process, and wide gene expression profiling studies are presented in Tables 1, 2, 3, 4 and 5 respectively.

The spectrum of surfaces investigated in *in vitro* studies of cellular aspects of the osseointegration process is widely represented by metallic and ceramic materials (Table 1). It is apparent that, when limited to critical appraisal of studies involving osteoblast-like or osteoblastic cell performance in relationship to endosseous implant material influences, studies performed in cell culture are possible and provide information regarding cytotoxicity, cell adhesion, proliferation and differentiation. The vast majority of these studies have been conducted using typical cell culture conditions that include the use of 5 – 15% serum, typically bovine derived. It is acknowledged that adhesion – related phenomena involved the interaction of cellular receptors with serum

derived proteins such as Fibronectin. The study of direct cell (or cell-derived protein) - surface interaction has not been widely pursued.

Interestingly, despite many preliminary studies of cell function with regard to bulk endosseous implant material, the majority have focused on osteoblastic or osteoblast-like cell behavior without regard to the key cellular components of the immune system. More recent interest in the role of immunomodulation of osteogenesis in general [18] suggests the importance of other cell types in the process of osseointegration. The more recent investigations of monocyte/macrophage function, platelet function and inflammatory gene regulation in vitro demonstrate that surface topography influences cellular processes beyond osteoblast functions and these processes may be evaluated in cell culture [19,20].

While the obvious variable in studies of topography-dependent modulation of osseointegration is the implant surface, the previous statement indicates that in vitro studies are highly dependent on the model system and particularly upon the cell line selected for investigation. Comprehensive review revealed approximately 50 different types of cells, the majority representing the osteoblastic lineage, has been used to study implant surface-cell interactions in culture (Table 3). The majority of studies employed one or another osteoblastic cell model able to differentiated under culture stimulation. Such models have included primary cultured bone marrow-derived stem cells (e.g., hMSCs), stem cell-like cell lines (e.g., C₃H₁₀T_{1/2}) or C₂C₁₂), bone-derived osteoprogenitors (e.g., RBM cells), transformed osteoblastic cells (e.g. FOB), osteoblastic cell lines (e.g., MC3T3-E1), and osteosarcoma derived cell lines (e.g., MG63). Cells of human, mouse and rat origin dominate these models, however, canine, chick and bovine cell models have also been utilized. Each model system offers select advantages and disadvantages [21], despite the generalized ability to adhere to and proliferate on the alloplastic substrates. Differences in phenotypes such as the relative expression of integrin receptors, matrix proteins or signal transduction molecules must be understood for proper deployment and interpretation of results. Irrespective of important distinctions that must be made for the different models deployed to investigate “osteoblast” – implant surface interactions, it may be generally concluded that osteoblastic cell adhesion and culture on titanium (or Zirconia) surfaces with enhanced surface topography in the micron-scale range results in increased osteoblastic differentiation as evidenced by a) increased osteoinductive transcription factor mRNA expression (RUNX-2 and Osterix), b) elevated type 1 collagen expression, c) increased bone

specific matrix protein expression including alkaline phosphatase, osteopontin, osteocalcin and bone sialoprotein, and d) cell matrix layer mineralization.

The array of surface topographies investigated to date spans the range of applicable technologies represented by clinical dentistry and orthopedics. They include grit blasting, acid etching, anodizing, laser ablating, micromachining, and photolithography methods among them. While most investigations have examined one or two surfaces representing the result of a modification process, a select few investigations have attempted to systematically interrogate the role of a specific surface modification parameter on adherent cell behavior. For example, Sjotstrom et al. (2009) [22] utilized titania nanopillar structures of 15 – 100 nm to examine hMSC osteoblastic differentiation as a function of nanoscale topography. In this instance, diameter and spacing parameters were not controlled. In this particular review, the biological activation of metallic and ceramic implant surfaces by linking of receptor targets (e.g., matrix proteins, growth factors, or cytokines) was not considered. [23]

Cell Adhesion – A general appreciation for cell adhesion phenomena at endosseous implant surfaces includes specific roles for adherent extracellular matrix proteins (ECM, e.g., fibronectin, osteopontin) and related transmembrane receptors (e.g., integrins) present on the adherent cells [24]. Adherent osteoprogenitors produce ECM proteins in a manner that is influenced by the nature of the titanium surface, suggesting that surface topography provides environmental cues that change cell signaling at the most fundamental levels [25]. Surface topography does influence the expression of integrins important in osteoblastic cell adhesion and differentiation [26]. The systematic knockdown of alpha 2 integrins in MG63 osteosarcoma cells revealed the requirement of alpha 2-beta1 integrin signaling of titanium topographic cues affecting osteoblastic differentiation [27]. The role of integrins in cell adhesion involves many different integrins and common integrin subunits (e.g., b1) appear to mediate binding to many different surfaces in cell culture [28], leaving open the question of precisely how specificity of adhesion is controlled at the cellular level. One other mechanistic evaluation of topographic cue-based signaling has focused on b-Catenin activation involving the cytoskeleton, RhoA, as well as WNT pathway mediators. Using reporter gene tools to study the activity of b-Catenin (a known mediator of osteoinduction), Macaluso and colleagues have provided among the few investigations probing the mechanisms by which surface topographic cues influence adherent cell function [29].

The surface cues imposed through adhesion –based signaling leads to functionally and structurally significant changes in the cultured cell layer, suggesting that similar influences are imposed at the implant bone interface *in vivo*. Ogawa and colleagues' comparison of rat BMC cultured on titanium and tissue culture polystyrene (TCPS) revealed a collagen rich, calcium phosphate layer at the titanium but not TCPS interface. The titanium interfacial tissue demonstrated greater hardness, elastic modulus and interfacial strength [30]. Changes of the titanium surface in fact alter abundance of key signaling proteins such as the small GTPase RAS and the MAP kinase pathway within adherent osteoblastic cells [31]. When considering the influence of topography, the stimulation of matrix formation can influence a range of cellular processes including migration, matrix organization, cytoskeletal organization and intracellular signaling [32]. An elegant investigation of hMSC adhesion to nanoporous TiO₂ surfaces measured displacement of adherent cells using atomic force microscopy methods which led to hypothesize that initial adsorption is a function of proteins adsorbed from serum (e.g., fibronectin; [33]). Additional studies have revealed that particular signals are mediated from topographically modified titanium substrates to cells via integrins including the α2β1 integrin [27]. Most recently, MC3T3-E1 osteoblastic cell culture on smooth versus SLA surfaces was examined at the level of ERK signaling. Greater Osterix (Sp7), osteopontin and osteocalcin expression were observed in cells cultured on SLA surfaces. Associated with this enhanced Osteoinduction was reduced ERK1/2 phosphorylation, suggesting that topography-mediated signals involve the downregulation of the ERK pathway [34]. Continued mechanistic investigations are needed to define precisely how cells perceive, signal and integrate topographic cues from alloplastic materials to physiologic changes that result in tissue integration.

Osteoblastic differentiation - Runx2 is an essential transcription factor for osteogenesis; its removal results in no bone formation or osteoblastogenesis. It binds to target gene promoters to affect their expression during osteoblastic differentiation and bone formation [35]. If surface topography alters adherent cellular differentiation, then one mechanism could involve topography-related changes in Runx2 expression. Earliest reports of surface topography influences on RUNX-2 included studies of Masaki et al (2005) [36] and Guo et al (2007) [37] that evaluated the influence of HF treatment of TiO₂ grit blasted implant surfaces on adherent MSC function. Recently, elevated RUNX-2 expression was reported for human periodontal ligament cells cultured on the SLactive surface [38].

Osterix (Sp7) represents the second key transcriptional regulator of Osteoinduction. Sp7 is required downstream of Runx2. Importantly, Sp7 is necessary for postnatal osteoblast and osteocyte function [39]. Masaki et al [36] first indicated that enhancing titanium substrate microtopography led to elevated Sp7 expression in adherent osteoprogenitor cells. Others including Perrotti et al (2012) [40] have demonstrated that compared to machined surfaces, adherent cell Sp7 expression on micron rough surfaces is elevated. hMSC Sp7 expression is positively influenced by culture on titanium substrated bearing nanoscale topographic enhancement [37,41-43] In confirmation of the significance of Osterix's role in promotion of osseointegration, *in vivo* studies reveal that Osterix overexpression in labeled mouse bone marrow stem cells led to accelerated osseointegration[44]. Thus, *in vitro* studies of surface topography effects on Osteoinduction suggest that greater bone formation *in vivo* is due, in part, to surface dependent modulation of the osteoinductive transcription factors Runx2 and Osterix (Sp7).

More recently, investigations have pursued descriptive studies of cell – implant surface interactions *in vitro* using genome wide expression profiling techniques. At least 13 publications report use of different arrayed gene assays for the purpose of characterizing the changes in gene expression that occur over time or as a function of surface modification. For example, Vlacic-Zischke et al (2011) compared human mandible derived osteoblast gene expression following growth on SLA vs. SLactive surfaces [45]. When subjected to pathway analysis, gene expression data revealed the up-regulation of BMP pathway signaling as well as molecules involved in Wnt signaling. Zhao et al (2010) examined rat osteoblastic cell culture on a unique porous Ti alloys surface [46]. When comparing data from studies using different cell models, markedly different results are observed (e.g. MG63 cells [47] vs. hMSC [48]). Culture of hMSCs on topographically modified titanium substrates led to increased expression of both Runx2 and BSP where as MG63 cell culture at 24 hours did not reveal elevations in these key markers of Osteoinduction.

The aggregate data from focused evaluations of directed studies of one or another osteoinductive regulatory gene or from gene profiling studies regarding cells adherent to different implant surfaces indicates that surface topography can influence Osteoinduction. With increasing surface roughness, elevated and / or earlier expression of Runx2, Osterix (Sp7), BMPs (notably BMP2 and BMP6), and Wnt pathway molecules including b catenin, has been reported. *In vitro*, cells adherent to modeled dental implant surfaces demonstrate

topography-dependent changes in the expression and function of several key regulators of Osteoinduction (Figure 1).

Extracellular matrix formation - Among the first observations of surface topography effects on adherent cell expression of ECM protein expression was the study of fibronectin mRNA levels that concluded that topography-induced changes of the cell led to increased fibronectin expression [49]. With specific emphasis on interfacial bone formation, attention has focused on bone matrix proteins known to be the product of osteoblastic cells [50].

Alkaline phosphatase is a commonly utilized marker of early osteoblastic differentiation that is repeatedly observed to be elevated in cells adherent to surfaces of increasing surface topography and Osteocalcin has been utilized as a marker of terminal osteoblastic differentiation [51,52]. Ogawa and colleagues have utilized both osteopontin and osteocalcin expression levels to indicate the extent of osteoblastic differentiation [53,54]. These and many other investigations have revealed that culture-induced differentiation of osteoblast-like cell lines and mesenchymal stem cells is surface topography dependent. This process is modeled by the sequential expression of alkaline phosphatase, osteonectin, osteopontin, and the penultimate emergence of bone sialoprotein and osteocalcin expression. With increasing topographic complexity and / or increasing R(a) or S(a) values, cultured cells produce greater abundance of mRNAs encoding these matrix proteins at earlier time points. Suggested is earlier and greater bone formation *in vivo* at implants with enhanced surface topography.

Bone matrix is largely composed of type I collagen. Cooper and co workers described the differential regulation of collagen biosynthesis in cells adherent to smooth and rough titanium surfaces [55]. This revealed greater collagen biosynthesis and higher levels of cross-linking gene expression within cells adherent to the topographically enhanced titanium substrates. Similar investigations have revealed the positive influence of surface roughness on type I collagen mRNA expression, as well as other bone matrix components including osteopontin, osteocalcin and alkaline phosphatase [26].

These different molecules and the molecular knowledge of their regulation enables investigators to pursue studies that may indicate the mechanisms by which surface topographic cues enable cellular differentiation along the osteoblast lineage. In vitro studies to date have **a)** confirmed that adherent cell expression of ECM protein and encoding mRNAs is affected by topography, **b)** demonstrated that changes in ECM expression in

turn affect adherent cell behavior, and c) shown how alterations in ECM protein biosynthesis of adherent cells is associated with changes in the physical properties of the protein / cell layer and its attachment to the modeled implant surface.

Osteoclastogenesis: The accrual of bone mass at the implant surface requires the formation of new bone matrix and its mineralization. The vast majority of cell culture studies addressing osseointegration have focused on osteoblastic production of bone matrix and mineralization. However, bone accrual is balanced by osteoclastogenesis. Few clinical, pre-clinical or in vitro studies of osseointegration have investigated osteoclastogenesis at the implant-bone interface or as a function of the implant surface per se.

Osteoclastogenesis is controlled by soluble inducing factors as well as insoluble membrane-bound ligands present on osteoprogenitor cells. These factors and ligands represent both positive and negative mediators of osteoclast production. The MSC expresses the central insoluble ligand that triggers monocyte differentiation to osteoclasts, namely RANKL. The MCS and osteoblastic cells produce and secrete the key inhibitor of osteoclastogenesis, termed osteoprotegerin (OPG). Additionally, osteoclastogenesis is modulated by immunoregulatory cytokines including TGF β and IL6. Other mediators include mechanostimulatory events and particulate debris that are beyond the scope of this review. Three similar investigations using MG63 osteosarcoma cells [56], human periodontal ligament cells [38], and primary human osteoblasts cultured on smooth versus SLA and / or SLactive substrates [57,58]. RANKL expression was lower, while OPG expression was increased in cells adherent to the rougher surfaces. Increased expression of OPG on a rough versus smooth surface was observed for both MG63 cells and alveolar primary osteoblasts [59]. In the MG63 model, integrin mediate signaling and protein kinase C activity were implicated in the increased expression of OPG [60], further demonstrating that surface cues directly impact adherent cell physiology.

Other cellular aspects of osseointegration modeled in vitro: While the majority of studies of osseointegration in cell culture have centered about the osteoblastic cell lineage, the process of osseointegration in vivo is not fully represented by surface – osteoblast interactions alone. Other cell types are clearly observed to adhere before the attachment of osteoprogenitor cells or mesenchymal stem cells [61]. Primary among these other cells are the components of extravasated blood, notably the platelet. Additionally, monocytes from the

circulation and cells of the innate immune system are eventually recruited to this site of surgical tissue damage. The direct interaction of these cells with the implant surface has received limited attention.

Davies and co-workers introduced the general concept that the topographic enhancement of blood platelet – implant surface interaction was central to the process of osteoconduction [62]. Subsequently, it was demonstrated that adhesion of platelets to microrough surfaces of increasing topographic complexity and dimension enhanced platelet activation [63,64]. More recently, assessment of the thrombogenic response with regard to surface topography was performed. Thor et al (2007) demonstrated that 15 fold greater activation (transglutaminase release) for whole blood plated on grit blasted vs machined or HA surfaces [65]. Cell culture investigation of thrombogenesis was further able to distinguish greater transglutaminase release from blood platelets on SLactive vs. SLA surfaces [66]. In the context of this review, it is important to recognize the lack of transcription and mRNA expression occurring in platelets. However, as remarkably rich sources of growth factors and cytokines, their regulated presence and activity may be important, indirect significance to the surface-mediated changes in osteoprogenitor cell phenotype that is of direct concern herein.

Monocytes or macrophages represent important cellular mediators of tissue responses to implanted biomaterials and have been known to be topography dependent in this function [67]. Monocytes display marked haptotaxis and monocyte adherence increases with surface topography [68]. Takebe et al (2003) [69] utilized anti beta3 integrin antibody treatment to demonstrate that J774A.1 cell adhesion and spreading as a function of surface topography was integrin- dependent and involved alterations in the cytoskeleton. When murine macrophage like cells RAW 264.7 cells were cultured on surfaces of increasing roughness, unstimulated macrophages increased TNF- α secretion . Upon LPS stimulation, cells cultured on roughest surfaces produced the highest levels of IL-1b, IL-6 and TNF- α [70]. Using the J744A.1 cell line, in the absence of inflammatory LPS stimulation, only IL-1 levels were increased on the rougher surface [71] , once again indicating the important role cell models play in modeling biologic events surrounding the impact of surface topography on adherent cell phenotypes *in vitro*. Further study of the role surface topography place in the initial interactions of an implant surface with blood and tissues is requires and can be facilitated using cell culture models and *in vitro* systems.

Conclusions:

The present literature concerning the molecular phenotype of cells adherent to and cultured on endosseous implant materials subjected to topographic and biological modification confirms *in vivo* and clinical data suggesting that topographic enhancement of the implant surface influences cell function directly. Depending upon the adherent cell type, different biological processes may be modeled in cell culture. With regard to osteoinduction and osteogenesis, cell culture studies clearly indicate that adhesion to surfaces of increasing topographic magnitude and complexity results in increased osteoinductive and bone matrix-specific gene expression. These changes are associated with increases in BMP expression and Wnt pathway gene expression, suggesting that these pathways are influential in promoting osteogenesis of adherent osteoprogenitors. The role of other adherent cell types, including platelets, monocytes, and lymphocytes has been recognized, but comprehensive evaluation of the impact of these cell types as well as the influence of surface topography upon their function adherent to the implant surface remains to be defined. Studies of cell – substrate interactions involving molecular assessment have largely provided descriptions of adherent cell phenotypes. Future studies can utilize the cell culture environment to investigate the mechanisms by which topographic cues influence adherent cell behavior related to the process of osseointegration.

Table 1: Surface modification and coatings examined in the in-vitro studies.

Material (Bulk)	Surface modification (With nanotopographic features*)	Coatings after surface modification	Coatings only (With nanotopographic features*)
Titanium	Untreated/mirror polished/machined/electromachined [52,72-93]		Hydroxyapatite coating- Calcium phosphate [94-111, 112*, 113-116, 117*, 118*, 119,120*, 121]
	Wet ground-grit [77,122-124]		Carbonated hydroxylapatite [125]
	Grooved [126-128]		Hydroxyapatite outer layer and Fluorhydroxyapatite inner layer [97]
	Drill channels [129]		Fluorhydroxyapatite [97]
	Porous-powder metallurgy [130]		Calcium metaphosphate Anodized[108]
	Acid etched [42,46,53,54,59,90,111,117,120,127,131-152]	Sputter deposited TiO ₂ [149,151*, 153*]	Octacalcium phosphate (OCP) coated Ti [154]
	Acid etching with chemical modification by exposing to NaOH (Alkali acid etched) [155]		Titania hydroxyapatite coatings (composite coating of HA+TiO(2)) [116] [156,157]
	Mod A [59,141-144]		Zinc Hydroxyapatite coating [115]
	Acid etched with Photofunctionalization of titanium oxide: ultraviolet light mediated changes [158-160]		dicalcium pyrophosphate (Ca ₂ P ₂ O ₇ , DCP) [110]
	Acid etched aged [160]		Mn(2+)-doped carbonate hydroxyapatite (Mn-CHA) [154]
	Acid etching/Anodization [46]*		Porous surface-Laser Engineered Net Shaping (LENS) method- ti powder[161]
	Blasted [43,69,118,120,134,135,137,145,162-180]	Hydroxyapatite[182] Calcium phosphate coating [172-174] Calcium phosphate coating with heat treatment [174]	Ag particles electrodeposited onto the TiO ₂ nanotubular surface [182*]
	Sandblasted with Photofunctionalization of titanium oxide: ultraviolet light mediated changes [160]		Hydroxyfluorine coating [95]
	Sandblasted aged [160]		Titanium nitrate coating[95]
Blasted Acid etched [27,36*, 41,43*, 48,51,52,55,57,58-60,71,94,95,106,107,111,118,120,126,134,139-145,164*, 166*, 167*, 168*, 183,184,185*, 186-228,236*]	Hydroxyapatite coating [210] Anatase coating [228]	Calcium titanate-amorphous carbon (CaTiO(3)-aC) coating [105]	
Blasted acid etched with heat treatment [226,227]		Ti-Plasma sprayed [51,57,60,94,107,114,134,135,140,162,163,190,191,193]	

		-199,201,207-209,229] ANODIZED [114,179,229-231]
Mod SLA [27, 36,48,58,59,141-144, 202,211-221]		Diamond-like carbon coating [95]
Blasted etched with modification using hydrogen peroxide [199]		Anatase titania coating [41*,47*,233*,234*]
Blasted Amino group ion implanted [179]		Rutile titania coating [41*]
Alkali heat treated [234-237]		Ti carbide coatings [238]
Anodized Alkali treatment [239]		Plasma sprayed and Amino group ion implanted [179]
Alkali heat treated with SBF [118,234,236]		Carbon-coated TiO(2) nanotubes [240*]
Oxidation: immersion in a solution of 8.8 M H ₂ O ₂ /0.1 M HCl at 80°C for 30 min [241]		
Oxidation of either PT or SLA [242*]		Coating with titanium nitride oxide [243]
Anodization[22*,136,165,182*,240*, 244*,245,246*,247,248,249*,250,251*, 252*,253*,254]	Hydroxyapatite [99*,255]	Titania coating non-specified [116,256,257]
Anodization Mg ion incorporated [165]		Phosphonic acid coated [258]
Anodization Mg ion incorporated with SBF [118]		Plasma-immersion implanting Si ion [259*]
Electrochemical treatment either with Ca or Ca and P [260]		Calcium ion implanted [261]
Heat treatment [73]		Hydrothermal treatment: Strontium ions and/or phosphate [262] phosphate [263] magnesium- [264*]; Calcium [265]
Glow discharge plasma (GDP) pretreatment[266]		A copolymeric hydrogel coating, poly-2-hydroxyethyl methacrylate-2-methacryloyloxyethyl phosphate (P(HEMA-MOEP)) [268]
Unspecified smooth/rough [268]		Zirconium coating [41*,99]
		Alumina coating [41*,42*]
		Anodized alumina coating [269*]
Titanium alloys		
Ti6Al4V alloy		
Grade polished/ grooved/ untreated [77,86,135,137,270-283]		Hydroxyapatite- calcium phosphate [284-288]
Wet ground [77,289-291]		Coating with porous alumina ceramics [292,293]
Acid etched [137,294,295]	Hydroxyapatite [295]	Titanium plasma spraying [297]
Blasted[180,270-273,277,293,298-309]	Hydroxyapatite [181] Titanium nitride coating [307]	Titanium plasma spraying in addition to titanium nitride coating [297]

Blasted acid etched [311]		CaO-ZrO ₂ -SiO ₂ (CZS) coating[311]
Shot peened [181]	Hydroxyapatite [181]	blends of hydroxyapatite and fluorapatite, with concentrations ranging from 0 to 100% fluorapatite[286]
Selective Laser Sintering (SLS) [294]		Electrochemically deposited dicalcium phosphate dehydrate, so-called brushite [312]
MAO [306*]		Silicon-substituted hydroxyapatite (Si-HA) coatings [286]
Severe plastic deformation [313*, 314*]		Fluorohydroxyapatite [315]
Nanopore [308*,316*]		Titanium plasma spraying in addition to HA[231]
Electron beam melting process [317]		silicon (Si) nanofibers coating [318*]
Oxidation [93,319]		silicon oxide (SiO ₂) nanofibers coating [318*]
Aged treatment (A:Passivated tt followed by aging in boiling deionized water for 10h)[320,321]		titanium oxide (TiO ₂) nanofibers surface coating [318*]
Unspecified smooth/rough [268]		Bioactive glass coating [322]
		Ion implantation with zinc (Zn-Ti-6Al-4V) [31]
		Ion implantation magnesium (Mg-Ti-6Al-4V) [31]
		Coating alkoxide-derived hydroxy carbonate apatite (CHAP-Ti-6Al-4V) [31]
TiMo ₁₂ Zr ₆ Fe ₂ (TMZF) discs [323]		
NiTi		
Mirror polished [75,93]		Hydroxyapatite[181]
Oxidized [93]		
Ti-6Al-7Nb		
Untreated [80]		
TiZr (Ti-50 wt %Zr)		
Grit ground [124]		
TiNb (Ti-50 wt %Nb) alloy discs		
Grit ground [124]		
fine-ground[135]		
Ti-5Zr-3Sn-5Mo-15Nb alloy		
MAO[324]		
Ti ₁₃ Nb ₁₃ Zr alloy		Hydroxyapatite coating [288*]
CrCoMo alloy Zimaloy		
Untreated/polished [73,85,135,273,274,277]		Porocoated [277]
Etched [147]		
Heat treatment [73]		
Blasted [273,305]		
Stainless steel		
[75,76,80,135,277,325,326]an		

	austenitic Ni-reduced SSt [276,281]	
	Etched [147]	
Tantalum	Untreated [73,85]	chemical vapour deposition (CVD) process [73]
Nickel	[75]	
ZrO	[326]	
ZrO ₂ ceramics		
	Untreated [327]	
Zirconia (yttria-stabilized tetragonal zirconia: ZrO ₂ 93.5%, Y ₂ O ₃ 5.1%)		
	Untreated [78,328,329]	Zi-Unite [250]
	Grooved [328]	
	UV light [330]	
Yttrium-stabilized tetragonal zirconia polycrystals zirconia discs reinforced with 25% alumina		
	Machined [225,250]	ATZ discs with a modified surface (ATZ-mod)[250]
	Abraded[225]	
	Abraded acid etched [225]	
Novel zirconia alloy ((Y,Nb)-TZP/alumina- zirconia/alumina composite		
	Smooth [331]	
Alumina (polycrystalline alumina ceramic Al ₂ O ₃ 99.5% purity) ceramics		
	Untreated [78,332]	Magnesium ion implanted [332]
		Polymeric powder coating with TiO ₂ or silica nanoparticles [333*]
Glass ceramics[84]		
CaSiO ₃ ceramic disks [334,335]		
calcium silicate ceramics, sphene (CaTiSiO ₅) coating [335]		
Hardystonite (Ca ₂ ZnSi ₂ O ₇) ceramics [334]		
Hydroxyapatite		
	As received [112,229,291,325,336-339]	Plasma sprayed with HA[229]
	Calcined [338]	
	Sintered [84,113,282,338,340]	
	Sintered with microchannels[342]	
calcium titanium phosphates CaTi ₄ (PO ₄) ₆ [106]		
calcium titanium zirconium phosphates CaZr ₄ (PO ₄) ₆ [106]		
Silicon wafers		
	Etched [49,342]	Coated with cpTi[49,342,343]
	Untreated smooth [49,342]	Coated with cpTi[49,342]
Polysterene culture plates		Sputter coated with titanium, titanium oxide, Alumina oxide,zirconia oxide and calcium phosphate [344] ; Titanium [30,72]
Polycarbonate membranes		Titanium [345*]
Fiber reinforced composites		
	Blasted [346]	Bioactive Glass [346]
Bioactive glass 45S5, S53P4 [256,325]		
Glass slides		
		Titanium- Tobacco Mosaic Virus and TMV

	-Phos [345,347*] Polyelectrolyte multilayer film self assembly[348]
	Nanocrystalline deposition of Cp Ti, Ti6Al4V, TiNb30 and TiNb13Zr13) [349]
PMMA [325]	
Ultra-high-molecular-weight polyethylene (UHMWPE) [339]	
Polyethylene [134]	
Carbon/carbon composite [134]	

Table2: Cell culture models used at different implant surfaces.

Cell models	References
SaOS-2	[106,107,120,124,162,163,186,187,189,190,260,274,275,279,281,305,321,340,350,351]
MC3T3-E1	[37,72,74,81,82,87,92,98,105,114,115,152,177-180,185,186,226-228,262-265,318,322,348,352-356]
MG-63	[27,47,51,52,58-60,79,93,95,99,102,108,134,136,137,140,143-145,157,169,170,188,189,192,195-197,201-203,206-209,215,216,218,221-224,231-233,235,242,247,255,261,267,281,285,292,293,298,300,304,308,316,326,327,329,357-359]
C3H10T1/2	[74]
C2C12	[354]
Osteosarcoma cell line U2OS	[113]
ROS-17/2.8 osteosarcoma cell line	[75]
Human osteosarcoma HOS TE85 cells	[96,97,331]
HEPM (Human Embryonic Palatal Mesenchymal Cells)	[36,121,155,168,171,272,338]
Primary human osteoblast cells	[31,57-59,73,76,80,83,86,106,107,116,118,125,129,130,135,176,181,184,198,199,211,212,214,215,218,220,225,229,238,239,244,273,279,283,294,301,302,309,319,320,323,332,334,335,341,360,361]
Human bone marrow derived osteoblast cells	[89,154,282,287,289,290,325]
Human mesenchymal stem cells(hMSCs) and human bone marrow cells	[22,41,43,48,58,85,111,125,146,150,158,160,164,166,167,183,216,217,240,241,252,254,269,277,280,284,288,295,297,307,311,315,339,345,362]
hFOB 1.19	[147,238,250,312,317,362]
Human fetal osteoblast cells (hFOB)	[119]
osteoblastic precursor cell line (OPC1) established from fetal bone tissue	[161,244,245]
Rat bone marrow (RBM) cells	[42,84,101,103,104,110,172-174,236,237,251,256,259,330,347,363]
Primary rat osteoblasts	[46,90,91,100,156,200,205,219,248,249,253,276,291,299,313,314,324,349,364]
Rat bone marrow derived osteoblasts	[30,53,54,132,137,151,153,159,257,346,365]
Rat periosteum derived cells	[131,149]
Rat osteoblastic cells-CRP10/30 cells	[258]
UMR-106-01-BSP /non-mineralizing subclone of UMR-BSP; UMR-U1 cells (negative mineralization control)	[271]
Rat osteoblastic cells (ROS.MER#14), an osteosarcoma line of immortalized cells	[238]
Calvarial chick osteoblasts	[336]
Bone formative group cells	[138]

(BFGCs) derived from bone marrow of beagle's femur : consisted of hematopoietic stem cells (HSC) and osteogenetic stem cells (OSC)	
2T9 mouse osteoblast progenitor cell line	[122]
Primary mouse osteoblasts	[74,112,234]
Mouse bone marrow derived mesenchymal stem cells	[296]
Rabbit bone marrow derived mesenchymal stem cells	[210]
Primary chondrocytes from Rats- resting zone and growth plate zone	[268,344]
J774A.1	[69,71,109,278]
RAW264.7	[117,122]
Mouse bone marrow cell culture along with osteoclast differentiation media M-CSF and RANKL	[266]
Human monocytes	[166,246,254,335]
Dendritic cells differentiated from human mononuclear cells	[213]
Human aortic endothelial cells (HAEC)	[218]
HUVECs	[88,141,144]
Purified and immortalized human dermal microvascular endothelial cells (HMEC-1)	[335]
Human gingival fibroblasts (HGF)	[49,127,128,182,204,328,342,343]
Rat oral fibroblasts	[133]
NIH3T3 fibroblasts	[152,366]
Adipose derived MSCs	[280]
Platelet concentrate- human	[142]
Schwann cells derived from neonatal rats	[94]

Table 3: Genes examined in in-vitro culture models with different implant surfaces along with their functional gene ontology annotation.

Genes examined	Biological process GO annotation	References
miRNA		[79,232,233,326,327]
Hsp47 (heat shock protein 47)	response to unfolded protein; negative regulation of endopeptidase activity; regulation of proteolysis	[55]
HSP70 (heat shock 70kDa protein)	protein folding; post-Golgi vesicle-mediated transport; cellular membrane organization	[275]
cyclin-dependent kinase 2; cyclin-dependent kinase 4; cyclin-dependent kinase 6	cell division	[127,128]
cyclin A1	Cell division	[250]
cyclin A2	Cell division	[128]
cyclin D1	Cell division	[112,127,128,331]
cyclin E	Cell division	[127,128]
cyclin-dependent kinase inhibitor 1A (p21, Cip1); cyclin-dependent kinase inhibitor 1B (p27, Kip1)	Cell cycle checkpoint	[127,128]
cyclin-dependent kinase inhibitor 2A	Cell cycle checkpoint	[250]
PCNA (proliferating cell nuclear antigen)	cell proliferation	[250]
antigen identified by monoclonal antibody Ki-67	cell cycle; meiosis; cell proliferation	[239]
c-myc	cell proliferation	[127]
Ubiquitin C	cell cycle checkpoint;DNA damage response	[85]
RP59	multicellular organismal development; cell differentiation; regulation of osteoblast differentiation	[234]
RUNX3 (runt-related transcription factor 3)	regulation of transcription, DNA-dependent; transcription from RNA polymerase II promoter; protein phosphorylation; induction of apoptosis; cell proliferation; negative regulation of cell cycle; negative regulation of epithelial cell proliferation	[250]
SOX9	cartilage condensation; regulation of	[149,296]

(SRY (sex determining region Y)-box 9)	transcription from RNA polymerase II promoter; transcription from RNA polymerase II promoter	
MSX-2 (msh homeobox 2)	Sequence-specific DNA binding transcription factor activity; osteoblast differentiation; multicellular organismal development; negative regulation of cell proliferation;	[234]
DLX5 (distal-less homeobox 5)	Skeletal system development; osteoblast differentiation; endochondral ossification; multicellular organismal development	[234,264]
RUNX2 (Runt-related transcription factor 2)	Ossification; osteoblast differentiation; transcription	[36,37,41-43, 46, 48, 55, 73,85, 90, 112, 114, 130,146,166,168,170,171,200,212,228,234,238, 243,248,249,260-262, 269-271,280, 283, 286, 289,290,294-296, 322, 324,333,345,347,362]
Sp7 transcription factor	Regulation of transcription; osteoblast differentiation	[36,37,41,43,55,90,112,166, 168,228,295]
ALP (alkaline phosphatase)	Skeletal system development; biomineral tissue development	[36,41,43,46,53,55,84-86, 90, 92,100,101,104-107, 112, 114,119,121,130,135,143, 144,146,152,161,168,180, 185,211,212,226,227,238, 239,241,243-245, 248-250, 260,262-265, 274, 279, 280, 284, 285, 287, 295, 301, 302, 311,312,317,333-335, 340, 345,354, 355,360,362]
BSP (integrin-binding sialoprotein)	Ossification; cell adhesion; extracellular matrix organization; biomineral tissue development	[36,37,41,43,48,73,84,86,106,107,112,116,125,162,164, 168,178,183,201,220,228, 234, 250, 253, 260, 262, 264, 271,274,277,286,294,295, 301,302,311,317,333,335, 345,346,348,362]
OC (Osteocalcin)	Skeletal system development; osteoblast differentiation; osteoblast development; bone mineralization; regulation of osteoclast differentiation	[22,30,36,41-43,46,52-55,57, 59, 73, 76, 80, 82, 83, 85, 86, 90-93,96-98, 100, 101, 103, 106, 107, 110, 112, 114, 115, 118,120,124,129,130,131, 134,136,139,143-147,150-153, 155-160, 164, 167, 168, 170, 171, 174, 176, 180, 185,188-190,195,196,199-202, 206, 207,209-212, 218, 220-229, 234,237,238,240,242,243, 246,248-253, 256, 257, 262-265,267,269,272,274,276, 277,280-282, 285, 286, 289, 290,292,295,297,300-302, 307,309, 311, 314,317-319,

		321,324,330,334,335,345-348, 351, 352,355,357,359-361,364,365]
OPN (Osteopontin)	Ossification; cell adhesion; positive regulation of cell-substrate adhesion; biomineral tissue development	[22,30,42,43,46,48,53-55, 72, 84-86,91,98,105-107, 112, 114,116,131,132,146,149-151,153,155,158-160, 162, 164,177,180,210,211,234, 239-241,248-251, 257, 260, 267,262,263,265,277,286, 288,289,291,294,295, 297, 309,311,314, 321, 324, 330, 334,347-349,353,355]
ON (secreted protein, acidic, cysteine-rich) (osteonectin)	Ossification; regulation of cell proliferation; cellular response to growth factor stimulus	[81,86,106,107,116,125,126, 250,288,291,294,296, 309, 321,331]
DMP1 (dentin matrix acidic phosphoprotein 1)	ossification; positive regulation of cell-substrate adhesion; extracellular matrix organization; biomineral tissue development	[234]
OMD (osteomodulin)	cell adhesion	[178]
Wnt 5a	multicellular organismal development; positive regulation of gene expression;	[48]
CTNNB (catenin (cadherin-associated protein), beta 1)	canonical Wnt receptor signaling pathway;	[283,354]
Axin2	intramembranous ossification; chondrocyte differentiation involved in endochondral bone morphogenesis; dorsal/ventral axis specification; regulation of Wnt receptor signaling pathway; bone mineralization;	[354]
Snail	osteoblast differentiation; mesoderm formation; multicellular organismal development; positive regulation of transcription, DNA-dependent; regulated by Wnt signaling pathway	[354]
Wisp2 (WNT1 inducible signaling pathway protein 2)	regulation of cell growth; cell adhesion; signal transduction; cell-cell signaling; negative regulation of cell proliferation	[354]
Connexin43	transport; apoptosis; muscle contraction; signal transduction; cell-cell signaling; gap junction assembly	[354]
BMP1 (bone morphogenetic protein 1)	skeletal system development; cartilage condensation; ossification; multicellular organismal development; cell differentiation	[55]
BMP2 (bone morphogenetic protein 2)	skeletal system development; osteoblast differentiation; positive regulation of bone mineralization	[46,69,71,109,114,164,171, 220,243,248,249,287,295, 324,362]
BMP4 (bone morphogenetic protein 4)	osteoblast differentiation; positive regulation of pathway-restricted SMAD protein phosphorylation; positive regulation of bone mineralization;	[324]
BMP6 (bone morphogenetic protein 6)	skeletal system development; positive regulation of pathway-restricted SMAD protein phosphorylation; positive regulation of bone mineralization	[220]
BMP7	skeletal system development; ossification;	[130,250]

(bone morphogenetic protein 7)	positive regulation of bone mineralization; SMAD protein signal transduction	
SMAD1 (SMAD family member 1)	osteoblast fate commitment; regulation of transcription, DNA-dependent; transforming growth factor beta receptor signaling pathway	[280]
TGFB1 (transforming growth factor, beta 1)	chondrocyte differentiation; SMAD protein complex assembly; regulation of cell proliferation; response to wounding; regulation of collagen biosynthetic process	[52,55,59,60,69,71,75,83,118,134-136, 140, 145, 154, 175, 195,196,201,207-209,221-224, 238, 243, 250, 268, 276, 278,281,300,314,356,357, 359]
TGFBR1(transforming growth factor, beta receptor 1); TGFBR2(transforming growth factor, beta receptor 2)	positive regulation of mesenchymal cell proliferation; positive regulation of SMAD protein import into nucleus	[127,128]
EGFR (Epidermal growth factor receptor)	cell morphogenesis; ossification; cell proliferation; positive regulation of cell proliferation; cell-cell adhesion	[127]
FGFR1 (fibroblast growth factor receptor 1)	skeletal system development; positive regulation of cell proliferation	[127]
FGF-2 (fibroblast growth factor 2 (basic))	regulation of cell proliferation; wound healing; positive regulation of blood vessel;regulation of cell cycle	[218]
EGF (epidermal growth factor)	angiogenesis; platelet degranulation; DNA replication; positive regulation of cell proliferation	[218]
IGF1 (insulin-like growth factor 1)	skeletal system development; blood coagulation; positive regulation of cell proliferation; bone mineralization involved in bone maturation; positive regulation of osteoblast differentiation	[314]
Collagen production	Skeletal system development; blood vessel development; osteoblast differentiation; intramembranous ossification; endochondral ossification	[30,46,51,55,76,82,89,98,102,129,133,147,151,154,157,170,181,186,197,219,231,248,258,268,276,292,295,305,315,323,336,341,344,350,357]
COL1 (collagen, type I, alpha 1)	Skeletal system development; blood vessel development; osteoblast differentiation; intramembranous ossification; endochondral ossification	[30,36,53,55,72,73,84-87, 90, 91,103,105-107, 112, 114, 116,121,125,130-133, 143, 146,149,152,153,158-160, 162-164, 167, 168, 177, 179, 182,185,187,211,212,226, 228,234,238,250,257,260, 265,274,277,279,280,285-288,296,298,302,309,311, 312,314,317,319,322,324, 328,333-335, 345, 347, 348, 353,355,360,361,365]

COL II	Skeletal system development	[133,149,250,277,296,339]
COL III (collagen, type III, alpha 1)	skeletal system development; blood vessel development; cell-matrix adhesion	[30,53,182,250,328,339]
COLIX (collagen, type IX, alpha 1)	chondrocyte differentiation; cell adhesion; organ morphogenesis	[149]
COL10a1 (collagen, type X, alpha 1)	skeletal system development	[296]
lysyl hydroxylases (LHs);LH1,LH2,LH3	protein modification process; hydroxylysine biosynthetic process; collagen fibril organization	[55,87]
Lysyl oxidases (LOX, LOXL1-4]	protein modification process; collagen fibril organization	[55]
Prolyl hydroxylases (LEPRE1, P4HA1)	collagen fibril organization	[53,55,133]
Sulfatase 1	Heparan sulfate proteoglycan metabolic process; negative regulation of fibroblast growth factor receptor signaling pathway; bone development	[178]
Decorin	organ morphogenesis; wound healing; extracellular matrix binding ;peptide cross-linking via chondroitin 4-sulfate glycosaminoglycan;	[55,87,250]
Biglycan	Blood vessel remodeling; peptide cross-linking via chondroitin 4-sulfate glycosaminoglycan; extracellular matrix binding	[55,87]
Fibromodulin	Transforming growth factor beta receptor complex assembly; wound healing	[87]
Lumican	collagen fibril organization; cartilage development; collagen binding	[87]
Laminin	regulation of cell adhesion; regulation of cell migration; extracellular matrix structural constituent;	[309,328,339,345]
Vitronectin	cell adhesion; cell-matrix adhesion; extracellular matrix organization	[88,119,161-163,280,309]
Vitronectin receptor	----	[88]
TN (tenascin)	cell adhesion; signal transduction; response to wounding	[162,163,187,188]
fibronectin	extracellular matrix structural constituent; angiogenesis; cell adhesion; response to wounding; cell migration; peptide cross-linking; platelet activation; substrate adhesion-dependent cell spreading; leukocyte migration; regulation of cell shape	[46,49,88,126-128, 133, 162, 163, 182, 186, 187, 248, 280, 292,293,309,321,324,328, 339,343,347]
CD44 molecule	cell-matrix adhesion; cell-cell adhesion; cytokine-mediated signaling pathway	[259,349]
ICAM-1 (intercellular adhesion molecule 1); selectin E	Leukocyte migration; cell-cell adhesion; leukocyte cell-cell adhesion	[141,182]
VCAM-1(vascular cell adhesion molecule 1)	Inflammatory response; cell adhesion; leukocyte cell-cell adhesion regulation of immune response; leukocyte tethering or	[135]

	rolling	
EPCR (Endothelial cell protein C-receptor)	Immune response; blood coagulation; antigen processing and presentation	[141]
CADHERIN E	Cell-cell adhesion	[162,292]
VE-cadherin	Cell-cell adhesion	[88,335]
N-cadherin	Cell-cell adhesion	[292,293]
MOUSE Emr(F4/80)	cell adhesion; G-protein coupled receptor protein signaling pathway; neuropeptide signaling pathway	[266]
Vinculin	blood vessel development; regulation of Wnt receptor signaling pathway; canonical Wnt receptor signaling pathway involved in positive regulation of wound healing	[244,245,251,283,293]
vWF (von Willebrand factor)	Cell adhesion; blood coagulation; response to wounding; cell-substrate adhesion	[88,141]
PECAM-1 (platelet/endothelial cell adhesion molecule)	platelet degranulation; cell adhesion; signal transduction; blood coagulation; cell recognition; platelet activation; leukocyte migration	[88]
vascular endothelial growth factor A	angiogenesis; patterning of blood vessels; vasculogenesis; response to hypoxia	[59,142,182,218,242]
iNOS	response to hypoxia; nitric oxide biosynthetic process; blood coagulation; positive regulation of vasodilation	[81]
PDGF (platelet-derived growth factor alpha polypeptide)	Angiogenesis; response to hypoxia; positive regulation of mesenchymal cell proliferation; platelet degranulation; cell-cell signaling	[142]
Ang-1 (angiopoietin 1)	regulation of endothelial cell proliferation; sprouting angiogenesis; leukocyte migration; positive chemotaxis	[218]
TM (Thrombomodulin)	Negative regulation of blood coagulation; leukocyte migration	[141]
integrin, alpha 1	cell adhesion; cell-matrix adhesion; integrin-mediated signaling pathway; cell chemotaxis	[128,172,173,187,264,273,305]
integrin, alpha 2	cell adhesion; cell-matrix adhesion; integrin-mediated signaling pathway; organ morphogenesis	[163,172,173,187,264,273,305]
integrin, alpha 3	cell adhesion; cell-matrix adhesion; integrin-mediated signaling pathway	[113,172,173,273,345]
integrin, alpha 4	cell adhesion; heterophilic cell-cell adhesion; leukocyte cell-cell adhesion;	[113,172,173,273,345]

	integrin-mediated signaling pathway; regulation of immune response; leukocyte migration	
integrin, alpha 5	angiogenesis; cell-substrate junction assembly; cell adhesion; heterophilic cell-cell adhesion; leukocyte cell-cell adhesion; integrin-mediated signaling pathway; leukocyte migration	[113,127,128,163,172,173,188,264,273,305,309]
integrin, alpha 6	cell-substrate junction assembly; cell adhesion; integrin-mediated signaling pathway; regulation of apoptosis; leukocyte migration	[113,172,173,187,273]
integrin, alpha V	cell adhesion; cell-matrix adhesion; integrin-mediated signaling pathway	[113,188,212,273,305,340,344]
integrin, beta 1	cell migration involved in sprouting angiogenesis; cellular defense response; cell adhesion; cell-matrix adhesion; integrin-mediated signaling pathway; multicellular organismal development; cellular response to mechanical stimulus	[31,46,104,113,163,172,173,182,187,188,203,212,248-250,259,264,273,305,309,313,324,328,331,332,340]
integrin, beta 3	cell adhesion; cell-matrix adhesion; integrin-mediated signaling pathway; regulation of bone resorption; leukocyte migration; angiogenesis involved in wound healing	[104,172,173,188,250,305]
integrin, beta 5	cell adhesion; cell-matrix adhesion; integrin-mediated signaling pathway; multicellular organismal development	[305,345,250]
integrin alpha2 beta1	platelet degranulation; cell adhesion; cell-matrix adhesion; integrin-mediated signaling pathway; blood coagulation; platelet activation	[292,332]
integrin alpha3 beta1	cell-matrix adhesion; integrin-mediated signaling pathway	[332]
Integrin alpha 5 beta 1	cell-matrix adhesion; integrin-mediated signaling pathway	[88,292,332]
Integrin, alpha V beta3	----	[88,163,246,332]
CSF (colony stimulating factor 1 (macrophage))	macrophage differentiation; regulation of ossification; osteoclast differentiation; positive regulation of cell migration; positive regulation of mononuclear cell proliferation; monocyte activation	[100,238,278]
OPG (tumor necrosis factor receptor superfamily, member 11b)	Skeletal system development; apoptosis; extracellular matrix organization; negative regulation of bone resorption	[41,57,59,60,73,100,143,144,166,167,190,196,199,202,206,242,243,278,286,300,319,334,335,354,358,361]
RANK (tumor necrosis factor receptor superfamily, member 11a, NFKB activator)	cell-cell signaling; positive regulation of cell proliferation; osteoclast differentiation	[122]
RANKL (tumor necrosis factor (ligand) superfamily,	Positive regulation of osteoclast differentiation; positive regulation of bone	[73,81,100,167,196,206,242,243,286,319,334,335,358,

member 11)	resorption; cytokine-mediated signaling pathway	361]
TRAF6 (TNF receptor-associated factor 6)	signal transduction; regulation of apoptosis; positive regulation of osteoclast differentiation; negative regulation of transcription, DNA-dependent; positive regulation of NF-kappaB transcription factor activity	[122]
catK (Cathepsin K)	Proteolysis; bone resorption	[122,336]
calcitonin receptor	Activation of adenylate cyclase activity by G-protein signaling pathway	[267,336]
carbonic anhydrase II	Positive regulation of osteoclast differentiation; positive regulation of bone resorption; secretion	[335]
TRAP (acid phosphatase 5, tartrate resistant)	response to cytokine stimulus; bone resorption; bone morphogenesis	[122,246,266,277]
MMP1 (matrix metalloproteinase 1)	Proteolysis; blood coagulation; metabolic process; collagen catabolic process; leukocyte migration	[135]
MMP2 (matrix metalloproteinase 2)	Angiogenesis; proteolysis; metabolic process; collagen catabolic process	[55,342]
MMP9 (matrix metalloproteinase 9)	Skeletal system development; proteolysis; extracellular matrix organization; collagen catabolic process	[55, 335]
TIMP2 (TIMP metalloproteinase inhibitor 2)	Negative regulation of cell proliferation; regulation of cAMP metabolic process; regulation of MAPKKK cascade	[335]
TIMP1-4 (TIMP metalloproteinase inhibitor1-4)	----	[55]
TNF- α (tumor necrosis factor)	Inflammatory response; immune response	[73,116,134,165,213,276, 278]
Interleukin 1, alpha- pro-inflammatory cytokine	Inflammatory response; immune response; cell proliferation; wound healing	[278]
Interleukin 1, beta	Inflammatory response; immune response; signal transduction; cell-cell signaling;	[71,117,213,278]
Interleukin 6	Inflammatory response; immune response	[71,75,117,187,238,276,281, 357]
Interleukin 8	Inflammatory response; immune response	[135,213]
Interleukin 10	Inflammatory response; cell-cell signaling; regulation of gene expression; leukocyte chemotaxis	[71,165,213,278]
Interleukin 11	Inflammatory response; immune response	[73]
interleukin 12, interleukin 17A	immune response	[117]
IL-1 R alpha , IL-12p70, IL-15, IL-18 ,IL-16	immune response	[213]

MCP-1 (CCL2)	angiogenesis; response to hypoxia; chemotaxis; inflammatory response; cytokine-mediated - signaling pathway	[117,213,278]
MIP-1 α (CCL3) ; MIP-1 β (CCL4) ; RANTES (CCL5); Eotaxin (CCL11);MDC (CCL22)	chemotaxis; inflammatory response; immune response	[117]; MIP-1 [213]
SDF-1 (CxCL12) (chemokine (C-X-C motif ligand 12)	chemotaxis; immune response; cell adhesion; signal transduction	[117]
Cox-2 (prostaglandin-endoperoxide synthase 2 (prostaglandin G/H synthase and cyclooxygenase)	regulation of inflammatory response; response to glucocorticoid stimulus	[354]
PGE2 (prostaglandin E synthase 2)	prostaglandin biosynthetic process; fatty acid biosynthetic process; cell redox homeostasis; secretion	[52,134,136,140,145,174,175,195,196,201,207,208, 221-224,268,300,352,359]
NPAS2(neuronal PAS domain protein 2)	Transcription, DNA-dependent; central nervous system development	[296]
BDNF (brain-derived neurotrophic factor)	Nervous system development; axon guidance	[94]
NGF (Nerve growth factor)	Peripheral nervous system development; regulation of neuron differentiation; regulation of axonogenesis	[94]
FAK		[171,214,299,332,340]
p-ERK; p-JNK ;p-FAK	-----	[81,192,309,340]
Erk; p-eErk1	-----	[31,74]
Akt-1; MEK1 ;ERK2	-----	[127]
c-fos	transcription, DNA-dependent	[31,299,340]
c-jun	transcription, DNA-dependent	[29,340]
RhoA; Rac1 ;cdc42 ;Rho Kinase		[127]
Shc (SHC (Src homology 2 domain containing) transforming protein 1)	angiogenesis; response to hypoxia; epidermal growth factor receptor signaling pathway; Ras protein signal transduction; positive regulation of cell proliferation; cell-cell adhesion; neuron differentiation; organ regeneration; actin cytoskeleton reorganization; intracellular signal transduction	[31,332]
PLD1a,1b,2a&2b (phospholipase D1, phosphatidylcholine-specific)	phosphatidic acid biosynthetic process; chemotaxis; cell communication; small GTPase mediated signal transduction; Ras protein signal transduction	[202]

phospholipase C-gamma2 intracellular signal transduction [298]
(Plc-gamma2)

protein kinase C, alpha intracellular signal transduction [127,202]

Table 4: Technique used in in-vitro culture models for molecular assessment of osseointegration with different implant surfaces

Method of testing	References
Northern blotting	[84,236,274,279,291,301,302,309,342]
RT-PCR	[30,53,54,69,71,73,98,100,103,109,116,122,127-129,131-133,137,138,143,147,149,150,151,153,158-160,164,170,171,178,198,202-204,214,234,238,253,257,260,261,266,277-279,285-290,294-296,298,301,302,312-314,324,328,330,331,333,364-366]
Quantitative real time RT-PCR	[27,36,37,41-43,46,48,71,72,85,87,90,91,94,101,104,105,112,114,121,122,130,141,144,146,152,168,177,180,182,183,185,187,188,200,206,210,212,215-217,220,226-228,235,238,240,241,243,248-250,254,259,262-265,267,271,272,280,284,293,311,317,321,322,333-335,340,345-348,353-355,358,360,362]
In situ hybridization	[86,106,107]
Immunoassay-ELISA (OC, PGE2, TGF-B1, IL-1 alpha, IL-1B, MCP-1, IL-10, IL-12, IL-17A, SDF-1 (CxCL12), RANTES (CCL5), MCP-1 (CCL2), MIP-1 α (CCL3), MIP-1 β (CCL4), MDC (CCL22) and Eotaxin (CCL11), FGF2, EGF, M-CSF, BDNF, NGF, IL-6, OPG, VEGFA, DKK1, DKK2, BMP2-BMP4, BMP6, OPN, RANKL, COLI, IGF-1, PDGF, TNF-alpha, MMP1, VCAM1)	[27,52,57-60,73,75,76,80,82,83,93,94,96,101,103,109,110,115,117,118,129,134-137,139,140,142,144,145,147,154-157,165,167,175,176,179,181,187,189,190,195,196,199,202,205-209,216-218,220-227,231,234,237,242,243,252,254,256,268,276,278,281,292,297,300,307,314,315,318,319,321,348,351,352,254,357,359,361]
Immunochemistry (Vinculin, ALP, PECAM-1, Vitronectin, Fibronectin receptor, VN receptor, VE-cadherin, von Willebrand factor, Fibronectin, $\alpha\beta$ 1 and α (v) β 3), OC, BSP, OPN, TN, Runx2, collagen)	[86,88,92,106,107,119,124,161,162,163,181,200,211,244-246,273,283,309]
Radioimmunoassay	[27,52,97,123,134,136,140,145,147,169,175,195,196,201,202,205,207,208-210,215-218,221-224,229-242,268,282,300,338,359]
Gelatin Zymography and reverse zymography/ MMP-TIMP2	MMP2 [342]
Immunoblotting	[31,74,81,98,127,192,235,275,292,293,305,309,332,340,356]
Immunofluorescence	[22,125,203,239,251,269,277,293,332,341]
Collagen synthesis: 3H-proline incorporation into collagen fibers; Sirius red based stain assay	[30,51,53,102,133,151,170,197,219,295,305,336,365]
Immunogold labeling & SEM	[126]
Cytochemical stain TRAP	[246,266]
Flow cytometry	[113,163,172-174,187,204,261,292,332,339,349]
[35S] Methionine-labeled fibronectin	[49,343]

[35S] Sulfate incorporation	[51,197,268]
miRNA microarrays	
miRNA microarrays containing 329 probes designed from the human miRNA sequence	[79,232,233,326,327]
Wider genome profiling	
Human 19.2 K DNA microarray	[304,308,316,329] [47]
Human 20K DNA microarray (MWG Biotech AG, Ebersberg, Germany) cDNA microarray-18,401 genes	[120]
GeneChip Mouse Genome 430 2.0 Array (34,000 genes)-affymetrix	[178]
Whole genome-Illumina Sentrix [®] Human-6 v2 expression BeadChips-47,000 probe sets	[48,220]
Genefilters GF211: 12,626 genes	[320]
cDNA microarray GCK 5.0 K human chip (Genocheck, Korea) - 5049 genes	[247]
Rat gene microarray: Research Genetics GF300 nylon microarray (Invitrogen Corporation, Carlsbad, CA). These arrays have 1633 named rat gene sequences.relative level of specific groups of genes related to bone and cartilage development, cell adhesion and extracellular matrix proteins, transcription factors, bone morphogenetic proteins, phospholipases, and protein kinases	[363]
Atlas [™] Human Cancer 1.2 gene array containing 1176 genes	[184,198]
Human cDNA microarray (1152 elements)	[95,99,108,255]
A microarray containing a total of 687 cDNA sequences	[325]
cDNA GEArray [™] kit for Human Osteogenesis, HS-026-4 www.superarray.com)	[110]
An array of osteogenesis-related genes (human osteogenesis RT ² Profiler PCR array, PAHS-0026A – SuperArray Bioscience, Frederick, MD)) 76 related genes	[41,55]
RT profiler PCR array for ECM and adhesion molecules	[345]
Murine PCR Array (PAMM-011, SABiosciences, Frederick, MD, USA). This array profiles 84 key genes involved in mediating immune cascade reactions during inflammation and includes chemokines, cytokines, interleukins and their receptors..	[116]
GE-Superarray system,>80 genes	[166]

Table 5: Genome wide expression profiling in in-vitro culture models for molecular assessment of osseointegration.

Model	Surface examined	Technique used	Days of analysis	Reference
Primary human osteoblasts - 3rd molar extraction sites	SLA, mod SLA vs. Glass cover slips	Whole genome-Illumina Sentrix [®] Human-6 v2 expression BeadChips-47,000 probe sets	72 hrs	[220]
hMSCs	SLA, SLActive, SMO (polished)	Whole genome-Illumina Sentrix [®] Human-6 v2 expression BeadChips-47,000 probe sets	3, 24, 72 or 120 h	[48]
MC3T3-E1 pre-osteoblastic cells	FN-immobilized titanium (Fibronectin coating using the tresyl chloride activation technique) vs untreated titanium	GeneChip Mouse Genome 430 2.0 Array (34,000 genes)-affymetrix	14 days	[178]
MG-63	Anatase coating of titanium	Human 20K DNA microarray (MWG Biotech AG, Ebersberg, Germany)	24 hrs	[47]
MG-63	Ti6Al4V disks machined (SR=0.77+ ₋ 0.28) vs. Biolok, Blasted with tricalcium phosphate and light nitric acid tt (SR=1.93+ ₋ 0.37) Biolok, Nanopore SR=1.05+ ₋ 0.34 vs. TPSS surface 2.74, or only medium and cells	Human 19.2 K DNA microarray	24 hrs	[308]
MG-63	zirconium oxide discs (Cercon, Degussa Dental, Hanau, Germany)	Human 19.2 K DNA microarray	24,48 hrs	[329]
MG-63	Disks of machined titanium , vs. nanoPORE (Out-Link, Sweden and Martina, Due Carrare, Padova, Italy).The surface roughness (Sa) was 0.77±0.28 for the machined disks and 1.05±0.34 for the nanoPORE disks	Human 19.2 K DNA microarray	24,48 hrs	[316]
MG-63	Machined grade 3 titanium vs. titanium pull spray superficial [TPSS]:produced through micromechanical removal of parts of the superficial oxide layer with the use of aluminum oxide 0.5 mm/micropoints.The Ra value was 0.30 for the machined surface and 2.74 for the TPSS surface.	Human 19.2 K DNA microarray	24,48 hrs	[304]

MG-63	Machined vs anodized Ti surface: The roughness of machined Ti surface was $0.54 \pm 0.16 \mu\text{m}$ and the roughness of anodized one was $0.88 \pm 0.13 \mu\text{m}$	cDNA microarray GCK 5.0 K human chip (Genocheck, Korea) - 5049 genes	24 hrs	[247]
Saos-2	1) Tapered Internal (BioHorizons Implant Systems, Inc., Birmingham, AL) and Resorbable Blast Texturing with Laser-Lok collar; (Ra, not available). 2) Nanotite (3i Implant Innovations, Inc., Palm Beach Gardens, FL), osseotite surface combined with a discrete crystalline deposition of nanometer scale calcium phosphate; (Ra, $0.28 \pm 0.06 \mu\text{m}$). 3) Full Osseotite (FOSS; 3i Implant Innovations, Inc.), osseotite surface: dual acid-etched with HF and then HCl/H ₂ SO ₄ ; (Ra, $0.86 \pm 0.14 \mu\text{m}$). 4) Straumann SLActive Standard Implant (Institut Straumann AG, Basel, Switzerland), sandblasted with large grits (0.25–0.50 mm), acid-etched with HCl/H ₂ SO ₄ , rinsed under N ₂ protection, and preserved in isotonic NaCl solution; (Ra, $2.93 \pm 0.46 \mu\text{m}$). 5) SwissPlus (Zimmer Dental, Inc., Carlsbad, CA), grit-blasted with hydroxylapatite (Microtextured Titanium, MTX). As referring control, cells grown in absence of dental implant were used ($1\text{--}2 \mu\text{m}$, as provided by the manufacturer). TCP was used as control	DNA microarray-18,401 genes	72 hrs	[120]
primary human osteoblasts (hOB)	Ti6Al4V polished (control) vs. passivated samples (P: nitric acid treatment-30%-1 hr) vs. Aged treatment (A: Passivated treatment followed by aging in boiling deionized water for 10h)	Gene filters GF211: 12,626 genes	4,24,48 and 120 hrs	[320]

Figure 1:

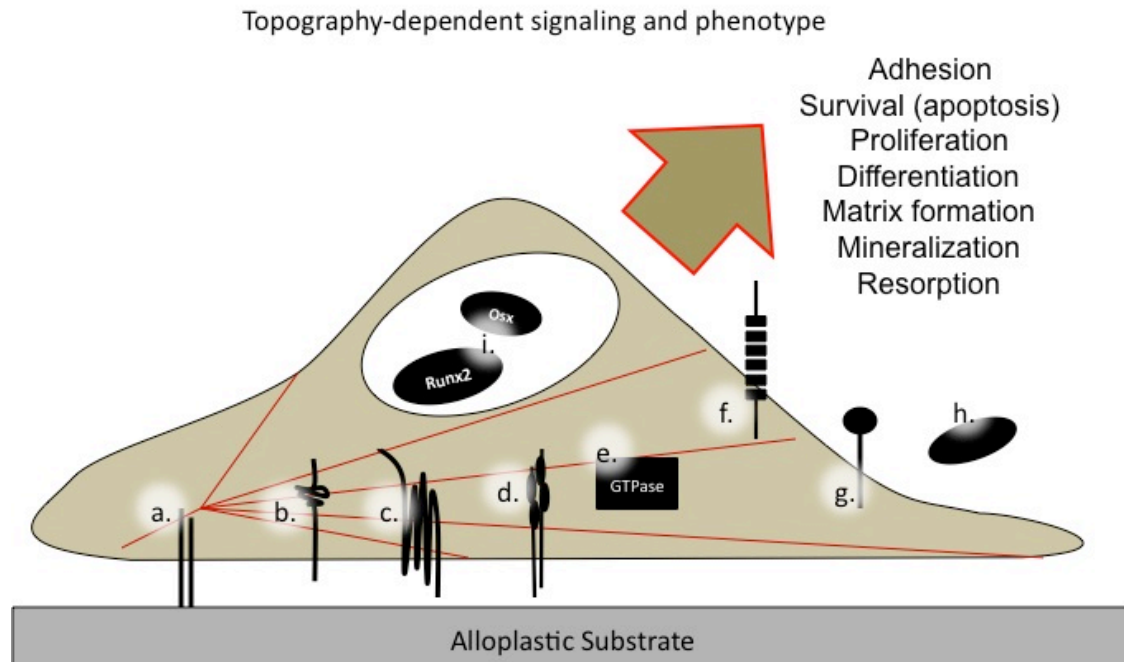


Figure 1: Topography-dependent signaling and phenotype. Alloplastic substrates vary widely in bulk composition and topography (Table 1). Multiple signaling pathways directly or indirectly mediate topography dependent changes in the adherent cell phenotype. Numerous primary, immortalized, and tumor-derived cell models have been involved (Table 2). These pathways represent those involved in cell-adhesion and bone development and repair. Included are (a) integrins [46,248,324] that interact directly with the surface, (b) serine/threonine kinase receptors (eg, TGF β and BMP signaling [69,196,224], (c) G-protein coupled receptors (eg, PTH, Wnt), (d) tyrosine kinase receptors (eg, PDGF, IFG-1 [142,314]) (e) GTPases (eg, Rho1, RAS), (f) b-cadherin, (g) RANKL [100], (OPG) [243], (i) osteoblast differentiation transcription factors (Runx2, Osx). Cellular responses examined focus on osteoblast-specific phenotype but include a wider range of physiologic responses (Table 3)

References

1. Baier RE, Meyer AE, Natiella JR, Natiella RR, Carter JM. Surface properties determine bioadhesive outcomes: methods and results. *J Biomed Mater Res* 1984;18:337-355.
2. Albrektsson T, Jacobsson M. Bone-metal interface in osseointegration. *J Prosthet Dent* 1987;57:597-607.
3. Buser D, Schenk RK, Steinemann S, Fiorellini JP, Fox CH, Stich H. Influence of surface characteristics on bone integration of titanium implants. A histomorphometric study in miniature pigs. *J Biomed Mater Res* 1991;25:889-902.
4. Albrektsson T, Wennerberg A. Oral implant surfaces: Part 1--review focusing on topographic and chemical properties of different surfaces and in vivo responses to them. *Int J Prosthodont* 2004;17:536-543.
5. Albrektsson T, Wennerberg A. Oral implant surfaces: Part 2--review focusing on clinical knowledge of different surfaces. *Int J Prosthodont* 2004;17:544-564.
6. Juodzbaly G, Sapragoniene M, Wennerberg A, Baltrukonis T. Titanium dental implant surface micromorphology optimization. *J Oral Implantol* 2007;33:177-185.
7. Wennerberg A, Albrektsson T. Effects of titanium surface topography on bone integration: a systematic review. *Clin Oral Implants Res* 2009;20 Suppl 4:172-184.
8. Wennerberg A, Albrektsson T. On implant surfaces: a review of current knowledge and opinions. *Int J Oral Maxillofac Implants* 2010;25:63-74.
9. Shalabi MM, Gortemaker A, Van't Hof MA, Jansen JA, Creugers NH. Implant surface roughness and bone healing: a systematic review. *J Dent Res* 2006;85:496-500.
10. Junker R, Dimakis A, Thoneick M, Jansen JA. Effects of implant surface coatings and composition on bone integration: a systematic review. *Clin Oral Implants Res* 2009;20 Suppl 4:185-206.
11. Degidi M, Perrotti V, Piattelli A, Iezzi G. Mineralized bone-implant contact and implant stability quotient in 16 human implants retrieved after early healing periods: a histologic and histomorphometric evaluation. *Int J Oral Maxillofac Implants* 2010;25:45-48.
12. Ivanoff CJ, Widmark G, Johansson C, Wennerberg A. Histologic evaluation of bone response to oxidized and turned titanium micro-implants in human jawbone. *Int J Oral Maxillofac Implants* 2003;18:341-348.
13. Ivanoff CJ, Hallgren C, Widmark G, Sennerby L, Wennerberg A. Histologic evaluation of the bone integration of TiO₂ blasted and turned titanium microimplants in humans. *Clin Oral Implants Res* 2001;12:128-134.
14. Trisi P, Rao W, Rebaudi A. A histometric comparison of smooth and rough titanium implants in human low-density jawbone. *Int J Oral Maxillofac Implants* 1999;14:689-698.
15. Thalji G, Cooper LF. Molecular Assessment of Osseointegration In Vivo: A review of the current literature. *Oral and Craniofacial Tissue Engineering*. 2012; 2: 9-22.
16. Thalji G, Gretzer C, Cooper LF. Comparative molecular assessment of early osseointegration in implant-adherent cells. *Bone* 2012.
17. Ivanovski S, Hamlet S, Salvi GE, Huynh-Ba G, Bosshardt DD, Lang NP, Donos N. Transcriptional profiling of osseointegration in humans. *Clin Oral Implants Res* 2011;22:373-381.
18. Takayanagi H. Osteoimmunology and the effects of the immune system on bone. *Nat Rev Rheumatol* 2009;5:667-676.

19. Hamlet S, Alfarsi M, George R, Ivanovski S. The effect of hydrophilic titanium surface modification on macrophage inflammatory cytokine gene expression. *Clin Oral Implants Res* 2012;23:584-590.
20. Milleret V, Tugulu S, Schlottig F, Hall H. Alkali treatment of microrough titanium surfaces affects macrophage/monocyte adhesion, platelet activation and architecture of blood clot formation. *Eur Cell Mater* 2011;21:430-44; discussion 444.
21. Cooper LF, Masuda T, Yliheikkila PK, Felton DA. Generalizations regarding the process and phenomenon of osseointegration. Part II. In vitro studies. *Int J Oral Maxillofac Implants* 1998;13:163-74.
22. Sjoström T, Dalby MJ, Hart A, Tare R, Oreffo RO, Su B. Fabrication of pillar-like titania nanostructures on titanium and their interactions with human skeletal stem cells. *Acta Biomater* 2009;5:1433-41.
23. Beutner R, Michael J, Schwenzer B, Scharnweber D. Biological nano-functionalization of titanium-based biomaterial surfaces: a flexible toolbox. *J R Soc Interface* 2010;7 Suppl 1:S93-S105.
24. Brunette DM. The effects of implant surface topography on the behavior of cells. *Int J Oral Maxillofac Implants* 1988;3:231-246.
25. Groessner-Schreiber B, Tuan RS. Enhanced extracellular matrix production and mineralization by osteoblasts cultured on titanium surfaces in vitro. *J Cell Sci* 1992;101 (Pt 1):209-217.
26. Klein MO, Bijelic A, Ziebart T, Koch F, Kammerer PW, Wieland M, Konerding MA, Al-Nawas B. Submicron Scale-Structured Hydrophilic Titanium Surfaces Promote Early Osteogenic Gene Response for Cell Adhesion and Cell Differentiation. *Clin Implant Dent Relat Res* 2011.
27. Olivares-Navarrete R, Raz P, Zhao G, Chen J, Wieland M, Cochran DL, Chaudhri RA, Ornoy A, Boyan BD, Schwartz Z. Integrin alpha2beta1 plays a critical role in osteoblast response to micron-scale surface structure and surface energy of titanium substrates. *Proc Natl Acad Sci U S A* 2008;105:15767-72.
28. Kramer PR, Janik Keith A, Cai Z, Ma S, Watanabe I. Integrin mediated attachment of periodontal ligament to titanium surfaces. *Dent Mater* 2009;25:877-883.
29. Galli C, Piemontese M, Lumetti S, Ravanetti F, Macaluso GM, Passeri G. Actin cytoskeleton controls activation of Wnt/beta-catenin signaling in mesenchymal cells on implant surfaces with different topographies. *Acta Biomater* 2012;8:2963-2968.
30. Saruwatari L, Aita H, Butz F, Nakamura HK, Ouyang J, Yang Y, Chiou WA, Ogawa T. Osteoblasts generate harder, stiffer, and more delamination-resistant mineralized tissue on titanium than on polystyrene, associated with distinct tissue micro- and ultrastructure. *J Bone Miner Res* 2005;20:2002-16.
31. Zreiqat H, Valenzuela SM, Nissan BB, Roest R, Knabe C, Radlanski RJ, Renz H, Evans PJ. The effect of surface chemistry modification of titanium alloy on signalling pathways in human osteoblasts. *Biomaterials* 2005;26:7579-86.
32. Kokubu E, Yoshinari M, Matsuzaka K, Inoue T. Behavior of rat periodontal ligament cells on fibroblast growth factor-2-immobilized titanium surfaces treated by plasma modification. *J Biomed Mater Res A* 2009;91:69-75.
33. Bertocini P, Le Chevalier S, Lavenus S, Layrolle P, Louarn G. Early adhesion of human mesenchymal stem cells on TiO₂ surfaces studied by single-cell force spectroscopy measurements. *J Mol Recognit* 2012;25:262-269.
34. Zhuang LF, Jiang HH, Qiao SC, Appert C, Si MS, Gu YX, Lai HC. The roles of extracellular signal-regulated kinase 1/2 pathway in regulating osteogenic differentiation of murine preosteoblasts MC3T3-E1 cells on roughened titanium surfaces. *J Biomed Mater Res A* 2012;100:125-133.
35. Nishimura R, Hata K, Matsubara T, Wakabayashi M, Yoneda T. Regulation of bone and cartilage development by network between BMP signalling and transcription factors. *J Biochem* 2012;151:247-254.

36. Masaki C, Schneider GB, Zaharias R, Seabold D, Stanford C. Effects of implant surface microtopography on osteoblast gene expression. *Clin Oral Implants Res* 2005;16:650-6.
37. Guo J, Padilla RJ, Ambrose W, De Kok IJ, Cooper LF. The effect of hydrofluoric acid treatment of TiO₂ grit blasted titanium implants on adherent osteoblast gene expression in vitro and in vivo. *Biomaterials* 2007;28:5418-25.
38. Mamalis AA, Markopoulou C, Vrotsos I, Koutsiliri M. Chemical modification of an implant surface increases osteogenesis and simultaneously reduces osteoclastogenesis: an in vitro study. *Clin Oral Implants Res* 2011;22:619-626.
39. Long F. Building strong bones: molecular regulation of the osteoblast lineage. *Nat Rev Mol Cell Biol* 2011;13:27-38.
40. Perrotti V, Palmieri A, Pellati A, Degidi M, Ricci L, Piattelli A, Carinci F. Effect of titanium surface topographies on human bone marrow stem cells differentiation in vitro. *Odontology* 2012.
41. Mendonca G, Mendonca DB, Simoes LG, Araujo AL, Leite ER, Duarte WR, Aragao FJ, Cooper LF. The effects of implant surface nanoscale features on osteoblast-specific gene expression. *Biomaterials* 2009;30:4053-62.
42. Mendonca G, Mendonca DB, Simoes LG, Araujo AL, Leite ER, Duarte WR, Cooper LF, Aragao FJ. Nanostructured alumina-coated implant surface: effect on osteoblast-related gene expression and bone-to-implant contact in vivo. *Int J Oral Maxillofac Implants* 2009;24:205-15.
43. Mendonca G, Mendonca DB, Aragao FJ, Cooper LF. The combination of micron and nanotopography by H₂SO₄/H₂O treatment and its effects on osteoblast-specific gene expression of hMSCs. *J Biomed Mater Res A* ;94:169-79.
44. Xu B, Zhang J, Brewer E, Tu Q, Yu L, Tang J, Krebsbach P, Wieland M, Chen J. Osterix enhances BMSC-associated osseointegration of implants. *J Dent Res* 2009;88:1003-1007.
45. Vlacic-Zischke J, Hamlet SM, Friis T, Tonetti MS, Ivanovski S. The influence of surface microroughness and hydrophilicity of titanium on the up-regulation of TGFbeta/BMP signalling in osteoblasts. *Biomaterials* 2011;32:665-671.
46. Zhao L, Mei S, Chu PK, Zhang Y, Wu Z. The influence of hierarchical hybrid micro/nano-textured titanium surface with titania nanotubes on osteoblast functions. *Biomaterials* ;31:5072-82.
47. Sollazzo V, Palmieri A, Pezzetti F, Scarano A, Martinelli M, Scapoli L, Massari L, Brunelli G, Caramelli E, Carinci F. Genetic effect of anatase on osteoblast-like cells. *J Biomed Mater Res B Appl Biomater* 2008;85:29-36.
48. Wall I, Donos N, Carlqvist K, Jones F, Brett P. Modified titanium surfaces promote accelerated osteogenic differentiation of mesenchymal stromal cells in vitro. *Bone* 2009;45:17-26.
49. Chou L, Firth JD, Uitto VJ, Brunette DM. Substratum surface topography alters cell shape and regulates fibronectin mRNA level, mRNA stability, secretion and assembly in human fibroblasts. *J Cell Sci* 1995;108 (Pt 4):1563-73.
50. Komori T. Regulation of bone development and extracellular matrix protein genes by RUNX2. *Cell Tissue Res* 2010;339:189-195.
51. Martin JY, Schwartz Z, Hummert TW, Schraub DM, Simpson J, J. L, Jr, Dean DD, Cochran DL, Boyan BD. Effect of titanium surface roughness on proliferation, differentiation, and protein synthesis of human osteoblast-like cells (MG63). *J Biomed Mater Res* 1995;29:389-401.
52. Zinger O, Zhao G, Schwartz Z, Simpson J, Wieland M, Landolt D, Boyan B. Differential regulation of osteoblasts by substrate microstructural features. *Biomaterials* 2005;26:1837-47.

53. Takeuchi K, Saruwatari L, Nakamura HK, Yang JM, Ogawa T. Enhanced intrinsic biomechanical properties of osteoblastic mineralized tissue on roughened titanium surface. *J Biomed Mater Res A* 2005;72:296-305.
54. Sato N, Kubo K, Yamada M, Hori N, Suzuki T, Maeda H, Ogawa T. Osteoblast mechanoresponses on Ti with different surface topographies. *J Dent Res* 2009;88:812-6.
55. Mendonca DB, Miguez PA, Mendonca G, Yamauchi M, Aragao FJ, Cooper LF. Titanium surface topography affects collagen biosynthesis of adherent cells. *Bone* 2011;49:463-472.
56. Lossdorfer S, Schwartz Z, Wang L, Lohmann CH, Turner JD, Wieland M, Cochran DL, Boyan BD. Microrough implant surface topographies increase osteogenesis by reducing osteoclast formation and activity. *J Biomed Mater Res A* 2004;70:361-9.
57. Galli C, Guizzardi S, Passeri G, Martini D, Tinti A, Mauro G, Macaluso GM. Comparison of human mandibular osteoblasts grown on two commercially available titanium implant surfaces. *J Periodontol* 2005;76:364-72.
58. Olivares-Navarrete R, Hyzy S, Wieland M, Boyan BD, Schwartz Z. The roles of Wnt signaling modulators Dickkopf-1 (Dkk1) and Dickkopf-2 (Dkk2) and cell maturation state in osteogenesis on microstructured titanium surfaces. *Biomaterials* ;31:2015-24.
59. Rausch-fan X, Qu Z, Wieland M, Matejka M, Schedle A. Differentiation and cytokine synthesis of human alveolar osteoblasts compared to osteoblast-like cells (MG63) in response to titanium surfaces. *Dent Mater* 2008;24:102-10.
60. Schwartz Z, Olivares-Navarrete R, Wieland M, Cochran DL, Boyan BD. Mechanisms regulating increased production of osteoprotegerin by osteoblasts cultured on microstructured titanium surfaces. *Biomaterials* 2009;30:3390-3396.
61. Masuda T, Salvi GE, Offenbacher S, Felton DA, Cooper LF. Cell and matrix reactions at titanium implants in surgically prepared rat tibiae. *Int J Oral Maxillofac Implants* 1997;12:472-485.
62. Park JY, Davies JE. Red blood cell and platelet interactions with titanium implant surfaces. *Clin Oral Implants Res* 2000;11:530-539.
63. Park JY, Gemmell CH, Davies JE. Platelet interactions with titanium: modulation of platelet activity by surface topography. *Biomaterials* 2001;22:2671-2682.
64. Kikuchi L, Park JY, Victor C, Davies JE. Platelet interactions with calcium-phosphate-coated surfaces. *Biomaterials* 2005;26:5285-5295.
65. Thor A, Rasmusson L, Wennerberg A, Thomsen P, Hirsch JM, Nilsson B, Hong J. The role of whole blood in thrombin generation in contact with various titanium surfaces. *Biomaterials* 2007;28:966-974.
66. Hong J, Kurt S, Thor A. A Hydrophilic Dental Implant Surface Exhibit Thrombogenic Properties In Vitro. *Clin Implant Dent Relat Res* 2011.
67. Rosengren A, Bjursten LM, Danielsen N, Persson H, Kober M. Tissue reactions to polyethylene implants with different surface topography. *J Mater Sci Mater Med* 1999;10:75-82.
68. Soskolne WA, Cohen S, Sennerby L, Wennerberg A, Shapira L. The effect of titanium surface roughness on the adhesion of monocytes and their secretion of TNF-alpha and PGE2. *Clin Oral Implants Res* 2002;13:86-93.
69. Takebe J, Champagne CM, Offenbacher S, Ishibashi K, Cooper LF. Titanium surface topography alters cell shape and modulates bone morphogenetic protein 2 expression in the J774A.1 macrophage cell line. *J Biomed Mater Res A* 2003;64:207-16.

70. Refai AK, Textor M, Brunette DM, Waterfield JD. Effect of titanium surface topography on macrophage activation and secretion of proinflammatory cytokines and chemokines. *J Biomed Mater Res A* 2004;70:194-205.
71. Tan KS, Qian L, Rosado R, Flood PM, Cooper LF. The role of titanium surface topography on J774A.1 macrophage inflammatory cytokines and nitric oxide production. *Biomaterials* 2006;27:5170-7.
72. Oya K, Tanaka Y, Moriyama Y, Yoshioka Y, Kimura T, Tsutsumi Y, Doi H, Nomura N, Noda K, Kishida A, Hanawa T. Differences in the bone differentiation properties of MC3T3-E1 cells on polished bulk and sputter-deposited titanium specimens. *J Biomed Mater Res A* ;94:611-8.
73. Findlay DM, Welldon K, Atkins GJ, Howie DW, Zannettino AC, Bobyn D. The proliferation and phenotypic expression of human osteoblasts on tantalum metal. *Biomaterials* 2004;25:2215-27.
74. Hata K, Ikebe K, Wada M, Nokubi T. Osteoblast response to titanium regulates transcriptional activity of Runx2 through MAPK pathway. *J Biomed Mater Res A* 2007;81:446-52.
75. Kapanen A, Kinnunen A, Ryhanen J, Tuukkanen J. TGF-beta1 secretion of ROS-17/2.8 cultures on NiTi implant material. *Biomaterials* 2002;23:3341-6.
76. Kudelska-Mazur D, Lewandowska-Szumiel M, Mazur M, Komender J. Osteogenic cell contact with biomaterials influences phenotype expression. *Cell and Tissue Banking* 2005;6:55-64.
77. Lincks J, Boyan BD, Blanchard CR, Lohmann CH, Liu Y, Cochran DL, Dean DD, Schwartz Z. Response of MG63 osteoblast-like cells to titanium and titanium alloy is dependent on surface roughness and composition. *Biomaterials* 1998;19:2219-32.
78. Oum'hamed Z, Garnotel R, Josset Y, Trenteseaux C, Laurent-Maquin D. Matrix metalloproteinases MMP-2, -9 and tissue inhibitors TIMP-1, -2 expression and secretion by primary human osteoblast cells in response to titanium, zirconia, and alumina ceramics. *J Biomed Mater Res A* 2004;68:114-22.
79. Palmieri A, Pezzetti F, Avantaggiato A, Lo Muzio L, Scarano A, Rubini C, Guerzoni L, Arlotti M, Ventrone D, Carinci F. Titanium acts on osteoblast translational process. *J Oral Implantol* 2008;34:190-5.
80. Schmidt C, Ignatius AA, Claes LE. Proliferation and differentiation parameters of human osteoblasts on titanium and steel surfaces. *J Biomed Mater Res* 2001;54:209-15.
81. Lee YH, Lee NH, Bhattarai G, Oh YT, Yu MK, Yoo ID, Jhee EC, Yi HK. Enhancement of osteoblast biocompatibility on titanium surface with Terrein treatment. *Cell Biochem Funct* 2010;28:678-685.
82. Yang F, Zhao SF, Zhang F, He FM, Yang GL. Simvastatin-loaded porous implant surfaces stimulate preosteoblasts differentiation: an in vitro study. *Oral Surg Oral Med Oral Pathol Oral Radiol Endod* .
83. Khadra M, Lyngstadaas SP, Haanaes HR, Mustafa K. Effect of laser therapy on attachment, proliferation and differentiation of human osteoblast-like cells cultured on titanium implant material. *Biomaterials* 2005;26:3503-9.
84. Ozawa S, Kasugai S. Evaluation of implant materials (hydroxyapatite, glass-ceramics, titanium) in rat bone marrow stromal cell culture. *Biomaterials* 1996;17:23-9.
85. Stiehler M, Lind M, Mygind T, Baatrup A, Dolatshahi-Pirouz A, Li H, Foss M, Besenbacher F, Kassem M, Bunger C. Morphology, proliferation, and osteogenic differentiation of mesenchymal stem cells cultured on titanium, tantalum, and chromium surfaces. *J Biomed Mater Res A* 2008;86:448-58.
86. Zreiqat H, Howlett CR. Titanium substrata composition influences osteoblastic phenotype: In vitro study. *J Biomed Mater Res* 1999;47:360-6.

87. Matsuura T, Tsubaki S, Tsuzuki T, Duarte WR, Yamauchi M, Sato H. Differential gene expression of collagen-binding small leucine-rich proteoglycans and lysyl hydroxylases, during mineralization by MC3T3-E1 cells cultured on titanium implant material. *European journal of oral sciences* 2005;113:225-231.
88. Breithaupt-Faloppa AC, de Lima WT, Oliveira-Filho RM, Kleinheinz J. In vitro behaviour of endothelial cells on a titanium surface. *Head Face Med* 2008;4:14.
89. Beloti MM, Bellesini LS, Rosa AL. The effect of purmorphamine on osteoblast phenotype expression of human bone marrow mesenchymal cells cultured on titanium. *Biomaterials* 2005;26:4245-8.
90. Hayes JS, Khan IM, Archer CW, Richards RG. The role of surface microtopography in the modulation of osteoblast differentiation. *Eur Cell Mater* ;20:98-108.
91. Kodama T, Goto T, Ishibe T, Kobayashi S, Takahashi T. Apolipoprotein E stimulates bone formation on titanium in vitro. *Asian Journal of Oral and Maxillofacial Surgery* 2007;19:96-100.
92. Davies JT, Lam J, Tomlins PE, Marshall D. An in vitro multi-parametric approach to measuring the effect of implant surface characteristics on cell behaviour. *Biomedical Materials* ;5 (1) , 2010:ate of Pubaton: 2010.
93. Michiardi A, Engel E, Aparicio C, Planell JA, Gil FJ. Oxidized NiTi surfaces enhance differentiation of osteoblast-like cells. *J Biomed Mater Res A* 2008;85:108-14.
94. Yuan Q, Liao D, Yang X, Li X, Wei N, Tan Z, Gong P. Effect of implant surface microtopography on proliferation, neurotrophin secretion, and gene expression of Schwann cells. *J Biomed Mater Res A* ;93:381-8.
95. Kim CS, Sohn SH, Jeon SK, Kim KN, Ryu JJ, Kim MK. Effect of various implant coatings on biological responses in MG63 using cDNA microarray. *J Oral Rehabil* 2006;33:368-79.
96. Kim HW, Kim HE, Salih V, Knowles JC. Sol-gel-modified titanium with hydroxyapatite thin films and effect on osteoblast-like cell responses. *J Biomed Mater Res A* 2005;74:294-305.
97. Kim HW, Knowles JC, Salih V, Kim HE. Hydroxyapatite and fluor-hydroxyapatite layered film on titanium processed by a sol-gel route for hard-tissue implants. *J Biomed Mater Res B Appl Biomater* 2004;71:66-76.
98. Lee KW, Bae CM, Jung JY, Sim GB, Rautray TR, Lee HJ, Kwon TY, Kim KH. Surface characteristics and biological studies of hydroxyapatite coating by a new method. *J Biomed Mater Res B Appl Biomater* 2011;98B:395-407.
99. Sohn S, Lee JB, Kim K, Kim IK, Lee SH, Kim HW, Seo S, Kim Y, Shin S, Ryu J, Kim M. Gene expression of osteosarcoma cells on various coated titanium materials. *Molecular & Cellular Toxicology* 2007;3:36-45.
100. Berube P, Yang Y, Carnes DL, Stover RE, Boland EJ, Ong JL. The effect of sputtered calcium phosphate coatings of different crystallinity on osteoblast differentiation. *J Periodontol* 2005;76:1697-709.
101. Hashimoto Y, Kawashima M, Hatanaka R, Kusunoki M, Nishikawa H, Hontsu S, Nakamura M. Cytocompatibility of calcium phosphate coatings deposited by an ArF pulsed laser. *J Mater Sci Mater Med* 2007;18:1457-64.
102. Sandrini E, Morris C, Chiesa R, Cigada A, Santin M. In vitro assessment of the osteointegrative potential of a novel multiphase anodic spark deposition coating for orthopaedic and dental implants. *J Biomed Mater Res B Appl Biomater* 2005;73:392-9.
103. Siebers MC, Walboomers XF, Leeuwenburgh SC, Wolke JG, Jansen JA. Electrostatic spray deposition (ESD) of calcium phosphate coatings, an in vitro study with osteoblast-like cells. *Biomaterials* 2004;25:2019-27.
104. Siebers MC, Walboomers XF, van den Dolder J, Leeuwenburgh SC, Wolke JG, Jansen JA. The behavior of osteoblast-like cells on various substrates with functional blocking of integrin-beta1 and integrin-beta3. *J Mater Sci Mater Med* 2008;19:861-8.

105. Inoue M, Rodriguez AP, Takagi T, Katase N, Kubota M, Nagai N, Nagatsuka H, Nagaoka N, Takagi S, Suzuki K. Effect of a new titanium coating material (CaTiO₃-aC) prepared by thermal decomposition method on osteoblastic cell response. *J Biomater Appl* ;24:657-72.
106. Knabe C, Berger G, Gildenhaar R, Klar F, Zreiqat H. The modulation of osteogenesis in vitro by calcium titanium phosphate coatings. *Biomaterials* 2004;25:4911-9.
107. Knabe C, Howlett CR, Klar F, Zreiqat H. The effect of different titanium and hydroxyapatite-coated dental implant surfaces on phenotypic expression of human bone-derived cells. *J Biomed Mater Res A* 2004;71:98-107.
108. Lee J, Seo SH, Kim Y, Shin S, Kim M, Ryu J. Effect of titanium coating on cell adhesion and extracellular matrix formation in human osteoblast-like MG-63 cells. *Molecular & Cellular Toxicology* 2008;4:192-198.
109. Takebe J, Ito S, Champagne CM, Cooper LF, Ishibashi K. Anodic oxidation and hydrothermal treatment of commercially pure titanium surfaces increases expression of bone morphogenetic protein-2 in the adherent macrophage cell line J774A.1. *J Biomed Mater Res A* 2007;80:711-8.
110. Yan Y, Wolke JG, De Ruijter A, Yubao L, Jansen JA. Growth behavior of rat bone marrow cells on RF magnetron sputtered hydroxyapatite and dicalcium pyrophosphate coatings. *J Biomed Mater Res A* 2006;78:42-9.
111. Mamalis A, Silvestros S. Modified Titanium Surfaces Alter Osteogenic Differentiation; a Comparative Microarray-Based Analysis of Human Mesenchymal Cell Response to Commercial Titanium Surfaces. *J Oral Implantol* 2011.
112. Murakami A, Arimoto T, Suzuki D, Iwai-Yoshida M, Otsuka F, Shibata Y, Igarashi T, Kamijo R, Miyazaki T. Antimicrobial and osteogenic properties of a hydrophilic-modified nanoscale hydroxyapatite coating on Titanium. *Nanomedicine* 2011.
113. de Ruijter JE, ter Brugge PJ, Dieudonne SC, van Vliet SJ, Torensma R, Jansen JA. Analysis of integrin expression in U2OS cells cultured on various calcium phosphate ceramic substrates. *Tissue Eng* 2001;7:279-89.
114. Fu Q, Hong Y, Liu X, Fan H, Zhang X. A hierarchically graded bioactive scaffold bonded to titanium substrates for attachment to bone. *Biomaterials* 2011;32:7333-7346.
115. Yang F, Wen-Jing-Dong, He FM, DE XX, Zhao SF, Yang GL. Osteoblast response to porous titanium surfaces coated with zinc-substituted hydroxyapatite. *Oral Surg Oral Med Oral Pathol Oral Radiol Endod* 2011.
116. Harle J, Kim HW, Mordan N, Knowles JC, Salih V. Initial responses of human osteoblasts to sol-gel modified titanium with hydroxyapatite and titania composition. *Acta Biomater* 2006;2:547-56.
117. Hamlet S, Ivanovski S. Inflammatory cytokine response to titanium chemical composition and nanoscale calcium phosphate surface modification. *Acta Biomater* 2011;7:2345-2353.
118. Goransson A, Arvidsson A, Currie F, Franke-Stenport V, Kjellin P, Mustafa K, Sul YT, Wennerberg A. An in vitro comparison of possibly bioactive titanium implant surfaces. *J Biomed Mater Res A* 2009;88:1037-47.
119. Bodhak S, Bose S, Bandyopadhyay A. Electrically polarized HAp-coated Ti: in vitro bone cell-material interactions. *Acta Biomater* ;6:641-51.
120. Baldi D, Longobardi M, Cartiglia C, La Maestra S, Pulliero A, Bonica P, Micale RT, Menini M, Pera P, Izzotti A. Dental Implants Osteogenic Properties Evaluated by cDNA Microarrays. *Implant Dent* 2011;20:299-305.
121. Du C, Schneider GB, Zaharias R, Abbott C, Seabold D, Stanford C, Moradian-Oldak J. Apatite/amelogenin coating on titanium promotes osteogenic gene expression. *J Dent Res* 2005;84:1070-4.

122. Makihira S, Mine Y, Kosaka E, Nikawa H. Titanium surface roughness accelerates RANKL-dependent differentiation in the osteoclast precursor cell line, RAW264.7. *Dent Mater J* 2007;26:739-45.
123. Ong JL, Carnes DL, Cardenas HL, Cavin R. Surface roughness of titanium on bone morphogenetic protein-2 treated osteoblast cells in vitro. *Implant Dent* 1997;6:19-24.
124. Sista S, Wen C, Hodgson PD, Pande G. The influence of surface energy of titanium-zirconium alloy on osteoblast cell functions in vitro. *J Biomed Mater Res A* 2011.
125. Sima LE, Stan GE, Morosanu CO, Melinescu A, Ianculescu A, Melinte R, Neamtu J, Petrescu SM. Differentiation of mesenchymal stem cells onto highly adherent radio frequency-sputtered carbonated hydroxylapatite thin films. *J Biomed Mater Res A* 2010;95:1203-1214.
126. Jayaraman M, Meyer U, Buhner M, Joos U, Wiesmann HP. Influence of titanium surfaces on attachment of osteoblast-like cells in vitro. *Biomaterials* 2004;25:625-31.
127. Kim SY, Oh N, Lee MH, Kim SE, Leesungbok R, Lee SW. Surface microgrooves and acid etching on titanium substrata alter various cell behaviors of cultured human gingival fibroblasts. *Clin Oral Implants Res* 2009;20:262-72.
128. Lee SW, Kim SY, Rhyu IC, Chung WY, Leesungbok R, Lee KW. Influence of microgroove dimension on cell behavior of human gingival fibroblasts cultured on titanium substrata. *Clin Oral Implants Res* 2009;20:56-66.
129. Frosch KH, Barvencik F, Viereck V, Lohmann CH, Dresing K, Breme J, Brunner E, Sturmer KM. Growth behavior, matrix production, and gene expression of human osteoblasts in defined cylindrical titanium channels. *J Biomed Mater Res A* 2004;68:325-34.
130. Rosa AL, Crippa GE, de Oliveira PT, M. T, Jr, Lefebvre LP, Beloti MM. Human alveolar bone cell proliferation, expression of osteoblastic phenotype, and matrix mineralization on porous titanium produced by powder metallurgy. *Clin Oral Implants Res* 2009;20:472-81.
131. Att W, Kubo K, Yamada M, Maeda H, Ogawa T. Biomechanical properties of jaw periosteum-derived mineralized culture on different titanium topography. *Int J Oral Maxillofac Implants* 2009;24:831-41.
132. Att W, Tsukimura N, Suzuki T, Ogawa T. Effect of supramicron roughness characteristics produced by 1- and 2-step acid etching on the osseointegration capability of titanium. *Int J Oral Maxillofac Implants* 2007;22:719-28.
133. Att W, Yamada M, Ogawa T. Effect of titanium surface characteristics on the behavior and function of oral fibroblasts. *Int J Oral Maxillofac Implants* 2009;24:419-31.
134. Batzer R, Liu Y, Cochran DL, Szmuckler-Moncler S, Dean DD, Boyan BD, Schwartz Z. Prostaglandins mediate the effects of titanium surface roughness on MG63 osteoblast-like cells and alter cell responsiveness to 1 alpha,25-(OH)2D3. *J Biomed Mater Res* 1998;41:489-96.
135. Kubies D, Himmlova L, Riedel T, Chanova E, Balik K, Douderova M, Bartova J, Pesakova V. The interaction of osteoblasts with bone-implant materials: 1. The effect of physicochemical surface properties of implant materials. *Physiol Res* 2011;60:95-111.
136. Zhao G, Zinger O, Schwartz Z, Wieland M, Landolt D, Boyan BD. Osteoblast-like cells are sensitive to submicron-scale surface structure. *Clin Oral Implants Res* 2006;17:258-64.
137. Naganawa T, Ishihara Y, Iwata T, Koide M, Ohguchi M, Ohguchi Y, Murase Y, Kamei H, Sato N, Mizuno M, Noguchi T. In vitro biocompatibility of a new titanium-29niobium-13tantalum-4.6zirconium alloy with osteoblast-like MG63 cells. *Journal of periodontology* 2004;75:1701-1707.
138. Nakamura HK, Butz F, Saruwatari L, Ogawa T. A role for proteoglycans in mineralized tissue-titanium adhesion. *J Dent Res* 2007;86:147-52.

139. Kawahara H, Soeda Y, Niwa K, Takahashi M, Kawahara D, Araki N. In vitro study on bone formation and surface topography from the standpoint of biomechanics. *J Mater Sci Mater Med* 2004;15:1297-307.
140. Kieswetter K, Schwartz Z, Hummert TW, Cochran DL, Simpson J, Dean DD, Boyan BD. Surface roughness modulates the local production of growth factors and cytokines by osteoblast-like MG-63 cells. *J Biomed Mater Res* 1996;32:55-63.
141. An N, Schedle A, Wieland M, Andrukhov O, Matejka M, Rausch-Fan X. Proliferation, behavior, and cytokine gene expression of human umbilical vascular endothelial cells in response to different titanium surfaces. *J Biomed Mater Res A* ;93:364-72.
142. Kammerer PW, Gabriel M, Al-Nawas B, Scholz T, Kirchmaier CM, Klein MO. Early implant healing: promotion of platelet activation and cytokine release by topographical, chemical and biomimetical titanium surface modifications in vitro. *Clin Oral Implants Res* 2011.
143. Qu Z, Rausch-Fan X, Wieland M, Matejka M, Schedle A. The initial attachment and subsequent behavior regulation of osteoblasts by dental implant surface modification. *J Biomed Mater Res A* 2007;82:658-68.
144. Zhang Y, Andrukhov O, Berner S, Matejka M, Wieland M, Rausch-Fan X, Schedle A. Osteogenic properties of hydrophilic and hydrophobic titanium surfaces evaluated with osteoblast-like cells (MG63) in coculture with human umbilical vein endothelial cells (HUVEC). *Dent Mater* 2010;26:1043-1051.
145. Boyan BD, Batzer R, Kieswetter K, Liu Y, Cochran DL, Szmuckler-Moncler S, Dean DD, Schwartz Z. Titanium surface roughness alters responsiveness of MG63 osteoblast-like cells to 1 alpha,25-(OH)2D3. *J Biomed Mater Res* 1998;39:77-85.
146. Morra M, Cassinelli C, Cascardo G, Bollati D, Baena RR. Gene expression of markers of osteogenic differentiation of human mesenchymal cells on collagen I-modified microrough titanium surfaces. *J Biomed Mater Res A* 2011;96:449-455.
147. Hendrich C, Noth U, Stahl U, Merklein F, Rader CP, Schutze N, Thull R, Tuan RS, Eulert J. Testing of skeletal implant surfaces with human fetal osteoblasts. *Clin Orthop Relat Res* 2002;278-89.
148. Arpornmaeklong P, Akarawatcharangura B, Pripatnanont P. Factors influencing effects of specific COX-2 inhibitor NSAIDs on growth and differentiation of mouse osteoblasts on titanium surfaces. *Int J Oral Maxillofac Implants* 2008;23:1071-1081.
149. Kubo K, Att W, Yamada M, Ohmi K, Tsukimura N, Suzuki T, Maeda H, Ogawa T. Microtopography of titanium suppresses osteoblastic differentiation but enhances chondroblastic differentiation of rat femoral periosteum-derived cells. *J Biomed Mater Res A* 2008;87:380-91.
150. Silva TS, Machado DC, Viezzer C, Silva Junior AN, Oliveira MG. Effect of titanium surface roughness on human bone marrow cell proliferation and differentiation: an experimental study. *Acta Cir Bras* 2009;24:200-5.
151. Hori N, Iwasa F, Ueno T, Takeuchi K, Tsukimura N, Yamada M, Hattori M, Yamamoto A, Ogawa T. Selective cell affinity of biomimetic micro-nano-hybrid structured TiO₂ overcomes the biological dilemma of osteoblasts. *Dent Mater* ;26:275-87.
152. Maekawa K, Yoshida Y, Mine A, van Meerbeek B, Suzuki K, Kuboki T. Effect of polyphosphoric acid pre-treatment of titanium on attachment, proliferation, and differentiation of osteoblast-like cells (MC3T3-E1). *Clin Oral Implants Res* 2008;19:320-5.
153. Sugita Y, Ishizaki K, Iwasa F, Ueno T, Minamikawa H, Yamada M, Suzuki T, Ogawa T. Effects of pico-nanometer-thin TiO₂ coating on the biological properties of microroughened titanium. *Biomaterials* 2011.
154. Bigi A, Bracci B, Cuisinier F, Elkaim R, Fini M, Mayer I, Mihailescu IN, Socol G, Sturba L, Torricelli P. Human osteoblast response to pulsed laser deposited calcium phosphate coatings. *Biomaterials* 2005;26:2381-9.

155. Protivinsky J, Appleford M, Strnad J, Helebrant A, Ong JL. Effect of chemically modified titanium surfaces on protein adsorption and osteoblast precursor cell behavior. *Int J Oral Maxillofac Implants* 2007;22:542-50.
156. Ramires PA, Cosentino F, Milella E, Torricelli P, Giavaresi G, Giardino R. In vitro response of primary rat osteoblasts to titania/hydroxyapatite coatings compared with transformed human osteoblast-like cells. *Journal of Materials Science: Materials in Medicine* 2002;13:797-801.
157. Ramires PA, Romito A, Cosentino F, Milella E. The influence of titania/hydroxyapatite composite coatings on in vitro osteoblasts behaviour. *Biomaterials* 2001;22:1467-74.
158. Aita H, Att W, Ueno T, Yamada M, Hori N, Iwasa F, Tsukimura N, Ogawa T. Ultraviolet light-mediated photofunctionalization of titanium to promote human mesenchymal stem cell migration, attachment, proliferation and differentiation. *Acta Biomater* 2009;5:3247-57.
159. Aita H, Hori N, Takeuchi M, Suzuki T, Yamada M, Anpo M, Ogawa T. The effect of ultraviolet functionalization of titanium on integration with bone. *Biomaterials* 2009;30:1015-25.
160. Hori N, Ueno T, Suzuki T, Yamada M, Att W, Okada S, Ohno A, Aita H, Kimoto K, Ogawa T. Ultraviolet light treatment for the restoration of age-related degradation of titanium bioactivity. *Int J Oral Maxillofac Implants* ;25:49-62.
161. Xue W, Krishna BV, Bandyopadhyay A, Bose S. Processing and biocompatibility evaluation of laser processed porous titanium. *Acta Biomater* 2007;3:1007-18.
162. Postiglione L, Di Domenico G, Ramaglia L, di Lauro AE, Di Meglio F, Montagnani S. Different titanium surfaces modulate the bone phenotype of SaOS-2 osteoblast-like cells. *Eur J Histochem* 2004;48:213-22.
163. Postiglione L, Di Domenico G, Ramaglia L, Montagnani S, Salzano S, Di Meglio F, Sbordone L, Vitale M, Rossi G. Behavior of SaOS-2 cells cultured on different titanium surfaces. *J Dent Res* 2003;82:692-6.
164. Cooper LF, Zhou Y, Takebe J, Guo J, Abron A, Holmen A, Ellingsen JE. Fluoride modification effects on osteoblast behavior and bone formation at TiO₂ grit-blasted c.p. titanium endosseous implants. *Biomaterials* 2006;27:926-36.
165. Goransson A, Gretzer C, Johansson A, Sul YT, Wennerberg A. Inflammatory response to a titanium surface with potential bioactive properties: an in vitro study. *Clin Implant Dent Relat Res* 2006;8:210-7.
166. Valencia S, Gretzer C, Cooper LF. Surface nanofeature effects on titanium-adherent human mesenchymal stem cells. *Int J Oral Maxillofac Implants* 2009;24:38-46.
167. Guida L, Annunziata M, Rocci A, Contaldo M, Rullo R, Oliva A. Biological response of human bone marrow mesenchymal stem cells to fluoride-modified titanium surfaces. *Clin Oral Implants Res* .
168. Isa ZM, Schneider GB, Zaharias R, Seabold D, Stanford CM. Effects of fluoride-modified titanium surfaces on osteoblast proliferation and gene expression. *Int J Oral Maxillofac Implants* 2006;21:203-11.
169. Kim MJ, Choi MU, Kim CW. Activation of phospholipase D1 by surface roughness of titanium in MG63 osteoblast-like cell. *Biomaterials* 2006;27:5502-11.
170. Kim MJ, Kim CW, Lim YJ, Heo SJ. Microrough titanium surface affects biologic response in MG63 osteoblast-like cells. *J Biomed Mater Res A* 2006;79:1023-32.
171. Ko YJ, Zaharias RS, Seabold DA, Lafoon JE, Schneider GB. Analysis of the attachment and differentiation of three-dimensional rotary wall vessel cultured human preosteoblasts on dental implant surfaces. *Int J Oral Maxillofac Implants* ;25:722-8.
172. Ter Brugge PJ, Jansen JA. Initial interaction of rat bone marrow cells with non-coated and calcium phosphate coated titanium substrates. *Biomaterials* 2002;23:3269-3277.

173. ter Brugge PJ, Torensma R, De Ruijter JE, Figdor CG, Jansen JA. Modulation of integrin expression on rat bone marrow cells by substrates with different surface characteristics. *Tissue Eng* 2002;8:615-26.
174. ter Brugge PJ, Wolke JG, Jansen JA. Effect of calcium phosphate coating crystallinity and implant surface roughness on differentiation of rat bone marrow cells. *J Biomed Mater Res* 2002;60:70-8.
175. Mustafa K, Rubinstein J, Lopez BS, Arvidson K. Production of transforming growth factor beta1 and prostaglandin E2 by osteoblast-like cells cultured on titanium surfaces blasted with TiO₂ particles. *Clin Oral Implants Res* 2003;14:50-6.
176. Mustafa K, Wennerberg A, Wroblewski J, Hultenby K, Lopez BS, Arvidson K. Determining optimal surface roughness of TiO₂ blasted titanium implant material for attachment, proliferation and differentiation of cells derived from human mandibular alveolar bone. *Clin Oral Implants Res* 2001;12:515-25.
177. Choi CR, Yu HS, Kim CH, Lee JH, Oh CH, Kim HW, Lee HH. Bone cell responses of titanium blasted with bioactive glass particles. *J Biomater Appl* ;25:99-117.
178. Pugdee K, Shibata Y, Yamamichi N, Tsutsumi H, Yoshinari M, Abiko Y, Hayakawa T. Gene expression of MC3T3-E1 cells on fibronectin-immobilized titanium using tresyl chloride activation technique. *Dent Mater J* 2007;26:647-55.
179. Yang Y, Tian J, Deng L, Ong JL. Morphological behavior of osteoblast-like cells on surface-modified titanium in vitro. *Biomaterials* 2002;23:1383-9.
180. Park JW, Kim YJ, Park CH, Lee DH, Ko YG, Jang JH, Lee CS. Enhanced osteoblast response to an equal channel angular pressing-processed pure titanium substrate with microrough surface topography. *Acta Biomater* 2009;5:3272-80.
181. Ball M, Grant DM, Lo W, Scotchford CA. The effect of different surface morphology and roughness on osteoblast-like cells. *Journal of Biomedical Materials Research* 2008;86A:637-647.
182. Ma Q, Mei S, Ji K, Zhang Y, Chu PK. Immobilization of Ag nanoparticles/FGF-2 on a modified titanium implant surface and improved human gingival fibroblasts behavior. *J Biomed Mater Res A* 2011;98:274-286.
183. Baschong W, Jaquier C, Martin I, Lambrecht TJ. Surface-induced modulation of human mesenchymal progenitor cells. An in vitro model for early implant integration. *Schweiz Monatsschr Zahnmed* 2007;117:906-10.
184. Harle J, Salih V, Olsen I, Brett P, Jones F, Tonetti M. Gene expression profiling of bone cells on smooth and rough titanium surfaces. *J Mater Sci Mater Med* 2004;15:1255-8.
185. He F, Zhang F, Yang G, Wang X, Zhao S. Enhanced initial proliferation and differentiation of MC3T3-E1 cells on HF/HNO₃ solution treated nanostructural titanium surface. *Oral Surg Oral Med Oral Pathol Oral Radiol Endod* ;110:e13-22.
186. Ramaglia L, Capece G, di Spigna G, Esposito D, Postiglione L. In vitro expression of osteoblastic phenotype on titanium surfaces. *Minerva Stomatol* ;59:259-66, 267-70.
187. Ramaglia L, Postiglione L, Di Spigna G, Capece G, Salzano S, Rossi G. Sandblasted-acid-etched titanium surface influences in vitro the biological behavior of SaOS-2 human osteoblast-like cells. *Dent Mater J* 2011;30:183-192.
188. Raz P, Lohmann CH, Turner J, Wang L, Poythress N, Blanchard C, Boyan BD, Schwartz Z. 1alpha,25(OH)₂D₃ regulation of integrin expression is substrate dependent. *J Biomed Mater Res A* 2004;71:217-25.
189. Shapira L, Halabi A. Behavior of two osteoblast-like cell lines cultured on machined or rough titanium surfaces. *Clin Oral Implants Res* 2009;20:50-5.

190. Galli C, Macaluso GM, Elezi E, Ravanetti F, Cacchioli A, Gualini G, Passeri G. The Effects of Er:YAG Laser Treatment on Titanium Surface Profile and Osteoblastic Cell Activity: An In Vitro Study. *J Periodontol* 2011;82:1169-1177.
191. Galli C, Passeri G, Ravanetti F, Elezi E, Pedrazzoni M, Macaluso GM. Rough surface topography enhances the activation of Wnt/beta-catenin signaling in mesenchymal cells. *J Biomed Mater Res A* ;95:682-90.
192. Keselowsky BG, Wang L, Schwartz Z, Garcia AJ, Boyan BD. Integrin alpha(5) controls osteoblastic proliferation and differentiation responses to titanium substrates presenting different roughness characteristics in a roughness independent manner. *J Biomed Mater Res A* 2007;80:700-10.
193. Lohmann CH, Bonewald LF, Sisk MA, Sylvia VL, Cochran DL, Dean DD, Boyan BD, Schwartz Z. Maturation state determines the response of osteogenic cells to surface roughness and 1,25-dihydroxyvitamin D3. *J Bone Miner Res* 2000;15:1169-80.
194. Lohmann CH, Tandy EM, Sylvia VL, Hell-Vocke AK, Cochran DL, Dean DD, Boyan BD, Schwartz Z. Response of normal female human osteoblasts (NHOst) to 17beta-estradiol is modulated by implant surface morphology. *J Biomed Mater Res* 2002;62:204-13.
195. Sisk MA, Lohmann CH, Cochran DL, Sylvia VL, Simpson JP, Dean DD, Boyan BD, Schwartz Z. Inhibition of cyclooxygenase by indomethacin modulates osteoblast response to titanium surface roughness in a time-dependent manner. *Clin Oral Implants Res* 2001;12:52-61.
196. Wang L, Zhao G, Olivares-Navarrete R, Bell BF, Wieland M, Cochran DL, Schwartz Z, Boyan BD. Integrin beta1 silencing in osteoblasts alters substrate-dependent responses to 1,25-dihydroxy vitamin D3. *Biomaterials* 2006;27:3716-25.
197. Martin JY, Dean DD, Cochran DL, Simpson J, Boyan BD, Schwartz Z. Proliferation, differentiation, and protein synthesis of human osteoblast-like cells (MG63) cultured on previously used titanium surfaces. *Clin Oral Implants Res* 1996;7:27-37.
198. Brett PM, Harle J, Salih V, Mihoc R, Olsen I, Jones FH, Tonetti M. Roughness response genes in osteoblasts. *Bone* 2004;35:124-33.
199. Passeri G, Cacchioli A, Ravanetti F, Galli C, Elezi E, Macaluso GM. Adhesion pattern and growth of primary human osteoblastic cells on five commercially available titanium surfaces. *Clin Oral Implants Res* ;21:756-65.
200. Miron RJ, Oates CJ, Molenberg A, Dard M, Hamilton DW. The effect of enamel matrix proteins on the spreading, proliferation and differentiation of osteoblasts cultured on titanium surfaces. *Biomaterials* ;31:449-60.
201. Bannister SR, Lohmann CH, Liu Y, Sylvia VL, Cochran DL, Dean DD, Boyan BD, Schwartz Z. Shear force modulates osteoblast response to surface roughness. *J Biomed Mater Res* 2002;60:167-74.
202. Fang M, Olivares-Navarrete R, Wieland M, Cochran DL, Boyan BD, Schwartz Z. The role of phospholipase D in osteoblast response to titanium surface microstructure. *J Biomed Mater Res A* ;93:897-909.
203. Lennon FE, Hermann CD, Olivares-Navarrete R, Rhee WJ, Schwartz Z, Bao G, Boyan BD. Use of molecular beacons to image effects of titanium surface microstructure on beta1 integrin expression in live osteoblast-like cells. *Biomaterials* ;31:7640-7.
204. Oates TW, Maller SC, West J, Steffensen B. Human gingival fibroblast integrin subunit expression on titanium implant surfaces. *J Periodontol* 2005;76:1743-50.
205. Olivares-Navarrete R, Hyzy SL, Chaudhri RA, Zhao G, Boyan BD, Schwartz Z. Sex dependent regulation of osteoblast response to implant surface properties by systemic hormones. *Biol Sex Differ* 2010;1:4.

206. Qu Z, Andrukhov O, Laky M, Ulm C, Matejka M, Dard M, Rausch-Fan X. Effect of enamel matrix derivative on proliferation and differentiation of osteoblast cells grown on the titanium implant surface. *Oral Surg Oral Med Oral Pathol Oral Radiol Endod* 2011;111:517-522.
207. Schwartz Z, Denison TA, Bannister SR, Cochran DL, Liu YH, Lohmann CH, Wieland M, Boyan BD. Osteoblast response to fluid induced shear depends on substrate microarchitecture and varies with time. *Journal of Biomedical Materials Research - Part A* 2007;83:20-32.
208. Schwartz Z, Lohmann CH, Sisk M, Cochran DL, Sylvia VL, Simpson J, Dean DD, Boyan BD. Local factor production by MG63 osteoblast-like cells in response to surface roughness and 1,25-(OH)₂D₃ is mediated via protein kinase C- and protein kinase A-dependent pathways. *Biomaterials* 2001;22:731-41.
209. Schwartz Z, Lohmann CH, Vocke AK, Sylvia VL, Cochran DL, Dean DD, Boyan BD. Osteoblast response to titanium surface roughness and 1 α ,25-(OH)₂D₃ is mediated through the mitogen-activated protein kinase (MAPK) pathway. *J Biomed Mater Res* 2001;56:417-26.
210. Wang CY, Zhao BH, Ai HJ, Wang YW. Comparison of biological characteristics of mesenchymal stem cells grown on two different titanium implant surfaces. *Biomed Mater* 2008;3:015004.
211. Klein MO, Bijelic A, Toyoshima T, Gotz H, von Koppenfels RL, Al-Nawas B, Duschner H. Long-term response of osteogenic cells on micron and submicron-scale-structured hydrophilic titanium surfaces: sequence of cell proliferation and cell differentiation. *Clin Oral Implants Res* ;21:642-9.
212. Klein MO, Bijelic A, Ziebart T, Koch F, Kammerer PW, Wieland M, Konerding MA, Al-Nawas B. Submicron Scale-Structured Hydrophilic Titanium Surfaces Promote Early Osteogenic Gene Response for Cell Adhesion and Cell Differentiation. *Clin Implant Dent Relat Res* 2011.
213. Kou PM, Schwartz Z, Boyan BD, Babensee JE. Dendritic cell responses to surface properties of clinical titanium surfaces. *Acta Biomater* 2011;7:1354-1363.
214. Lai HC, Zhuang LF, Liu X, Wieland M, Zhang ZY. The influence of surface energy on early adherent events of osteoblast on titanium substrates. *J Biomed Mater Res A* ;93:289-96.
215. Olivares-Navarrete R, Hyzy SL, Hutton DL, Dunn GR, Appert C, Boyan BD, Schwartz Z. Role of non-canonical Wnt signaling in osteoblast maturation on microstructured titanium surfaces. *Acta Biomater* 2011;7:2740-2750.
216. Olivares-Navarrete R, Hyzy SL, Hutton DL, Erdman CP, Wieland M, Boyan BD, Schwartz Z. Direct and indirect effects of microstructured titanium substrates on the induction of mesenchymal stem cell differentiation towards the osteoblast lineage. *Biomaterials* ;31:2728-35.
217. Olivares-Navarrete R, Hyzy SL, Park JH, Dunn GR, Haithcock DA, Wasilewski CE, Boyan BD, Schwartz Z. Mediation of osteogenic differentiation of human mesenchymal stem cells on titanium surfaces by a Wnt-integrin feedback loop. *Biomaterials* 2011;32:6399-6411.
218. Raines AL, Olivares-Navarrete R, Wieland M, Cochran DL, Schwartz Z, Boyan BD. Regulation of angiogenesis during osseointegration by titanium surface microstructure and energy. *Biomaterials* ;31:4909-17.
219. Togashi AY, Cirano FR, Marques MM, Pustiglioni FE, Lang NP, Lima LA. Effect of recombinant human bone morphogenetic protein-7 (rhBMP-7) on the viability, proliferation and differentiation of osteoblast-like cells cultured on a chemically modified titanium surface. *Clin Oral Implants Res* 2009;20:452-7.
220. Vlacic-Zischke J, Hamlet SM, Friis T, Tonetti M, Ivanovski S. The influence of surface microroughness and hydrophilicity of titanium on the up-regulation of TGFbeta/BMP signalling in osteoblasts. *Biomaterials* .
221. Zhao G, Schwartz Z, Wieland M, Rupp F, Geis-Gerstorfer J, Cochran DL, Boyan BD. High surface energy enhances cell response to titanium substrate microstructure. *J Biomed Mater Res A* 2005;74:49-58.

222. Boyan BD, Schwartz Z, Lohmann CH, Sylvia VL, Cochran DL, Dean DD, Puzas JE. Pretreatment of bone with osteoclasts affects phenotypic expression of osteoblast-like cells. *J Orthop Res* 2003;21:638-47.
223. Bell BF, Schuler M, Tosatti S, Textor M, Schwartz Z, Boyan BD. Osteoblast response to titanium surfaces functionalized with extracellular matrix peptide biomimetics. *Clin Oral Implants Res* 2011;22:865-872.
224. Tosatti S, Schwartz Z, Campbell C, Cochran DL, VandeVondele S, Hubbell JA, Denzer A, Simpson J, Wieland M, Lohmann CH, Textor M, Boyan BD. RGD-containing peptide GCRGYGRGDSPG reduces enhancement of osteoblast differentiation by poly(L-lysine)-graft-poly(ethylene glycol)-coated titanium surfaces. *J Biomed Mater Res A* 2004;68:458-72.
225. Kohal RJ, Baechle M, Han JS, Hueren D, Huebner U, Butz F. In vitro reaction of human osteoblasts on alumina-toughened zirconia. *Clin Oral Implants Res* 2009;20:1265-71.
226. Shi GS, Ren LF, Wang LZ, Lin HS, Wang SB, Tong YQ. H₂O₂/HCl and heat-treated Ti-6Al-4V stimulates pre-osteoblast proliferation and differentiation. *Oral Surg Oral Med Oral Pathol Oral Radiol Endod* 2009;108:368-75.
227. Zhang F, Yang GL, He FM, Zhang LJ, Zhao SF. Cell response of titanium implant with a roughened surface containing titanium hydride: an in vitro study. *J Oral Maxillofac Surg* ;68:1131-9.
228. Yang XF, Chen Y, Yang F, He FM, Zhao SF. Enhanced initial adhesion of osteoblast-like cells on an anatase-structured titania surface formed by H₂O₂/HCl solution and heat treatment. *Dent Mater* 2009;25:473-80.
229. De Santis D, Guerriero C, Nocini PF, Ungersbock A, Richards G, Gotte P, Armato U. Adult human bone cells from jaw bones cultured on plasma-sprayed or polished surfaces of titanium or hydroxylapatite discs. *Journal of Materials Science: Materials in Medicine* 1996;7:21-28.
230. Carinci F, Pezzetti F, Volinia S, Francioso F, Arcelli D, Marchesini J, Scapoli L, Piattelli A. Analysis of osteoblast-like MG63 cells' response to a rough implant surface by means of DNA microarray. *J Oral Implantol* 2003;29:215-20.
231. Borsari V, Giavaresi G, Fini M, Torricelli P, Salito A, Chiesa R, Chiusoli L, Volpert A, Rimondini L, Giardino R. Physical characterization of different-roughness titanium surfaces, with and without hydroxyapatite coating, and their effect on human osteoblast-like cells. *J Biomed Mater Res B Appl Biomater* 2005;75:359-68.
232. Palmieri A, Brunelli G, Guerzoni L, Lo Muzio L, Scarano A, Rubini C, Scapoli L, Martinelli M, Pezzetti F, Carinci F. Comparison between titanium and anatase miRNAs regulation. *Nanomedicine* 2007;3:138-43.
233. Palmieri A, Pezzetti F, Brunelli G, Arlotti M, Lo Muzio L, Scarano A, Rubini C, Sollazzo V, Massari L, Carinci F. Anatase nanosurface regulates microRNAs. *J Craniofac Surg* 2008;19:328-33.
234. Isaac J, Galtayries A, Kizuki T, Kokubo T, Berda A, Sautier JM. Bioengineered titanium surfaces affect the gene-expression and phenotypic response of osteoprogenitor cells derived from mouse calvarial bones. *Eur Cell Mater* ;20:178-96.
235. Nebe JB, Muller L, Luthen F, Ewald A, Bergemann C, Conforto E, Muller FA. Osteoblast response to biomimetically altered titanium surfaces. *Acta Biomater* 2008;4:1985-95.
236. Nishio K, Neo M, Akiyama H, Nishiguchi S, Kim HM, Kokubo T, Nakamura T. The effect of alkali- and heat-treated titanium and apatite-formed titanium on osteoblastic differentiation of bone marrow cells. *J Biomed Mater Res* 2000;52:652-61.
237. Cai K, Lai M, Yang W, Hu R, Xin R, Liu Q, Sung KL. Surface engineering of titanium with potassium hydroxide and its effects on the growth behavior of mesenchymal stem cells. *Acta Biomater* ;6:2314-21.

238. Brama M, Rhodes N, Hunt J, Ricci A, Teghil R, Migliaccio S, Rocca CD, Leccisotti S, Lioi A, Scandurra M, De Maria G, Ferro D, Pu F, Panzini G, Politi L, Scandurra R. Effect of titanium carbide coating on the osseointegration response in vitro and in vivo. *Biomaterials* 2007;28:595-608.
239. Franco Rde L, Chiesa R, Beloti MM, de Oliveira PT, Rosa AL. Human osteoblastic cell response to a Ca- and P-enriched titanium surface obtained by anodization. *J Biomed Mater Res A* 2009;88:841-8.
240. Brammer KS, Choi C, Frandsen CJ, Oh S, Johnston G, Jin S. Comparative cell behavior on carbon-coated TiO₂ nanotube surfaces for osteoblasts vs. osteo-progenitor cells. *Acta Biomater* 2011;7:2697-2703.
241. Akintoye SO, Giavis P, Stefanik D, Levin L, Mante FK. Comparative osteogenesis of maxilla and iliac crest human bone marrow stromal cells attached to oxidized titanium: a pilot study. *Clin Oral Implants Res* 2008;19:1197-201.
242. Gittens RA, McLachlan T, Olivares-Navarrete R, Cai Y, Berner S, Tannenbaum R, Schwartz Z, Sandhage KH, Boyan BD. The effects of combined micron-/submicron-scale surface roughness and nanoscale features on cell proliferation and differentiation. *Biomaterials* 2011;32:3395-3403.
243. Durual S, Pernet F, Rieder P, Mekki M, Cattani-Lorente M, Wiskott HW. Titanium nitride oxide coating on rough titanium stimulates the proliferation of human primary osteoblasts. *Clin Oral Implants Res* 2011;22:552-559.
244. Das K, Bose S, Bandyopadhyay A. TiO₂ nanotubes on Ti: Influence of nanoscale morphology on bone cell-materials interaction. *J Biomed Mater Res A* 2009;90:225-37.
245. Das K, Bose S, Bandyopadhyay A. Surface modifications and cell-materials interactions with anodized Ti. *Acta Biomater* 2007;3:573-85.
246. Park J, Bauer S, Schlegel KA, Neukam FW, von der Mark K, Schmuki P. TiO₂ nanotube surfaces: 15 nm-- an optimal length scale of surface topography for cell adhesion and differentiation. *Small* 2009;5:666-71.
247. Kim Y, Jang JH, Ku Y, Koak JY, Chang IT, Kim HE, Lee JB, Heo SJ. Microarray-based expression analysis of human osteoblast-like cell response to anodized titanium surface. *Biotechnol Lett* 2004;26:399-402.
248. Zhao L, Mei S, Wang W, Chu PK, Wu Z, Zhang Y. The role of sterilization in the cytocompatibility of titania nanotubes. *Biomaterials* ;31:2055-63.
249. Zhao L, Mei S, Wang W, Chu PK, Zhang Y, Wu Z. Suppressed primary osteoblast functions on nanoporous titania surface. *J Biomed Mater Res A* 2011;96:100-107.
250. Setzer B, Bachle M, Metzger MC, Kohal RJ. The gene-expression and phenotypic response of hFOB 1.19 osteoblasts to surface-modified titanium and zirconia. *Biomaterials* 2009;30:979-90.
251. Lai M, Cai K, Zhao L, Chen X, Hou Y, Yang Z. Surface functionalization of TiO₂ nanotubes with bone morphogenetic protein 2 and its synergistic effect on the differentiation of mesenchymal stem cells. *Biomacromolecules* 2011;12:1097-1105.
252. Annunziata M, Oliva A, Buosciolo A, Giordano M, Guida A, Guida L. Bone marrow mesenchymal stem cell response to nano-structured oxidized and turned titanium surfaces. *Clin Oral Implants Res* 2011.
253. Kim JH, Cho KP, Chung YS, Kim OS, Chung SS, Lee KK, Lee DJ, Lee KM, Kim YJ. The effect of nanotubular titanium surfaces on osteoblast differentiation. *J Nanosci Nanotechnol* ;10:3581-5.
254. Omar OM, Graneli C, Ekstrom K, Karlsson C, Johansson A, Lausmaa J, Wexell CL, Thomsen P. The stimulation of an osteogenic response by classical monocyte activation. *Biomaterials* 2011.
255. Sohn SH, Jun HK, Kim CS, Kim KN, Chung SM, Shin SW, Ryu JJ, Kim MK. Biological responses in osteoblast-like cell line according to thin layer hydroxyapatite coatings on anodized titanium. *J Oral Rehabil* 2006;33:898-911.

256. Dieudonne SC, van den Dolder J, de Ruijter JE, Paldan H, Peltola T, van 't Hof MA, Happonen RP, Jansen JA. Osteoblast differentiation of bone marrow stromal cells cultured on silica gel and sol-gel-derived titania. *Biomaterials* 2002;23:3041-51.
257. Tsukimura N, Kojima N, Kubo K, Att W, Takeuchi K, Kameyama Y, Maeda H, Ogawa T. The effect of superficial chemistry of titanium on osteoblastic function. *J Biomed Mater Res A* 2008;84:108-16.
258. Viornery C, Guenther HL, Aronsson BO, Pechy P, Descouts P, Gratzel M. Osteoblast culture on polished titanium disks modified with phosphonic acids. *J Biomed Mater Res* 2002;62:149-55.
259. Chen L, Sun J, Zhu Z, Wu K, Li W, Liu H, Xu S. The adhesion and proliferation of bone marrow-derived mesenchymal stem cells promoted by nanoparticle surface. *J Biomater Appl* 2011.
260. De Angelis E, Ravanetti F, Cacchioli A, Corradi A, Giordano C, Candiani G, Chiesa R, Gabbi C, Borghetti P. Attachment, proliferation and osteogenic response of osteoblast-like cells cultured on titanium treated by a novel multiphase anodic spark deposition process. *J Biomed Mater Res B Appl Biomater* 2009;88:280-9.
261. Nayab SN, Jones FH, Olsen I. Effects of calcium ion-implantation of titanium on bone cell function in vitro. *J Biomed Mater Res A* 2007;83:296-302.
262. Park JW, Kim YJ, Jang JH. Enhanced osteoblast response to hydrophilic strontium and/or phosphate ions-incorporated titanium oxide surfaces. *Clin Oral Implants Res* ;21:398-408.
263. Park JW, Kim YJ, Jang JH, Kwon TG, Bae YC, Suh JY. Effects of phosphoric acid treatment of titanium surfaces on surface properties, osteoblast response and removal of torque forces. *Acta Biomater* ;6:1661-70.
264. Park JW, Kim YJ, Jang JH, Song H. Osteoblast response to magnesium ion-incorporated nanoporous titanium oxide surfaces. *Clin Oral Implants Res* .
265. Park JW, Suh JY, Chung HJ. Effects of calcium ion incorporation on osteoblast gene expression in MC3T3-E1 cells cultured on microstructured titanium surfaces. *J Biomed Mater Res A* 2008;86:117-26.
266. Kawai H, Shibata Y, Miyazaki T. Glow discharge plasma pretreatment enhances osteoclast differentiation and survival on titanium plates. *Biomaterials* 2004;25:1805-11.
267. De Giglio E, Cometa S, Ricci MA, Zizzi A, Cafagna D, Manzotti S, Sabbatini L, Mattioli-Belmonte M. Development and characterization of rhVEGF-loaded poly(HEMA-MOEP) coatings electrosynthesized on titanium to enhance bone mineralization and angiogenesis. *Acta Biomater* ;6:282-90.
268. Boyan BD, Lincks J, Lohmann CH, Sylvia VL, Cochran DL, Blanchard CR, Dean DD, Schwartz Z. Effect of surface roughness and composition on costochondral chondrocytes is dependent on cell maturation state. *J Orthop Res* 1999;17:446-57.
269. McNamara LE, Sjostrom T, Burgess KE, Kim JJ, Liu E, Gordonov S, Moghe PV, Meek RM, Oreffo RO, Su B, Dalby MJ. Skeletal stem cell physiology on functionally distinct titania nanotopographies. *Biomaterials* 2011;32:7403-7410.
270. Linez-Bataillon P, Monchau F, Bigerelle M, Hildebrand HF. In vitro MC3T3 osteoblast adhesion with respect to surface roughness of Ti6Al4V substrates. *Biomol Eng* 2002;19:133-41.
271. Schneider GB, Perinpanayagam H, Clegg M, Zaharias R, Seabold D, Keller J, Stanford C. Implant surface roughness affects osteoblast gene expression. *J Dent Res* 2003;82:372-6.
272. Schneider GB, Zaharias R, Seabold D, Keller J, Stanford C. Differentiation of preosteoblasts is affected by implant surface microtopographies. *J Biomed Mater Res A* 2004;69:462-8.
273. Sinha RK, Tuan RS. Regulation of human osteoblast integrin expression by orthopedic implant materials. *Bone* 1996;18:451-7.

274. Ahmad M, McCarthy M, Gronowicz G. An in vitro model for mineralization of human osteoblast-like cells on implant materials. *Biomaterials* 1999;20:211-220.
275. Borghetti P, De Angelis E, Caldara G, Corradi A, Cacchioli A, Gabbi C. Adaptive response of osteoblasts grown on a titanium surface: Morphology, cell proliferation and stress protein synthesis. *Veterinary research communications* 2005;29:ate of Pubaton: Aug 2005.
276. Fini M, Nicoli Aldini N, Torricelli P, Giavaresi G, Borsari V, Lenger H, Bernauer J, Giardino R, Chiesa R, Cigada A. A new austenitic stainless steel with negligible nickel content: an in vitro and in vivo comparative investigation. *Biomaterials* 2003;24:4929-39.
277. Jager M, Urselmann F, Witte F, Zanger K, Li X, Ayers DC, Krauspe R. Osteoblast differentiation onto different biometals with an endoprosthetic surface topography in vitro. *J Biomed Mater Res A* 2008;86:61-75.
278. Jakobsen SS, Larsen A, Stoltenberg M, Bruun JM, Soballe K. Effects of as-cast and wrought Cobalt-Chrome-Molybdenum and Titanium-Aluminium-Vanadium alloys on cytokine gene expression and protein secretion in J774A.1 macrophages. *Eur Cell Mater* 2007;14:45-54; discussion 54-5.
279. Zhang H, Ahmad M, Gronowicz G. Effects of transforming growth factor-beta 1 (TGF-beta1) on in vitro mineralization of human osteoblasts on implant materials. *Biomaterials* 2003;24:2013-20.
280. Tognarini I, Sorace S, Zonefrati R, Galli G, Gozzini A, Carbonell Sala S, Thyron GD, Carossino AM, Tanini A, Mavilia C, Azzari C, Sbaiz F, Facchini A, Capanna R, Brandi ML. In vitro differentiation of human mesenchymal stem cells on Ti6Al4V surfaces. *Biomaterials* 2008;29:809-24.
281. Torricelli P, Fini M, Borsari V, Lenger H, Bernauer J, Tschon M, Bonazzi V, Giardino R. Biomaterials in orthopedic surgery: effects of a nickel-reduced stainless steel on in vitro proliferation and activation of human osteoblasts. *Int J Artif Organs* 2003;26:952-7.
282. Kim KJ, Itoh T, Kotake S. Effects of recombinant human bone morphogenetic protein-2 on human bone marrow cells cultured with various biomaterials. *J Biomed Mater Res* 1997;35:279-85.
283. Anselme K, Bigerelle M, Loison I, Noel B, Hardouin P. Kinetic study of the expression of beta-catenin, actin and vinculin during osteoblastic adhesion on grooved titanium substrates. *Biomed Mater Eng* 2004;14:545-56.
284. Pallu S, Fricain JC, Bareille R, Bourget C, Dard M, Sewing A, Amedee J. Cyclo-DfKRG peptide modulates in vitro and in vivo behavior of human osteoprogenitor cells on titanium alloys. *Acta Biomater* 2009;5:3581-92.
285. Richard D, Dumelie N, Benhayoune H, Bouthors S, Guillaume C, Lalun N, Balossier G, Laurent-Maquin D. Behavior of human osteoblast-like cells in contact with electrodeposited calcium phosphate coatings. *Journal of Biomedical Materials Research* 2006;79B:108-115.
286. Bhadang KA, Holding CA, Thissen H, McLean KM, Forsythe JS, Haynes DR. Biological responses of human osteoblasts and osteoclasts to flame-sprayed coatings of hydroxyapatite and fluorapatite blends. *Acta Biomater* ;6:1575-83.
287. Gomes PS, Botelho C, Lopes MA, Santos JD, Fernandes MH. Evaluation of human osteoblastic cell response to plasma-sprayed silicon-substituted hydroxyapatite coatings over titanium substrates. *J Biomed Mater Res B Appl Biomater* ;94:337-46.
288. Bigi A, Nicoli-Aldini N, Bracci B, Zavan B, Boanini E, Sbaiz F, Panzavolta S, Zorzato G, Giardino R, Facchini A, Abatangelo G, Cortivo R. In vitro culture of mesenchymal cells onto nanocrystalline hydroxyapatite-coated Ti13Nb13Zr alloy. *J Biomed Mater Res A* 2007;82:213-21.

289. Kokkinos PA, Zarkadis IK, Panidis TT, Deligianni DD. Estimation of hydrodynamic shear stresses developed on human osteoblasts cultured on Ti-6Al-4V and strained by four point bending. Effects of mechanical loading to specific gene expression. *J Mater Sci Mater Med* 2009;20:655-65.
290. Kokkinos PA, Zarkadis IK, Kletsas D, Deligianni DD. Effects of physiological mechanical strains on the release of growth factors and the expression of differentiation marker genes in human osteoblasts growing on Ti-6Al-4V. *J Biomed Mater Res A* 2009;90:387-95.
291. Puleo DA, Preston KE, Shaffer JB, Bizios R. Examination of osteoblast-orthopaedic biomaterial interactions using molecular techniques. *Biomaterials* 1993;14:111-4.
292. Di Palma F, Chamson A, Lafage-Proust MH, Jouffray P, Sabido O, Peyroche S, Vico L, Rattner A. Physiological strains remodel extracellular matrix and cell-cell adhesion in osteoblastic cells cultured on alumina-coated titanium alloy. *Biomaterials* 2004;25:2565-75.
293. Di Palma F, Guignandon A, Chamson A, Lafage-Proust MH, Laroche N, Peyroche S, Vico L, Rattner A. Modulation of the responses of human osteoblast-like cells to physiologic mechanical strains by biomaterial surfaces. *Biomaterials* 2005;26:4249-57.
294. Mangano C, De Rosa A, Desiderio V, d'Aquino R, Piattelli A, De Francesco F, Tirino V, Mangano F, Papaccio G. The osteoblastic differentiation of dental pulp stem cells and bone formation on different titanium surface textures. *Biomaterials* ;31:3543-51.
295. Balloni S, Calvi EM, Damiani F, Bistoni G, Calvitti M, Locci P, Becchetti E, Marinucci L. Effects of titanium surface roughness on mesenchymal stem cell commitment and differentiation signaling. *Int J Oral Maxillofac Implants* 2009;24:627-35.
296. Mengatto CM, Mussano F, Honda Y, Colwell CS, Nishimura I. Circadian rhythm and cartilage extracellular matrix genes in osseointegration: a genome-wide screening of implant failure by vitamin D deficiency. *PLoS One* 2011;6:e15848.
297. Marco A, Adriana O, Maria Assunta B, Michele G, Nello M, Antonietta R, Alessandro L, Luigi G. The effects of titanium nitride-coating on the topographic and biological features of TPS implant surfaces. *J Dent* 2011.
298. Kim HJ, Kim SH, Kim MS, Lee EJ, Oh HG, Oh WM, Park SW, Kim WJ, Lee GJ, Choi NG, Koh JT, Dinh DB, Hardin RR, Johnson K, Sylvia VL, Schmitz JP, Dean DD. Varying Ti-6Al-4V surface roughness induces different early morphologic and molecular responses in MG63 osteoblast-like cells. *J Biomed Mater Res A* 2005;74:366-73.
299. Krause A, Cowles EA, Gronowicz G. Integrin-mediated signaling in osteoblasts on titanium implant materials. *J Biomed Mater Res* 2000;52:738-47.
300. Schwartz Z, Raz P, Zhao G, Barak Y, Tauber M, Yao H, Boyan BD. Effect of micrometer-scale roughness of the surface of Ti6Al4V pedicle screws in vitro and in vivo. *J Bone Joint Surg Am* 2008;90:2485-98.
301. Zhang H, Aronow MS, Gronowicz GA. Transforming growth factor-beta 1 (TGF-beta1) prevents the age-dependent decrease in bone formation in human osteoblast/implant cultures. *J Biomed Mater Res A* 2005;75:98-105.
302. Zhang H, Lewis CG, Aronow MS, Gronowicz GA. The effects of patient age on human osteoblasts' response to Ti-6Al-4V implants in vitro. *J Orthop Res* 2004;22:30-8.
303. Marinucci L, Balloni S, Becchetti E, Belcastro S, Guerra M, Calvitti M, Lilli C, Calvi EM, Locci P. Effect of titanium surface roughness on human osteoblast proliferation and gene expression in vitro. *Int J Oral Maxillofac Implants* 2006;21:719-25.

304. Carinci F, Volinia S, Pezzetti F, Francioso F, Tosi L, Piattelli A. Titanium-cell interaction: analysis of gene expression profiling. *J Biomed Mater Res B Appl Biomater* 2003;66:341-6.
305. Gronowicz G, McCarthy MB. Response of human osteoblasts to implant materials: integrin-mediated adhesion. *J Orthop Res* 1996;14:878-87.
306. Lim YW, Kwon SY, Sun DH, Kim HE, Kim YS. Enhanced cell integration to titanium alloy by surface treatment with microarc oxidation: a pilot study. *Clin Orthop Relat Res* 2009;467:2251-8.
307. Annunziata M, Guida L, Perillo L, Aversa R, Passaro I, Oliva A. Biological response of human bone marrow stromal cells to sandblasted titanium nitride-coated implant surfaces. *J Mater Sci Mater Med* 2008;19:3585-91.
308. Arcelli D, Palmieri A, Pezzetti F, Brunelli G, Zollino I, Carinci F. Genetic effects of a titanium surface on osteoblasts: a meta-analysis. *J Oral Sci* 2007;49:299-309.
309. Shah AK, Lazatin J, Sinha RK, Lennox T, Hickok NJ, Tuan RS. Mechanism of BMP-2 stimulated adhesion of osteoblastic cells to titanium alloy. *Biol Cell* 1999;91:131-42.
310. Klinger A, Tadir A, Halabi A, Shapira L. The effect of surface processing of titanium implants on the behavior of human osteoblast-like Saos-2 cells. *Clin Implant Dent Relat Res* 2011;13:64-70.
311. Yang F, Xie Y, Li H, Tang T, Zhang X, Gan Y, Zheng X, Dai K. Human bone marrow-derived stromal cells cultured with a plasma sprayed CaO-ZrO₂-SiO₂ coating. *Journal of Biomedical Materials Research* ;95B:192-201.
312. Ince A, Schutze N, Hendrich C, Thull R, Eulert J, Lohr JF. In Vitro Investigation of Orthopedic Titanium-Coated and Brushite-Coated Surfaces Using Human Osteoblasts in the Presence of Gentamycin. *Journal of Arthroplasty* 2008;23:762-771.
313. Ji W, Han P, Zhao C, Jiang Y, Zhang X. Increased osteoblast adhesion on nanophase Ti6Al4V. *Chinese Science Bulletin* 2008;53:1757-1762.
314. Han P, Ji WP, Zhao CL, Zhang XN, Jiang Y. Improved osteoblast proliferation, differentiation and mineralization on nanophase Ti6Al4V. *Chin Med J (Engl)* 2011;124:273-279.
315. Campoccia D, Arciola CR, Cervellati M, Maltarello MC, Montanaro L. In vitro behaviour of bone marrow-derived mesenchymal cells cultured on fluorohydroxyapatite-coated substrata with different roughness. *Biomaterials* 2003;24:587-96.
316. Carinci F, Pezzetti F, Volinia S, Francioso F, Arcelli D, Marchesini J, Caramelli E, Piattelli A. Analysis of MG63 osteoblastic-cell response to a new nanoporous implant surface by means of a microarray technology. *Clin Oral Implants Res* 2004;15:180-6.
317. Ponader S, Vairaktaris E, Heintz P, Wilmowsky CV, Rottmair A, Korner C, Singer RF, Holst S, Schlegel KA, Neukam FW, Nkenke E. Effects of topographical surface modifications of electron beam melted Ti-6Al-4V titanium on human fetal osteoblasts. *J Biomed Mater Res A* 2008;84:1111-9.
318. Huang Z, Daniels RH, Enzerink RJ, Hardev V, Sahi V, Goodman SB. Effect of nanofiber-coated surfaces on the proliferation and differentiation of osteoprogenitors in vitro. *Tissue Eng Part A* 2008;14:1853-9.
319. Saldana L, Vilaboa N, Valles G, Gonzalez-Cabrero J, Munuera L. Osteoblast response to thermally oxidized Ti6Al4V alloy. *J Biomed Mater Res A* 2005;73:97-107.
320. Ku CH, Browne M, Gregson PJ, Corbeil J, Pioletti DP. Large-scale gene expression analysis of osteoblasts cultured on three different Ti-6Al-4V surface treatments. *Biomaterials* 2002;23:4193-202.
321. Ku CH, Pioletti DP, Browne M, Gregson PJ. Effect of different Ti-6Al-4V surface treatments on osteoblasts behaviour. *Biomaterials* 2002;23:1447-54.

322. Foppiano S, Marshall SJ, Marshall GW, Saiz E, Tomsia AP. Bioactive glass coatings affect the behavior of osteoblast-like cells. *Acta Biomater* 2007;3:765-71.
323. Trentani L, Pelillo F, Pavesi FC, Ceciliani L, Cetta G, Forlino A. Evaluation of the TiMo12Zr6Fe2 alloy for orthopaedic implants: in vitro biocompatibility study by using primary human fibroblasts and osteoblasts. *Biomaterials* 2002;23:2863-9.
324. Zhao L, Wei Y, Li J, Han Y, Ye R, Zhang Y. Initial osteoblast functions on Ti-5Zr-3Sn-5Mo-15Nb titanium alloy surfaces modified by microarc oxidation. *J Biomed Mater Res A* ;92:432-40.
325. Bombonato-Prado KF, Bellesini LS, Junta CM, Marques MM, Passos GA, Rosa AL. Microarray-based gene expression analysis of human osteoblasts in response to different biomaterials. *J Biomed Mater Res A* 2009;88:401-8.
326. Palmieri A, Pezzetti F, Brunelli G, Zollino I, Lo Muzio L, Martinelli M, Scapoli L, Arlotti M, Masiero E, Carinci F. Zirconium oxide regulates RNA interfering of osteoblast-like cells. *J Mater Sci Mater Med* 2008;19:2471-6.
327. Palmieri A, Pezzetti F, Brunelli G, Lo Muzio L, Scarano A, Scapoli L, Martinelli M, Arlotti M, Guerzoni L, Rubini C, Carinci F. Short-period effects of zirconia and titanium on osteoblast microRNAs. *Clin Implant Dent Relat Res* 2008;10:200-5.
328. Pae A, Lee H, Kim HS, Kwon YD, Woo YH. Attachment and growth behaviour of human gingival fibroblasts on titanium and zirconia ceramic surfaces. *Biomed Mater* 2009;4:025005.
329. Carinci F, Pezzetti F, Volinia S, Francioso F, Arcelli D, Farina E, Piattelli A. Zirconium oxide: analysis of MG63 osteoblast-like cell response by means of a microarray technology. *Biomaterials* 2004;25:215-28.
330. Att W, Takeuchi M, Suzuki T, Kubo K, Anpo M, Ogawa T. Enhanced osteoblast function on ultraviolet light-treated zirconia. *Biomaterials* 2009;30:1273-1280.
331. Ko HC, Han JS, Bachle M, Jang JH, Shin SW, Kim DJ. Initial osteoblast-like cell response to pure titanium and zirconia/alumina ceramics. *Dent Mater* 2007;23:1349-55.
332. Zreiqat H, Howlett CR, Zannettino A, Evans P, Schulze-Tanzil G, Knabe C, Shakibaei M. Mechanisms of magnesium-stimulated adhesion of osteoblastic cells to commonly used orthopaedic implants. *J Biomed Mater Res* 2002;62:175-84.
333. Mozumder MS, Zhu J, Perinpanayagam H. TiO₂ -enriched polymeric powder coatings support human mesenchymal cell spreading and osteogenic differentiation. *Biomed Mater* 2011;6:035009.
334. Ramaswamy Y, Wu C, Zhou H, Zreiqat H. Biological response of human bone cells to zinc-modified Ca-Si-based ceramics. *Acta Biomater* 2008;4:1487-97.
335. Ramaswamy Y, Wu C, Dunstan CR, Hewson B, Eindorf T, Anderson GI, Zreiqat H. Sphene ceramics for orthopedic coating applications: an in vitro and in vivo study. *Acta Biomater* 2009;5:3192-204.
336. Layman DL, Ardoin RC. An in vitro system for studying osteointegration of dental implants utilizing cells grown on dense hydroxyapatite disks. *Canadian Association of Radiologists Journal* 1998;49:282-290.
337. Lin L, Chow KL, Leng Y. Study of hydroxyapatite osteoinductivity with an osteogenic differentiation of mesenchymal stem cells. *J Biomed Mater Res A* 2009;89:326-35.
338. Ong JL, Hoppe CA, Cardenas HL, Cavin R, Carnes DL, Sogal A, Raikar GN. Osteoblast precursor cell activity on HA surfaces of different treatments. *Journal of Biomedical Materials Research* 1998;39:176-183.
339. Wilke A, Orth J, Lomb M, Fuhrmann R, Kienapfel H, Griss P, Franke RP. Biocompatibility analysis of different biomaterials in human bone marrow cell cultures. *J Biomed Mater Res* 1998;40:301-6.

340. Rouahi M, Champion E, Hardouin P, Anselme K. Quantitative kinetic analysis of gene expression during human osteoblastic adhesion on orthopaedic materials. *Biomaterials* 2006;27:2829-44.
341. Holthaus MG, Stolle J, Treccani L, Rezwan K. Orientation of human osteoblasts on hydroxyapatite-based microchannels. *Acta Biomater* 2011.
342. Chou L, Firth JD, Uitto VJ, Brunette DM. Effects of titanium substratum and grooved surface topography on metalloproteinase-2 expression in human fibroblasts. *J Biomed Mater Res* 1998;39:437-45.
343. Chou L, Firth JD, Nathanson D, Uitto VJ, Brunette DM. Effects of titanium on transcriptional and post-transcriptional regulation of fibronectin in human fibroblasts. *J Biomed Mater Res* 1996;31:209-17.
344. Hambleton J, Schwartz Z, Khare A, Windeler SW, Luna M, Brooks BP, Dean DD, Boyan BD. Culture surfaces coated with various implant materials affect chondrocyte growth and metabolism. *J Orthop Res* 1994;12:542-52.
345. Lavenus S, Berreur M, Trichet V, Louarn G, Layrolle P. Adhesion and osteogenic differentiation of human mesenchymal stem cells on titanium nanopores. *Eur Cell Mater* 2011;22:84-96.
346. Ballo AM, Kokkari AK, Meretoja VV, Lassila LL, Vallittu PK, Narhi TO. Osteoblast proliferation and maturation on bioactive fiber-reinforced composite surface. *J Mater Sci Mater Med* 2008;19:3169-77.
347. Kaur G, Wang C, Sun J, Wang Q. The synergistic effects of multivalent ligand display and nanotopography on osteogenic differentiation of rat bone marrow stem cells. *Biomaterials* ;31:5813-24.
348. Angwarawong T, Dubas ST, Arksornnukit M, Pavasant P. Differentiation of MC3T3-E1 on poly(4-styrenesulfonic acid-co-maleic acid)sodium salt-coated films. *Dent Mater J* 2011;30:158-169.
349. Monsees TK, Barth K, Tippelt S, Heidel K, Gorbunov A, Pompe W, Funk RH. Effects of different titanium alloys and nanosize surface patterning on adhesion, differentiation, and orientation of osteoblast-like cells. *Cells Tissues Organs* 2005;180:81-95.
350. Fassina L, Visai L, Cusella De Angelis MG, Benazzo F, Magenes G. Physically enhanced coating of titanium plasma-spray with human osteoblasts and bone matrix. *Journal of Applied Biomaterials and Biomechanics* 2007;5:200.
351. Klinger A, Tadir A, Halabi A, Shapira L. The Effect of Surface Processing of Titanium Implants on the Behavior of Human Osteoblast-Like Saos-2 Cells. *Clin Implant Dent Relat Res* .
352. Arpornmaeklong P, Akarawatcharangura B, Pripatnanont P. Factors influencing effects of specific COX-2 inhibitor NSAIDs on growth and differentiation of mouse osteoblasts on titanium surfaces. *Int J Oral Maxillofac Implants* 2008;23:1071-81.
353. Dye K, Tanaka Y, Moriyama Y, Yoshioka Y, Kimura T, Tsutsumi Y, Doi H, Nomura N, Noda K, Kishida A, Hanawa T. Differences in the bone differentiation properties of MC3T3-E1 cells on polished bulk and sputter-deposited titanium specimens. *Journal of Biomedical Materials Research* ;94A:611-618.
354. Galli C, Passeri G, Ravanetti F, Elezi E, Pedrazzoni M, Macaluso GM. Rough surface topography enhances the activation of Wnt/beta-catenin signaling in mesenchymal cells. *J Biomed Mater Res A* 2010;95:682-690.
355. Rodriguez AP, Takagi T, Katase N, Kubota M, Nagai N, Nagatsuka H, Inoue M, Nagaoka N, Takagi S, Suzuki K. Effect of a new titanium coating material (CaTiO₃-aC) prepared by thermal decomposition method on osteoblastic cell response. *Journal of Biomaterials Applications* ;24:657-672.
356. Zhu L, Wang H, Xu J, Wei D, Zhao W, Wang X, Wu N. Effects of titanium implant surface coated with natural nacre on MC3T3E1 cell line in vitro. *Progress in Biochemistry and Biophysics* 2008;35:671-675.

357. Borsari V, Giavaresi G, Fini M, Torricelli P, Tschon M, Chiesa R, Chiusoli L, Salito A, Volpert A, Giardino R. Comparative in vitro study on a ultra-high roughness and dense titanium coating. *Biomaterials* 2005;26:4948-55.
358. Yang XY, Liu CH, Lei X, Su Y, Li WH, Wang HY, Xu WC, Xian SQ. Influence of surface modification of titanium on OPG/RANKL mRNA expression in MG-63 human osteoblast-like cells. *Nan Fang Yi Ke Da Xue Xue Bao* 2011;31:1353-1356.
359. Zhao G, Raines AL, Wieland M, Schwartz Z, Boyan BD. Requirement for both micron- and submicron scale structure for synergistic responses of osteoblasts to substrate surface energy and topography. *Biomaterials* 2007;28:2821-9.
360. Sagomonyants KB, Jarman-Smith ML, Devine JN, Aronow MS, Gronowicz GA. The in vitro response of human osteoblasts to polyetheretherketone (PEEK) substrates compared to commercially pure titanium. *Biomaterials* 2008;29:1563-72.
361. Saldana L, Gonzalez-Carrasco JL, Rodriguez M, Munuera L, Vilaboa N. Osteoblast response to plasma-spray porous Ti6Al4V coating on substrates of identical alloy. *J Biomed Mater Res A* 2006;77:608-17.
362. Verrier S, Peroglio M, Voisard C, Lechmann B, Alini M. The osteogenic differentiation of human osteoprogenitor cells on Anodic-Plasma-Chemical treated Ti6Al7Nb. *Biomaterials* .
363. Leven RM, Virdi AS, Sumner DR. Patterns of gene expression in rat bone marrow stromal cells cultured on titanium alloy discs of different roughness. *J Biomed Mater Res A* 2004;70:391-401.
364. Li Z, Kong Q, Wang Y. Effect of the chemical-vapor-deposited diamond film materials on expression of osteocalcin mRNA of osteoblast. *Journal of China Medical University* 2005;34:326-327.
365. Kubo K, Tsukimura N, Iwasa F, Ueno T, Saruwatari L, Aita H, Chiou WA, Ogawa T. Cellular behavior on TiO₂ nanonodular structures in a micro-to-nanoscale hierarchy model. *Biomaterials* 2009;30:5319-29.
366. Kodama T, Goto T, Miyazaki T, Takahashi T. Bone formation on apatite-coated titanium incorporated with bone morphogenetic protein and heparin. *Int J Oral Maxillofac Implants* 2008;23:1013-9.

Chapter 2

Molecular Assessment of Osseointegration *In Vivo*; A review of current literature

Abstract:

This paper reports on the results of a structured review of the literature concerning in vivo molecular assessment of osseointegrated endosseous dental implants. A search of electronic databases was performed up to and including August 2011. Thirty articles met the inclusion criteria. A descriptive evaluation and analysis of the gene expression data concerning the process of osseointegration were performed. Broad consensus was observed among the study results, perhaps as a result of the similar targeted gene expression events. More recent investigations using gene arrays or gene profiling techniques offer new insights into the fundamental molecular events that support the osseointegration process. Evidence for the influence of surface topography on osteogenesis and osteoinduction has been reported. Additional investigations are required to further solidify the functional associations between individual or orchestrated gene expression events and the clinical result of osseointegration.

Introduction:

Current tooth replacement strategies typically consider the alloplastic-integrated replacement of missing teeth using endosseous dental implants as a primary choice among available modes of therapy. Among the many reasons for selection of this mode of therapy include the often-cited reproducibility of the biologic integration of the endosseous implant. Such reproducibility in the clinical management of a biological response is accepted without question. Yet, important questions remain. Do current implant technologies address all current needs? Can clinicians explain experienced failures? Answers to such questions require careful understanding of the biologic process of osseointegration.

Osseointegration is defined as a direct structural and functional connection between ordered living bone and the surface of a load-carrying implant [1]. Essential elements of this definition include the implicit understanding that vital bone remains in apposition to the endosseous implant surface throughout its functional (loaded) lifetime. Implant success is often discussed in qualitative and quantitative terms of the amount of bone formed at the endosseous implant interface. The earliest identifiable influences on this feature of osseointegration were the qualitative and quantitative clinical perceptions of local bone prior to implant placement. [2] Early failures were attributed to clinical error leading to lack of primary stability or infection. Delayed failures were attributed to reduced bone volume (low bone to implant contact) attributable to diminished bone volume and quality. The role of systemic diseases or conditions on osseointegration further suggested that the healing potential of the local bone tissues affected bone formation at the endosseous implant.

The past decade has revealed an increasing interest in the improvement of osseointegration through modification of the endosseous dental implant surface. Implant surface topography, as recently reviewed by Wennerberg and Albrektsson [3] can be modified to alter the interfacial bone response. With the caveat that our definition of a 'rough surface' is limited, moderately rough ($S(a) > 1-2$ micron) surfaces show stronger bone responses (increased BIC, increased torque removal) than other surfaces. Another recent review of experimental surface alterations ranging from the application of structural peptides and proteins (e.g., collagen) to diverse growth factors and morphogens (e.g., BMPs) revealed more diverse positive and negative outcomes for these different approaches. New techniques to apply ultra thin CaP coatings (vapor deposition, sputter coating, ESD, biomimetic deposition) were observed to improve bone integration as compared to non-coated

titanium implants [4]. These recent reviews display a wide range of current activities that seek to improve the osseointegration result in attempts to address the increasing challenges clinicians address by placing implants in individuals with reduced bone volume, reduced bone density, and impaired wound healing (e.g., diabetes, osteoporosis, radiation therapy, chemotherapy).

Evaluation of the result of osseointegration is possible by simple clinical methods. Tactile approaches that include tapping and reverse torque estimations serve the majority of clinicians well in discerning successful versus failed osseointegration. While more controversial in its physical interpretation, quantifying stability using resonance frequency (ISQ) can reveal changes in implant integration over time that reflect the gain or loss of interfacial bone supporting the osseointegration result [5]. When the body of literature concerning bone-to-implant contact was reviewed at the histological level, a clear advantage for increased surface topography was revealed [6]. Human clinical investigations comparing different implant surfaces also suggest that modification of surface topography leads to alteration in the local bone responses leading to increased bone-to-implant contact [7-10]. There is sufficient data at multiple levels ranging from animal studies to direct human histology indicating that the process of osseointegration can be modulated to increase bone to implant contact. Precisely how this is achieved has not been clearly delineated. Without a complete understanding of the molecular and cellular process of osseointegration, therapeutically relevant targets for improving the result may be poorly defined.

The molecular basis of biology and of disease has been established as a principle determinant in managing human health. Only recently has the molecular basis of osseointegration been considered (Figure 1). The nature of tissue biology at, on or adjacent to the implant surface has not been carefully elucidated. However, recent activities have begun to highlight both the fundamental processes that contribute to interfacial bone formation and how different implant-surface parameters may influence these processes that eventually lead to bone formation at the alloplastic / tissue interface. Several laboratories demonstrated that it is possible to interrogate these molecular processes by retrieval of tissues and implanted endosseous devices from animal models (Figure 2). Early reports focused on demonstrating that gene expression events known to be evident in the process of bone formation were recapitulated at the forming bone to implant interface [11] and others demonstrated that the osteoinductive genes that promote stem cell differentiation to osteoprogenitor cells (namely RUNX-2 and Osterix) were expressed by implant-adherent cells in vivo and were elevated on surfaces

with topographies that enhanced bone to implant contact [12]. Most recently, wider evaluations of gene expression in tissues surrounding dental implants have indicated that other significant biologic processes may be involved in healing of the endosseous implant [13,14]. The aim of this review is to identify the model systems, molecular platforms and targeted gene expression events involved in existing phenotype at the level of protein-encoding mRNA expression. Anticipated (and repeatedly demonstrated in the literature) is the surface-dependent modulation of mRNA expression within the implant-surface adherent cells.

Materials and methods:

For the literature to be included in this review, the following eligibility criteria were used: in vivo reports assessing the molecular process of osseointegration, and articles published only in English. Studies related to wear particles, letters to the editor and reviews were excluded.

Search Strategy: A thorough search was performed up to and including August, 2011 through the following databases: PubMed (1948 to August, 2011), using the following terms: (titanium[tw] OR zirconium[tw] OR dental implant*[tw]) AND (gene expression[MeSH Terms] OR gene expression[tw] OR differentiation[tw] OR rna[MeSH Terms] OR rna[tw] OR messenger rna[tw] OR mrna[tw]), EMBASE via OVID (1947 to August,2011) using: (Titanium.mp. or zirconium.mp. or tooth implantation/ or dental implant*.mp. and gene expression.mp. or exp gene expression/ or exp DIFFERENTIATION/ or differentiation.mp. or ena.mp. or exp RNA/ or messenger rna.mp.[mp=title,abstract,subject headings,heading words, drug trade name, original title,device manufacturer, drug manufacturer] or mrna.mp.[mp=title,abstract,subject headings,heading words, drug trade name, original title,device manufacturer, drug manufacturer], and BIOSIS Previews via ISI Web of Science (1969 to August,2011), ISI Citation via ISI Web of Science (1955 to date) using the following words: Topic=((titanium OR zirconium OR "dental implant*") AND ("gene expression" OR differentiation OR rna OR rna OR "messenger rna" OR mrna)). Titles and abstracts were screened for possible inclusion in the review. The full text of the articles judged to be relevant by the title and abstract was read and independently evaluated against the eligibility criteria. In addition, a hand search of the reference lists of original studies that were found to be relevant was conducted.

Results:

Thirty articles met the inclusion criteria. Characteristics of the included in-vivo reports including model systems used, techniques used for molecular assessment of the osseointegration process, genes examined and wide gene expression profiling studies are presented in Table 1,2,3 and 4 respectively.

Different in vivo models are represented and include mouse, rat, mini-pig and rabbit animal models. Human studies have recently provided additional molecular data concerning the molecular processes surrounding osseointegration. These various studies all share similar major observations. The molecular processes of bone formation suggested by previous histological assessments and in vitro examinations of implant surface effects on osteoblast function are supported by these targeted assessments of osseointegration. Broad consensus is observed among these study results. One possible explanation for this consensus is that the early questions asked regarding the molecular process underscoring osseointegration have been directed about known aspects of bone formation and repair in general.

The spectrum of molecular events targeted in these studies is narrow. Osteoinduction represented by the expression or abundance of Runx-2 and Osterix, key transcriptional regulators of stem cell commitment to osteoblastogenesis, has been explored in many of these investigations. Osteogenesis reflected by the expression of collagen type I and bone-specific or enriched protein encoding mRNAs has also been observed. The increased expression of mRNAs including Collagen type I, osteopontin, osteonectin, bone sialoprotein, and decorin has been observed as a function of time as well as 'enhanced' surface topography in all of the reported studies. One general conclusion is that, irrespective of possible modulation of mRNA abundance temporally or quantitatively, osseointegration involves osteoinduction from progenitor cells and the subsequent elaboration of a bone matrix comprised of the basic components involved in bone repair.

Genome wide assessment of bone formation and repair conducted in vivo reveal a standard progression of cellular events indicated by gene expression [15]. Most investigations have focused on the impact of implant surface on the molecular process of osseointegration. Seventeen studies have specifically explored bone-specific gene expression as a function of implant surface and time. The general observation is that surface topography influences the pattern of gene expression for bone-related proteins (OPN, ON, BSP, COLI, ALP).

Perhaps more significantly, the impact of surface topography (and related chemistry) on osteoinduction has also been specifically addressed by measuring expression of *Osx* and *Runx2*.

Gene profiling studies ask a much broader question and can explore a wide range of possible biological processes including osteoinduction and osteogenesis. Only several gene profiling studies involving osseointegration have yet to be reported. For example, results from a human model reported on biological events surrounding osteogenesis, related angiogenesis and some interest on osteoclast recruitment and activity [13]. In a most recent report using targeted gene arrays, Bryington et al [14] explored gene expression events surrounding inflammation as related to early wound healing. Most interestingly, these reporting of these studies have focused on osteogenesis and related angiogenesis. The full value of >20,000 genes representing multiple processes remain underexplored.

Discussion:

Model systems: The selection of models for in vivo investigations involves understanding the value of desired endpoints and the applicability and translation to the human clinical situation. Much of the early research involving osseointegration was performed in extraoral sites that proved valuable in assessment of the extent of bone formation along the implant surface [16]. Mechanical testing of the implant / bone interface required the use of surrogate tests of function that include push out or reverse torque testing that do not fully replicate the biomechanics of dental implant function [17]. Typically, these models involved implants that approximated the dimension and form of clinical implants, but often were designed to best meet the demands of the animal model. (e.g., [18]). Despite these limitations, use of in vivo models to study osseointegration in extraoral sites has contributed to our knowledge of surface topography and mechanical loading on the histological result of osseointegration [3,6].

Studies on dental implant osseointegration have focused broadly on the effects of implant design, local bone physiology effects, masticatory (dys)function effects, or oral environmental effects (biofilm-mediated processes of peri-mucositis and peri-implantitis) largely through the histological evaluations of osseointegration. The majority of studies published represent single time-point studies that infer one or several biological processes were responsible for the results observed through histology (and radiography). A molecular and cellular interrogation of the biologic processes that contribute to osseointegration of endosseous implants requires

careful model selection. In addition to anatomic, dimensional and biomechanical concerns, an *in vivo* examination of the molecular and / or cellular processes contributing to osseointegration requires selection of model systems for which sufficient molecular and cellular tools of assessment are readily available. Unfortunately, the commonly utilized models for histology (rabbits, dogs, and to a lesser extent mini-pigs and sheep) provide fewer advantages for molecular assessment than do small animal models including rats and mice. The main advantages of using rats and mice for studies of biologic processes of physiology and pathology include 1) known genomes [19,20], 2) ready access to tools for molecular assessment, 3) relative low cost, 4) a wealth of knowledge regarding the molecular basis of biologic processes (including osteoinduction, osteogenesis, and osteoclastogenesis) in these specific models, and 5) the ability to specifically alter the genomes of mice and rats to create models that test individual genes encoding proteins that may directly affect osseointegration. Recent review of this field suggests that mice have become a preferred model system for bone research because of their genetic and pathophysiological similarities to humans, relatively low costs and the availability of the genome sequence information [21]. The value of genetic mouse models of bone physiology was recently underscored in a review of osteoclastogenesis where the authors stated that this approach has identified novel molecules and highlighted their involvement *in vivo*, confirmed human mutations and expanded the knowledge of mechanisms [22].

The rat model for study of bone physiology and repair is advantageous because of its relatively large size that facilitates surgical intervention. Several mutations or conditions of the rat have permitted forward genetic studies. For example, diabetic or osteopetroic conditions have been evaluated in terms of osseointegration using mutant rat strains [22,23]. Further advances are now promised with using reverse genetic approaches that can systematically and controllably alter the genome to affect phenotypic changes. Only recent technical advances in manipulating the rat genome have made this a realistic possibility [24]. Anticipated is the use of this technology to demonstrate the role of specific genes in the process of osseointegration.

Methods to assess gene expression: A major advantage of studying the process of osseointegration at the molecular level is the potential to identify key steps in the process that may be clinically influenced. These ‘targets’ are identifiable, but are dependent on the methods used to assess gene expression. Gene expression data is readily available at the level of mRNA that encodes proteins, which define the phenotype of interest (here interfacial bone formation). At the level of mRNA, assessments can be made using exploratory methods

(identification of novel or relatively high or low expressed molecules), qualitative methods (present or not), semi-quantitative methods, and quantitative methods. Most techniques all depend upon nucleotide complimentary and RNA hybridization methods that require knowledge of all mRNA sequences now available through the sequencing of the rat genome[25].

Building on histological methods, sections of tissues representing the implant/bone interface can be treated with antibodies for specific proteins and these proteins can be identified using immunohistochemistry. This technique, widely used in pathology, is not readily applied to ground sections embedded in acrylic resins that are frequently used for endosseous implants. When applied to fractured sections with the implant removed, the risk of interface damage exists. If successful, the result remains semi-quantitative. Another means of phenotypic characterization involves identification of specific mRNAs within tissues on histologic sections. In situ hybridization is the process of RNA hybridization of known RNA sequences within tissues (i.e. express by a particular cell). The methodology is robust, yet technically challenging. When accomplished it too offers a semi-quantitative assessment of the expression of an individual RNA encoding a protein within cells and tissue.

Ogawa and colleagues [26] used a exploratory method termed Differential display to identify differences among mRNAs expressed on two different implant surfaces in vivo. This approach identified at least three mRNAs (TO1, TO2, TO3) with elevated expression in tissues adjacent to implant surfaces following placement in the rat tibia. This and other subtractive gene cloning methods reveal differences by dismissing what appear to be the more common and similar mRNAs and is a powerful exploratory tool in biology. The ultimate role or impact of these identified genes on the process of osseointegration remains to be fully elucidated.

mRNA quantification has been enabled by a process termed quantitative-Reverse Transcription Polymerase chain reaction (qRT-PCR). This method has been largely automated and today it is possible to perform this process on sets of targeted mRNAs or on all mRNAs represented in a tissue (gene profiling) simultaneously. These approaches offer opportunities to explore many aspects of physiology through interpretation of large datasets using complex computer based algorithms. One such data base is ‘the Gene Ontology’, a project that collaboratively assists in structuring vocabularies that describe gene products in terms of a) biologic processes, c) cellular components and c) molecular functions. Genes observed by a process of gene profiling (looking at the relative abundance of all genes expressed) can be organized according to specific functions or

processes[27]. With respect to osseointegration, some of these processes might include "differentiation" or "ossification" or "skeletal development" and they are identified by the GO program based upon the expression of mRNA molecules. Where one or another single mRNA expression event might not provide insight to an important process, the organized expression of multiple mRNAs can often point toward a specific cellular components, molecular function or biologic process. These powerful tools can be applied to defining in more complete terms the process of osseointegration. This elucidation can provide new clues to the questions all clinicians have regarding the underlying causes of implant failure.

Genes examined: Distinct yet overlapping phases of healing are associated with osseointegration including clot formation, inflammation, bone repair and remodeling. The sequential changes in cell populations are orchestrated in a manner to weigh the balance toward bone formation. This involves the migration of mesenchymal stem cells, proliferation and promotion of osteoblastic differentiation.

Cell proliferation around implants in-vivo was modestly investigated (3,11). Proliferating cell nuclear antigen (PCNA) ; a protein that acts as a processivity factor for DNA polymerase delta in eukaryotic cells [28]was used to indicate cell proliferation(3). This protein is also involved during DNA repair (Bravo R, Celis JE, 1980). Period Homolog 2 (Per2); involved in the circadian rhythm also plays a role in the regulation of the cell proliferation [29]Expression of *Per* genes in osteoblasts negatively regulates osteoblast proliferation. In the context of osseointegration, per2 expression period homolog 2 (Per2), were upregulated around implants vs. osteotomy sites at 2 weeks and diminished by vitamin D deficiency [30]. This may be expected as proliferation and differentiation of osteoblastic cells are inversely related.

Osseointegration at endosseous implants requires activation of processes relevant to osteoinduction, osteoconduction and osteogenesis [31]. Osteoinduction is the process by which primitive, undifferentiated cells are stimulated to develop into osteoprogenitor cells [32]. Key effectors of osteoinduction include Runx2 and Osx. Both are transcription factors necessary for osteoblast differentiation by controlling osteoblast-specific gene expression at target genes such as ALP, COLI, OPN and OC [33-38]. Runx2 or Osx gene ablation in mice results in complete absence of bone development [39,40]. Modulation of Runx2 and Osx expression by the implant surface topography has been observed by several investigations. In-vivo reports modestly investigated the role of Osx (1 study). Runx2 and Osx expression are positively influenced by increased surface roughness

[12,41-43]. The elevated expression of Runx2 or Osx are paralleled by upregulation of bone-specific proteins (ALP, OC, BSP expression [12,42,43]. PPAR- γ ; a key transcription factor for adipocyte differentiation, is also implicated in the proliferation and differentiation of several cell types including osteogenic cells [44] and macrophages [45]. The PPAR- γ directs MSC differentiation toward the adipocyte lineage with a negative dominant regulatory effect on osteoblast differentiation [46]. Omar et al [43], investigated the expression of PPAR- γ as a function of time and surface treatment. PPAR γ was significantly higher at the machined surface (0.3 μ m) compared to oxidized (Ra=1.2 μ m) surface 1 day after implantation. Nevertheless, at day 3, the expression of PPAR- γ was higher at the oxidized surface. The authors proposed further studies are needed to establish the role of this transcription factor in implant adherent cells.

Osteogenesis was monitored by measurement of bone-specific proteins (ALP, BSP, OPN, ON, OC and COL1). Greater expression of bone-specific proteins is suggestive of greater osteogenesis and more bone formation. Elevations in expression of specific-bone proteins were reflected by higher torque removal values [41,47] at rougher implant surfaces at the micron and nanoscale levels. Collagen type I is the most abundant protein in bone [48] and is secreted at the early stages of osteoblast differentiation. The mechanical strength of bone reflects the inherent properties of its constituents. Collagen biosynthesis at the implant surfaces has been investigated in-vivo widely by means of type I COL expression. On the other hand, stability of collagen is largely dependent on several posttranslational modifications catalyzed by prolyl 4-hydroxylase, prolyl 3-hydroxylase and the family of Lysyl hydroxylases. Additional modifications by Lysyl oxidase (LOX) allow intermolecular and interfibrillar crosslinks between collagen fibrils [49,50]. An in-vitro investigation [51] demonstrated a positive influence of surface roughness on expression of the aforementioned collagen modifying genes. Current in-vivo reports have not examined the potential role of collagen modifying genes in the process of osseointegration. Other ECM components investigated in the context of osseointegration include vinculin [52], fibronectin [53] and various proteoglycans [54]; decorin and biglycan. Proteoglycans role in establishing bone-titanium interfacial adhesion has been established in-vitro by demonstrating that administration of GAG degradation enzyme reduced the bond strength of titanium and cultured rat bone marrow-derived osteoblastic cells [55].

The process of osteogenesis is affected by several growth and differentiation factors. BMPs (Bone morphogenic proteins), members of transforming growth factor family, are one group of stimuli known to induce MSCs or osteoblast progenitors to undergo osteogenic differentiation. The role of BMP signaling pathway in in-vivo osseointegration was mostly investigated through monitoring expression levels of BMP2 (7 studies). However, BMP signal transduction is regulated at different levels in the cell. It can be influenced by extracellular antagonists such as noggin, chordin, follistatin, etc which bind to BMPs and prevent their interaction with receptors [56]. The only extracellular BMP antagonist that was examined in vivo was Noggin. The reported study was examining the effects of local application rh-TGF- β 2 in an implant model on modulating gene expression [57]. Elucidation of the role of the various regulatory mechanisms in BMP signaling in osseointegration requires further elucidation. Reports on factors that may play a role in osseointegration also included studies examining TGF- β and its receptors [43,54,57]. TGF β acts as an important autocrine and paracrine factor in the regulation of bone formation and resorption. It has been implicated to stimulate the replication of precursor cells of the osteoblastic lineage, in addition to its stimulatory effect on bone collagen synthesis [58]. Yet, it also plays a role in stimulating bone resorption by differentiated osteoclasts [59]. TGF- β exerts its function by interacting with a heterotetrameric complex of type I and type II TGF- β receptors. The expression of dominant-negative TGF β receptors in osteoblast cells in vivo causes an age-dependent increase in trabecular bone mass, due to decreased bone resorption by osteoclasts [60].

Angiogenesis is of pivotal importance during the initial healing process of osseointegration. Factors that play a role in angiogenesis include but not limited to VEGF, bFGF, Ang-1 [61], PDGF-B, Insulin-like growth factor and HIF (Hypoxia-inducible transcription factor). VEGF, a molecule known to induce neovascularization, has also been shown to stimulate bone healing and skeletal growth [62,63]. VEGFA acts through its receptor Flk-1/KDR. VEGF leads to an upregulation of BMP2 in endothelial cells that can act reciprocally on the osteoblast lineage inducing osteogenesis [64]. Few studies investigated angiogenesis in the context of osseointegration.

Modulation of the inflammatory process in the early phases of healing following implant placement provides a key element in implant fixation. Inflammatory related processes in implant adherent cells may pioneer biological mechanisms for driving differentiation of cells, including osteoprogenitors, osteoclast precursors, etc that affect osseointegration. Furthermore, differential expression of chemokines and their

receptors affects recruitment of several cells including inflammatory cells, osteogenic cells and their progenitors [65,66]. Inflammatory response to different implant surfaces was investigated by the quantification of the relevant gene expression of TNF- α (7 studies), IL-1 β (3 studies), IL-6 (2 studies), IL-8R (1 study), IL-10 (1 study), IL-11 (1 study), CCL2 (2 studies) and CXCR4 (1 study).

Bone accrual at the implant surface also involves resorption and remodeling. Osteoclast differentiation is a tightly regulated process dependent on an osteoblast-derived member of the tumor necrosis factor (TNF) superfamily; RANKL (receptor activator of the NF κ B ligand), which binds to its receptor RANK on monocytes [67]. Osteoprotegerin (OPG) plays an essential role in the control of bone resorption by acting as soluble decoy receptor for RANKL. Thus, OPG functions to decrease osteoclast formation and activity [68,69]. Efficient degradation of bone is dependent on the production and activation of various matrix-degrading enzymes; cathepsin K [70,71], several MMPs [72,73] and TRAP [74]. Activation of the matrix-degrading enzymes is dependent on the acidification of the lacunar space [75] achieved by the action of an essential enzyme carbonic anhydrase II, in addition to a vacuolar ATPase electrogenic proton pump [76,77]. Another phenotypic marker for osteoclast is Calcitonin receptor, which expression correlates well with bone resorption [78,79]. Quantification of osteoclast-related genes was investigated briefly *in vivo*. Implant surface features modulated expression of bone resorption transcripts [47,80,81].

In an extraoral model of bone healing against endosseous implant surfaces; Donos et al (2011) [82] extended previous investigations of guided bone regeneration that indicated more broad gene regulation involving increased skeletogenesis and reduced inflammatory gene regulation over a 7 – 14 day period. In this study, they found that SLA surfaces displayed relevant gene ontology changes for many cellular processes, particularly at 14 days. Included were skeletal system development and signaling changes associated with the Wnt pathway, and Ras and Rho pathways. The authors highlighted 41 genes upregulated in the mesenchymal stem cell differentiation, angiogenesis ontologies as well. They concluded that regeneration associated with microrough and polished implant surfaces is associated with unique gene expression profiles. Another gene profiling study focused on early healing (days 4, 7 and 14) of SLActive implants inserted in the retromolar pad area of human volunteers [83]. Large numbers of differentially regulated genes (increasing and decreasing) were observed at each time point. At 4 days, several central inflammation-related biological processes were represented (NF κ B cascade, lymphocyte proliferation, macrophage activation). Several osteoinductive genes

including SATB2 and Sp7 (Osterix) were elevated between 4 and 14 days. This investigation highlights important molecular differences between early healing events that include inflammation and Wnt signaling and late healing events that included VEGF signaling, skeletal system development, and continued Wnt signaling. Further investigations have included use of gene profiling to compare the molecular events that occur at SLA vs. SLActive implant surfaces. Clear differences were observed in gene ontologies. For example, at day 7, the MAPK signaling pathway was significantly elevated ($P < 0.0004$) in tissues associated with the SLActive implant. At day 14, for example, BMP signaling pathway was also increased ($P < 0.03$). In general, these early gene profiling studies of the osseointegration process have confirmed that surface topography or hydrophobicity influences the behavior of tissues in ways that include fundamental processes of inflammation and wound healing, as well as many aspects of osteogenesis and biomineralization.

Conclusions:

In vivo molecular assessment of osseointegration can be achieved at multiple levels involving protein and mRNA. The quantitative assessment of bone-related mRNA expression is commonly reported with data supporting the concept that implant surface features that are associated with increased bone to implant contact are able to positively influence the process of bone formation. Several reports demonstrate that surface features also promote osteoinduction by the elevated expression of key transcriptional regulators of this process. Recent studies using gene profiling successfully characterized gene expression events in the tissues surrounding implants and within implant adherent cells. Processes preceding osteoinduction and events that follow the elaboration of a mineralized matrix have been highlighted by gene profiling studies. These molecular details may represent additional targets for therapeutic improvement. Further investigations using in vivo molecular assessment, combined with reverse genetic approaches will enable identification of biological factors that both promote osseointegration and underscore its failure.

Figure 1:

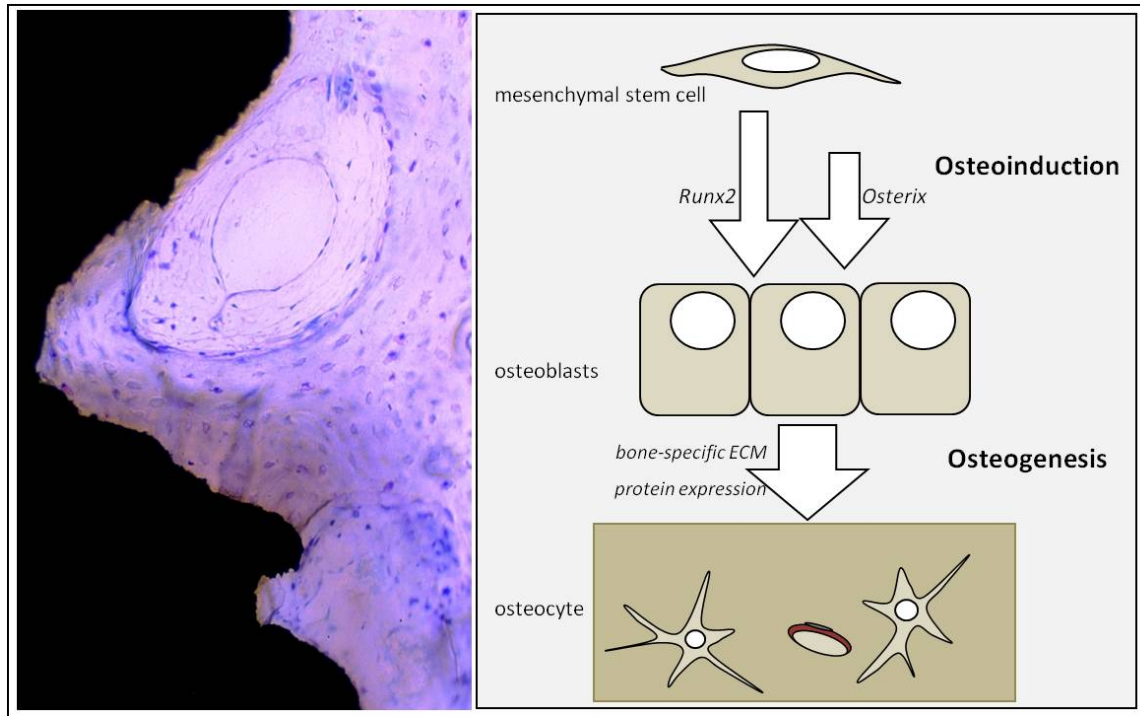


Figure 1. The result of osseointegration can be appreciated histologically (left). Note the presence of cells within the bone and adjacent to the implant surface as bone has formed over a four week period in a canine model. The process(es) that lead to this result are dependent on the differentiation of mesenchymal stem cells to osteoblasts by the process of osteoinduction(right). The key transcriptional regulators that control osteoblastogenesis are Runx2 and Osterix. One important question regarding implant surface influence on osseointegration is “what is the effect of surface on the expression of these transcriptional regulators in implant adherent or adjacent cells?” Committed osteoblasts elaborate a collagen-rich matrix that is embellished with bone-specific extracellular matrix proteins that control tissue formation and mineralization. Many studies have revealed that the nature of the implant surface alters the expression of bone-specific extracellular matrix proteins. These fundamental relationships between the implant and cells that produce bone matrix are accompanied by many other cell type-implant relationships that have not yet been elucidated.

Figure2:

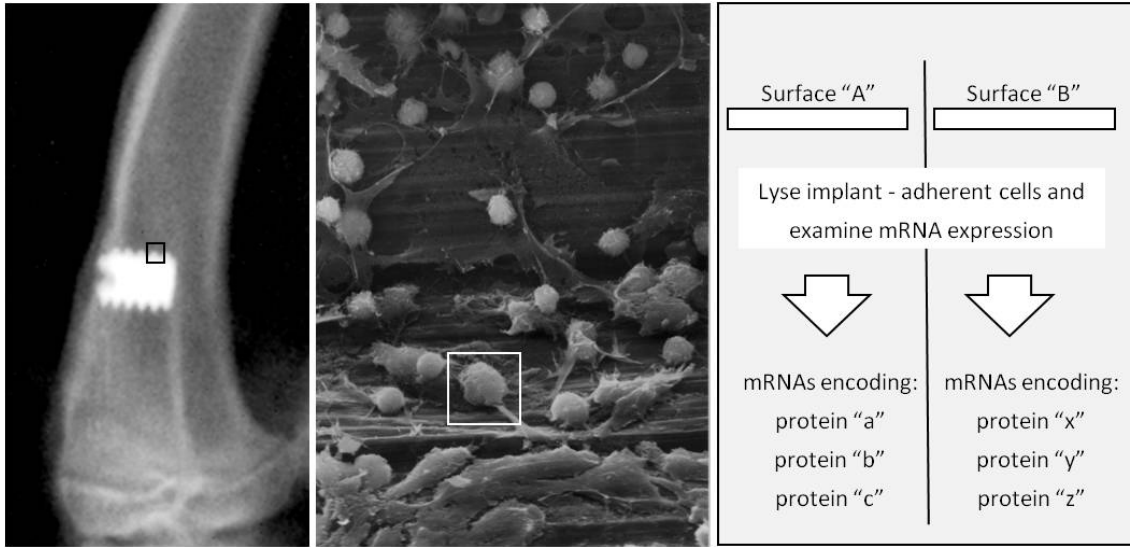


Figure 2: Obtaining molecular information from endosseous implants begins by placement of an implant with defined surface character into the bone marrow (left). Intentional explantation of the implant at early time points relative to mineralization leads to implant retrieval with adherent cells (center). When different implant surfaces are implanted, retrieval of implants with adherent cells permits the evaluation of adherent cell phenotype at the level of protein-encoding mRNA expression. Anticipated (and repeatedly demonstrated in the literature) is the surface-dependent modulation of mRNA expression within the implant-surface adherent cells.

Table1: In vivo models used for molecular assessment of osseointegration

Model	Site –intervention if present	References
Rats – Sprague Dawley;Wistar	Tibiae	[84] [85] [12] [86] [41] [52] [43] [47]
	Femurs	[87] [30] [26] [11] [54][53]
	Femurs- Intramedullary implants	[57] [88]
	Femurs - nicotine exposure	[89]
	Ovariectomized female rats	[11] [90]
	Tibiae-unloaded by tail suspension-osteopenic model	[91]
	Maxilla	[92]
	Calvarial defects covered by teflon membrane and Ti disks	[82]
New Zealand white rabbits	[81] [93] [94] [95]	
Minipigs	Frontal skull	[42]
Mice	Mouse Tibiae	[96]
	Femurs ; COX-2 ^{-/-} and COX-2 ^{+/+} mice	[97]
Human volunteers	The retromolar area-trephine	[13] [83]

Table2: Methods used to assess gene expression adjacent to different implant surfaces in in-vivo models.

Method used	References	Role
Differential display-polymerase chain-reaction	[11]	Exploratory
Immunohistology	[95] [88] [30] [84] [86] [52][43]	Qualitative
Immunofluorescence	[85]	Qualitative
In situ hybridization	[87] [96] [92]	Qualitative and semi-quantitative
Histochemistry; TRAP and ALP	[96] [84]	Qualitative and semi-quantitative
RT-PCR	[57] [30] [26] [54] [90]	Semi-quantitative
qReal-Time-PCR	[97] [12] [53] [41] [81] [52] [43] [47] [93] [94] [91] [42] [89]	Quantitative
Wide genome expression profiling	[13] [83] [82] [30]	Quantitative

Table 3: Molecular assessment of osseointegration in in-vivo models along with Gene Ontology classification

Genes examined	Gene Ontology Classification	References
PCNA (proliferating cell nuclear antigen)	Cell proliferation	[85]
Per2 (period homolog 2)	regulation of transcription, DNA-dependent; circadian rhythm	[30]
PPAR γ (peroxisome proliferator-activated receptor gamma)	Transcription, DNA-dependent; positive regulation of fat cell differentiation	[43]
RUNX2 (runt-related transcription factor 2)	Ossification; osteoblast differentiation; transcription	[96] [57] [12] [41] [81] [43] [47] [93] [94] [89]
Sp7 transcription factor	Regulation of transcription; osteoblast differentiation	[42]
ALP (alkaline phosphatase)	Skeletal system development; biomineral tissue development	[96] [57] [84] [12] [41] [43] [47] [42]
BSP (integrin-binding sialoprotein)	Ossification; cell adhesion; extracellular matrix organization; biomineral tissue development	[12] [41] [26] [90] [95] [89]
OC (Osteocalcin)	Skeletal system development; osteoblast differentiation; osteoblast development; bone mineralization; regulation of osteoclast differentiation	[97] [96] [57] [84] [85] [87] [41] [81] [26] [54] [43] [47] [90] [93] [94]
OPN (Osteopontin)	Ossification; cell adhesion; positive regulation of cell-substrate adhesion; biomineral tissue development	[96] [57] [53] [41] [30] [26] [54] [90] [95] [89] [57]
ON (secreted protein, acidic, cysteine-rich) (osteonectin)	Ossification; regulation of cell proliferation; cellular response to growth factor stimulus	[53] [87] [30] [26] [90] [95]
COL1A (collagen, type I, alpha 1)	Skeletal system development; blood vessel development; osteoblast differentiation; intramembranous ossification; endochondral ossification	[96] [57] [87] [30] [81] [26] [54] [90] [93] [95] [94] [42]
COL IIA (collagen, type II, alpha 1)	Skeletal system development	[96] [30] [26] [54] [95] [89]
COL IIIA (collagen, type III, alpha 1)	skeletal system development; blood vessel development; cell-matrix adhesion	[90]
COLIXA (collagen, type IX, alpha 1)	chondrocyte differentiation; cell adhesion; organ morphogenesis	[54]
COLXA1 (collagen, type X, alpha 1)	skeletal system development	[30]
collagen XIIA1 (collagen, type XII, alpha 1)	skeletal system development; cell adhesion; collagen fibril organization	[92]
Vinculin	Blood vessel development; regulation of Wnt receptor signaling pathway; canonical Wnt receptor signaling pathway involved in positive regulation of	[52]

	wound healing	
Fibronectin	Extracellular matrix structural constituent; angiogenesis; cell adhesion; response to wounding; cell migration; peptide cross-linking; platelet activation; substrate adhesion-dependent cell spreading; leukocyte migration; regulation of cell shape	[53]
integrin, beta 1	cell migration involved in sprouting angiogenesis; cellular defense response; cell adhesion; cell-matrix adhesion; integrin-mediated signaling pathway; multicellular organismal development; cellular response to mechanical stimulus	[26] [52] [90]
integrin, beta 2	cell-matrix adhesion; integrin-mediated signaling pathway; cell-cell signaling; multicellular organismal development	[52]
integrin, beta 3	cell adhesion; cell-matrix adhesion; integrin-mediated signaling pathway; regulation of bone resorption; leukocyte migration; angiogenesis involved in wound healing	[26] [52] [90]
Decorin & Biglycan	organ morphogenesis; wound healing; extracellular matrix binding ;peptide cross-linking via chondroitin 4-sulfate glycosaminoglycan;	[54]
BMP2 (bone morphogenetic protein 2)	skeletal system development; osteoblast differentiation;positive regulation of bone mineralization	[57] [84] [85] [54] [43] [89]
BMP4 (bone morphogenetic protein 4); BMP7 (bone morphogenetic protein 7);	osteoblast differentiation; positive regulation of pathway-restricted SMAD protein phosphorylation; positive regulation of bone mineralization;	[57]
The BMP antagonist Noggin	skeletal system development; osteoblast differentiation; negative regulation of BMP signaling pathway	[57]
TGF-β 1 (transforming growth factor, beta 1)	chondrocyte differentiation; SMAD protein complex assembly; regulation of cell proliferation; response to wounding; regulation of collagen biosynthetic process	[57] [54] [43]
TGF-β2 (transforming growth factor, beta 2); TGF-β3 (transforming growth factor, beta 3)	SMAD protein import into nucleus; cell proliferation	[57]
TGF-BR1(transforming growth factor, beta receptor 1); TGF-	positive regulation of mesenchymal cell proliferation;	[57]

BR2(transforming growth factor, beta receptor 2)	positive regulation of SMAD protein import into nucleus	
IGF1 (insulin-like growth factor 1)	skeletal system development; blood coagulation; positive regulation of cell proliferation; bone mineralization involved in bone maturation; positive regulation of osteoblast differentiation	[57] [81]
IGF-1 Receptor [IGF-1R]	signal transduction; positive regulation of cell proliferation; positive regulation of cell migration	[57]
FGF-2 (fibroblast growth factor 2 (basic))	regulation of cell proliferation; wound healing; positive regulation of blood vessel;regulation of cell cycle	[91]
PDGF-B (platelet-derived growth factor beta polypeptide)	positive regulation of endothelial cell proliferation; monocyte chemotaxis; platelet degranulation; response to wounding	[43]
Hif-1 α (hypoxia inducible factor 1, alpha subunit)	response to hypoxia; positive regulation of endothelial cell proliferation;transcription, DNA-dependent; positive regulation vascular endothelial growth factor production; positive regulation of chemokine production; regulation of transforming growth factor-beta2 production	[91]
vascular endothelial growth factor A	Angiogenesis; patterning of blood vessels; vasculogenesis; response to hypoxia	[57] [84] [91]
Fms-like tyrosine kinase 1 [Flt-1])	patterning of blood vessels; response to hypoxia; sprouting angiogenesis; vascular endothelial growth factor receptor signaling pathway	[57]
Epas1 (endothelial PAS domain protein 1)	angiogenesis; response to hypoxia; multicellular organismal development; cell differentiation	[91]
Ang-1 (angiopoietin 1)	regulation of endothelial cell proliferation; sprouting angiogenesis; leukocyte migration; positive chemotaxis	[91]
OPG (tumor necrosis factor receptor superfamily, member 11b)	Skeletal system development; apoptosis; extracellular matrix organization; negative regulation of bone resorption	[86]
RANK (tumor necrosis factor receptor superfamily, member 11a, NFKB activator)	Cell-cell signaling; positive regulation of cell proliferation; osteoclast differentiation	[86]
RANKL (tumor necrosis factor (ligand) superfamily, member	Positive regulation of osteoclast differentiation; positive regulation	[86] [91]

11)	of bone resorption; cytokine-mediated signaling pathway	
TRAP (acid phosphatase 5, tartrate resistant)	response to cytokine stimulus; bone resorption; bone morphogenesis	[96] [81] [47] [93] [94] [42] [43] [91]
catK (Cathepsin K)	Proteolysis; bone resorption	[53] [43] [47]
calcitonin receptor	Activation of adenylate cyclase activity by G-protein signaling pathway	[81]
H ⁺ -ATPase	ATP hydrolysis coupled proton transport; proton transport	[81]
TNF- α (tumor necrosis factor)	Inflammatory response; immune response	[81] [52] [43] [47] [91] [57] [94]
Interleukin 1, beta	Inflammatory response; immune response; signal transduction; cell-cell signaling;	[52] [43] [47]
Interleukin 6	Inflammatory response; immune response	[81] [94]
Interleukin 8 receptor	Inflammatory response; immune response	[52]
Interleukin 10	Inflammatory response; cell-cell signaling; regulation of gene expression; leukocyte chemotaxis	[81] [94]
Interleukin 11	Inflammatory response; immune response	[91]
MCP-1 (CCL2)	Angiogenesis; response to hypoxia; chemotaxis; inflammatory response; cytokine-mediated - signaling pathway	[52] [53]
CXCR4 (chemokine (C-X-C motif) receptor 4)	Response to hypoxia; inflammatory response; regulation of chemotaxis	[52]
Cox-1 (prostaglandin-endoperoxide synthase 1 (prostaglandin G/H synthase and cyclooxygenase)	Prostaglandin biosynthetic process; regulation of cell proliferation	[97]
Cox-2 (prostaglandin-endoperoxide synthase 2 (prostaglandin G/H synthase and cyclooxygenase)	Regulation of inflammatory response; response to glucocorticoid stimulus	[97] [57]
ED1 (CD68 molecule)	Marker of macrophages	[88]
CD 163	A marker for tissue macrophage	[43]
Periostin	A marker for osteogenic cells	[43]
PGP 9.5 (marker of axons), Calcitonin Gene-Related peptide (constituent of sensory axons and neuropeptide involved in bone remodeling), GAP-43 (marker of sprouting axons)		[88]

Table 4: Wide genome expression profiling studies in vivo.

Model	Surface examined	Technique used	Day of analysis	Reference
Retromolar area - human volunteers-trephine	SLA surface vs. SLActive	Human WG-6 V3 array (Illumina)	4,7 and 14 days	Donos et al, 2011[13]
Retromolar area - human volunteers-trephine	SLActive	Human WG-6 V3 array (Illumina)	4,7 and 14 days	Ivanovski,S. et al,2011[83]
Calvarial defects - Wistar rats total covered by teflon membrane and Ti disks	Polished Ti- SMO vs. microrough surface SLA	Affymetrix Gene Chip Rat Expression Set 230 v 2.0	7 and 14 days	Donos et al, 2011[82]
Rat femur	T-shaped Ti4Al6V implant-surface treated by dual acid-etching followed by crystalline deposition of HA particles –(tissue collected in the hollow chamber vs. osteotomy sites without implants were analyzed) – control vs. vitamin D deficient diet	Agilent Rat Whole Genome- two color channel microarray-41,000 genes	2 weeks	Mengatto,C.M et al,2011[30]
Rat femur	cp Titanium implants vs osteotomy healing sites	DNA microarray where 20,000 rat genes (Agilent Rat Oligo array, Agilent Technologies)	1 wk,2 wks and 4 wks	Kojima et al, 2008 [53]
Rat femur	Experimental cp Ti T-shaped implants .The implant surface was either machined (turned by a lathe) or treated by acid-etching (Osseotite)-(1) the osteotomy control group, (2) the machined titanium implant group, and (3) the acid-etched titanium implant group (4) untreated control group	Differential display-polymerase chain-reaction	3 days, 1,2 and 4 weeks post-surgery	Ogawa,T.et al, 2006[11]

References:

1. Branemark PI, Hansson BO, Adell R, Breine U, Lindstrom J, Hallen O, Ohman A. Osseointegrated implants in the treatment of the edentulous jaw. Experience from a 10-year period. *Scand J Plast Reconstr Surg Suppl* 1977;16:1-132.
2. Lekholm U, Zarb GA. Patient selection and preparation. In: Branemark, P-I., Zarb, G.A. & Albrektsson, T., eds. *Tissue Integrated Prostheses: Osseointegration in Clinical Dentistry*. Chicago: Quintessence Publishing. 1985: 199– 209.
3. Wennerberg A, Albrektsson T. Effects of titanium surface topography on bone integration: a systematic review. *Clin Oral Implants Res* 2009;20 Suppl 4:172-184.
4. Junker R, Dimakis A, Thoneick M, Jansen JA. Effects of implant surface coatings and composition on bone integration: a systematic review. *Clin Oral Implants Res* 2009;20 Suppl 4:185-206.
5. Degidi M, Perrotti V, Piattelli A, Iezzi G. Mineralized bone-implant contact and implant stability quotient in 16 human implants retrieved after early healing periods: a histologic and histomorphometric evaluation. *Int J Oral Maxillofac Implants* 2010;25:45-48.
6. Shalabi MM, Gortemaker A, Van't Hof MA, Jansen JA, Creugers NH. Implant surface roughness and bone healing: a systematic review. *J Dent Res* 2006;85:496-500.
7. Telleman G, Albrektsson T, Hoffman M, Johansson CB, Vissink A, Meijer HJ, Raghoobar GM. Peri-implant endosseous healing properties of dual acid-etched mini-implants with a nanometer-sized deposition of CaP: a histological and histomorphometric human study. *Clin Implant Dent Relat Res* 2010;12:153-160.
8. Trisi P, Lazzara R, Rebaudi A, Rao W, Testori T, Porter SS. Bone-implant contact on machined and dual acid-etched surfaces after 2 months of healing in the human maxilla. *J Periodontol* 2003;74:945-956.
9. Ivanoff CJ, Hallgren C, Widmark G, Sennerby L, Wennerberg A. Histologic evaluation of the bone integration of TiO₂ blasted and turned titanium microimplants in humans. *Clin Oral Implants Res* 2001;12:128-134.
10. Lang NP, Salvi GE, Huynh-Ba G, Ivanovski S, Donos N, Bosshardt DD. Early osseointegration to hydrophilic and hydrophobic implant surfaces in humans. *Clin Oral Implants Res* 2011;22:349-356.
11. Ogawa T, Nishimura I. Genes differentially expressed in titanium implant healing. *J Dent Res* 2006;85:566-70.
12. Guo J, Padilla RJ, Ambrose W, De Kok IJ, Cooper LF. The effect of hydrofluoric acid treatment of TiO₂ grit blasted titanium implants on adherent osteoblast gene expression in vitro and in vivo. *Biomaterials* 2007;28:5418-25.
13. Donos N, Hamlet S, Lang NP, Salvi GE, Huynh-Ba G, Bosshardt DD, Ivanovski S. Gene expression profile of osseointegration of a hydrophilic compared with a hydrophobic microrough implant surface. *Clin Oral Implants Res* 2011;22:365-372.
14. Bryington M, Mendonca G, Nares S, Cooper LF. Osteoblastic and cytokine gene expression of implant adherent cells in human. *Clin Oral Implants Res* 2012.
15. Hadjiargyrou M, Lombardo F, Zhao S, Ahrens W, Joo J, Ahn H, Jurman M, White DW, Rubin CT. Transcriptional profiling of bone regeneration. Insight into the molecular complexity of wound repair. *J Biol Chem* 2002;277:30177-30182.
16. Albrektsson T, Wennerberg A. Oral implant surfaces: Part 1--review focusing on topographic and chemical properties of different surfaces and in vivo responses to them. *Int J Prosthodont* 2004;17:536-543.

17. Brunski JB. In vivo bone response to biomechanical loading at the bone/dental-implant interface. *Adv Dent Res* 1999;13:99-119.

18. Pearce AI, Richards RG, Milz S, Schneider E, Pearce SG. Animal models for implant biomaterial research in bone: a review. *Eur Cell Mater* 2007;13:1-10.

19. Mouse Genome Sequencing Consortium, Waterston RH, Lindblad-Toh K, Birney E, Rogers J, Abril JF, Agarwal P, Agarwala R, Ainscough R, Alexandersson M, An P, Antonarakis SE, Attwood J, Baertsch R, Bailey J, Barlow K, Beck S, Berry E, Birren B, Bloom T, Bork P, Botcherby M, Bray N, Brent MR, Brown DG, Brown SD, Bult C, Burton J, Butler J, Campbell RD, Carninci P, Cawley S, Chiaromonte F, Chinwalla AT, Church DM, Clamp M, Clee C, Collins FS, Cook LL, Copley RR, Coulson A, Couronne O, Cuff J, Curwen V, Cutts T, Daly M, David R, Davies J, Delehaunty KD, Deri J, Dermitzakis ET, Dewey C, Dickens NJ, Diekhans M, Dodge S, Dubchak I, Dunn DM, Eddy SR, Elnitski L, Emes RD, Eswara P, Eyraas E, Felsenfeld A, Fewell GA, Flicek P, Foley K, Frankel WN, Fulton LA, Fulton RS, Furey TS, Gage D, Gibbs RA, Glusman G, Gnerre S, Goldman N, Goodstadt L, Grafham D, Graves TA, Green ED, Gregory S, Guigo R, Guyer M, Hardison RC, Haussler D, Hayashizaki Y, Hillier LW, Hinrichs A, Hlavina W, Holzer T, Hsu F, Hua A, Hubbard T, Hunt A, Jackson I, Jaffe DB, Johnson LS, Jones M, Jones TA, Joy A, Kamal M, Karlsson EK, Karolchik D, Kasprzyk A, Kawai J, Keibler E, Kells C, Kent WJ, Kirby A, Kolbe DL, Korfi I, Kucherlapati RS, Kulbokas EJ, Kulp D, Landers T, Leger JP, Leonard S, Letunic I, Levine R, Li J, Li M, Lloyd C, Lucas S, Ma B, Maglott DR, Mardis ER, Matthews L, Mauceli E, Mayer JH, McCarthy M, McCombie WR, McLaren S, McLay K, McPherson JD, Meldrim J, Meredith B, Mesirov JP, Miller W, Miner TL, Mongin E, Montgomery KT, Morgan M, Mott R, Mullikin JC, Muzny DM, Nash WE, Nelson JO, Nhan MN, Nicol R, Ning Z, Nusbaum C, O'Connor MJ, Okazaki Y, Oliver K, Overton-Larty E, Pachter L, Parra G, Pepin KH, Peterson J, Pevzner P, Plumb R, Pohl CS, Poliakov A, Ponce TC, Ponting CP, Potter S, Quail M, Reymond A, Roe BA, Roskin KM, Rubin EM, Rust AG, Santos R, Sapojnikov V, Schultz B, Schultz J, Schwartz MS, Schwartz S, Scott C, Seaman S, Searle S, Sharpe T, Sheridan A, Shownkeen R, Sims S, Singer JB, Slater G, Smit A, Smith DR, Spencer B, Stabenau A, Stange-Thomann N, Sugnet C, Suyama M, Tesler G, Thompson J, Torrents D, Trevaskis E, Tromp J, Ucla C, Ureta-Vidal A, Vinson JP, Von Niederhausern AC, Wade CM, Wall M, Weber RJ, Weiss RB, Wendl MC, West AP, Wetterstrand K, Wheeler R, Whelan S, Wierzbowski J, Willey D, Williams S, Wilson RK, Winter E, Worley KC, Wyman D, Yang S, Yang SP, Zdobnov EM, Zody MC, Lander ES. Initial sequencing and comparative analysis of the mouse genome. *Nature* 2002;420:520-562.

20. Gibbs RA, Weinstock GM, Metzker ML, Muzny DM, Sodergren EJ, Scherer S, Scott G, Steffen D, Worley KC, Burch PE, Okwuonu G, Hines S, Lewis L, DeRamo C, Delgado O, Dugan-Rocha S, Miner G, Morgan M, Hawes A, Gill R, Celera, Holt RA, Adams MD, Amanatides PG, Baden-Tillson H, Barnstead M, Chin S, Evans CA, Ferriera S, Fosler C, Glodek A, Gu Z, Jennings D, Kraft CL, Nguyen T, Pfannkoch CM, Sitter C, Sutton GG, Venter JC, Woodage T, Smith D, Lee HM, Gustafson E, Cahill P, Kana A, Doucette-Stamm L, Weinstock K, Fechtel K, Weiss RB, Dunn DM, Green ED, Blakesley RW, Bouffard GG, De Jong PJ, Osoegawa K, Zhu B, Marra M, Schein J, Bosdet I, Fjell C, Jones S, Krzywinski M, Mathewson C, Siddiqui A, Wye N, McPherson J, Zhao S, Fraser CM, Shetty J, Shatsman S, Geer K, Chen Y, Abramson S, Nierman WC, Havlak PH, Chen R, Durbin KJ, Egan A, Ren Y, Song XZ, Li B, Liu Y, Qin X, Cawley S, Worley KC, Cooney AJ, D'Souza LM, Martin K, Wu JQ, Gonzalez-Garay ML, Jackson AR, Kalafus KJ, McLeod MP, Milosavljevic A, Virk D, Volkov A, Wheeler DA, Zhang Z, Bailey JA, Eichler EE, Tuzun E, Birney E, Mongin E, Ureta-Vidal A, Woodward C, Zdobnov E, Bork P, Suyama M, Torrents D, Alexandersson M, Trask BJ, Young JM, Huang H, Wang H, Xing H, Daniels S, Gietzen D, Schmidt J, Stevens K, Vitt U, Wingrove J, Camara F, Mar Alba M, Abril JF, Guigo R, Smit A, Dubchak I, Rubin EM, Couronne O, Poliakov A, Hubner N, Ganten D, Goesele C, Hummel O, Kreitler T, Lee YA, Monti J, Schulz H, Zimdahl H, Himmelbauer H, Lehrach H, Jacob HJ, Bromberg S, Gullings-Handley J, Jensen-Seaman MI, Kwitek AE, Lazar J, Pasko D, Tonellato PJ, Twigger S, Ponting CP, Duarte JM, Rice S, Goodstadt L, Beatson SA, Emes RD, Winter EE, Webber C, Brandt P, Nyakatura G, Adetobi M, Chiaromonte F, Elnitski L, Eswara P, Hardison RC, Hou M, Kolbe D, Makova K, Miller W, Nekrutenko A, Riemer C, Schwartz S, Taylor J, Yang S, Zhang Y, Lindpaintner K, Andrews TD, Caccamo M, Clamp M, Clarke L, Curwen V, Durbin R, Eyraas E, Searle SM, Cooper GM, Batzoglu S, Brudno M, Sidow A, Stone EA, Venter JC, Payseur BA, Bourque G, Lopez-Otin C, Puente XS, Chakrabarti K, Chatterji S, Dewey C, Pachter L, Bray N, Yap VB, Caspi A, Tesler G, Pevzner PA, Haussler D, Roskin KM, Baertsch R, Clawson H, Furey TS, Hinrichs AS, Karolchik D, Kent WJ, Rosenbloom KR, Trumbower H, Weirauch M, Cooper DN, Stenson PD, Ma B, Brent M, Arumugam M, Shteynberg D, Copley RR, Taylor MS, Riethman H, Mudunuri U, Peterson J, Guyer M, Felsenfeld A, Old S, Mockrin S, Collins F, Rat Genome Sequencing Project

Consortium. Genome sequence of the Brown Norway rat yields insights into mammalian evolution. *Nature* 2004;428:493-521.

21. Elefteriou F, Yang X. Genetic mouse models for bone studies--strengths and limitations. *Bone* 2011;49:1242-1254.

22. Edwards JR, Mundy GR. Advances in osteoclast biology: old findings and new insights from mouse models. *Nat Rev Rheumatol* 2011;7:235-243.

23. Hasegawa H, Ozawa S, Hashimoto K, Takeichi T, Ogawa T. Type 2 diabetes impairs implant osseointegration capacity in rats. *Int J Oral Maxillofac Implants* 2008;23:237-246.

24. Glosel B, Kuchler U, Watzek G, Gruber R. Review of dental implant rat research models simulating osteoporosis or diabetes. *Int J Oral Maxillofac Implants* 2010;25:516-524.

25. Dwinell MR, Lazar J, Geurts AM. The emerging role for rat models in gene discovery. *Mamm Genome* 2011;22:466-475.

26. Ogawa T, Nishimura I. Different bone integration profiles of turned and acid-etched implants associated with modulated expression of extracellular matrix genes. *Int J Oral Maxillofac Implants* 2003;18:200-10.

27. Gene Ontology Consortium. The Gene Ontology project in 2008. *Nucleic Acids Res* 2008;36:D440-4.

28. Tsurimoto T. PCNA, a multifunctional ring on DNA. *Biochim Biophys Acta* 1998;1443:23-39.

29. Fu L, Patel MS, Bradley A, Wagner EF, Karsenty G. The molecular clock mediates leptin-regulated bone formation. *Cell* 2005;122:803-815.

30. Mengatto CM, Mussano F, Honda Y, Colwell CS, Nishimura I. Circadian rhythm and cartilage extracellular matrix genes in osseointegration: a genome-wide screening of implant failure by vitamin D deficiency. *PLoS One* 2011;6:e15848.

31. Cooper LF. Biologic determinants of bone formation for osseointegration: clues for future clinical improvements. *J Prosthet Dent* 1998;80:439-449.

32. Albrektsson T, Johansson C. Osteoinduction, osteoconduction and osseointegration. *Eur Spine J* 2001;10 Suppl 2:S96-101.

33. Lian JB, Javed A, Zaidi SK, Lengner C, Montecino M, van Wijnen AJ, Stein JL, Stein GS. Regulatory controls for osteoblast growth and differentiation: role of Runx/Cbfa/AML factors. *Crit Rev Eukaryot Gene Expr* 2004;14:1-41.

34. Kobayashi T, Kronenberg H. Minireview: transcriptional regulation in development of bone. *Endocrinology* 2005;146:1012-1017.

35. Harada H, Tagashira S, Fujiwara M, Ogawa S, Katsumata T, Yamaguchi A, Komori T, Nakatsuka M. Cbfa1 isoforms exert functional differences in osteoblast differentiation. *J Biol Chem* 1999;274:6972-6978.

36. Harada S, Rodan GA. Control of osteoblast function and regulation of bone mass. *Nature* 2003;423:349-355.

37. Byers BA, Garcia AJ. Exogenous Runx2 expression enhances in vitro osteoblastic differentiation and mineralization in primary bone marrow stromal cells. *Tissue Eng* 2004;10:1623-1632.

38. Byers BA, Pavlath GK, Murphy TJ, Karsenty G, Garcia AJ. Cell-type-dependent up-regulation of in vitro mineralization after overexpression of the osteoblast-specific transcription factor Runx2/Cbfa1. *J Bone Miner Res* 2002;17:1931-1944.

39. Komori T, Yagi H, Nomura S, Yamaguchi A, Sasaki K, Deguchi K, Shimizu Y, Bronson RT, Gao YH, Inada M, Sato M, Okamoto R, Kitamura Y, Yoshiki S, Kishimoto T. Targeted disruption of *Cbfa1* results in a complete lack of bone formation owing to maturational arrest of osteoblasts. *Cell* 1997;89:755-764.
40. Nakashima K, Zhou X, Kunkel G, Zhang Z, Deng JM, Behringer RR, de Crombrughe B. The novel zinc finger-containing transcription factor osterix is required for osteoblast differentiation and bone formation. *Cell* 2002;108:17-29.
41. Mendonca G, Mendonca DB, Simoes LG, Araujo AL, Leite ER, Duarte WR, Cooper LF, Aragao FJ. Nanostructured alumina-coated implant surface: effect on osteoblast-related gene expression and bone-to-implant contact in vivo. *Int J Oral Maxillofac Implants* 2009;24:205-15.
42. Wang N, Li H, Lu W, Li J, Wang J, Zhang Z, Liu Y. Effects of TiO₂ nanotubes with different diameters on gene expression and osseointegration of implants in minipigs. *Biomaterials* 2011;32:6900-6911.
43. Omar O, Svensson S, Zoric N, Lenneras M, Suska F, Wigren S, Hall J, Nannmark U, Thomsen P. In vivo gene expression in response to anodically oxidized versus machined titanium implants. *J Biomed Mater Res A* ;92:1552-66.
44. Bruedigam C, Koedam M, Chiba H, Eijken M, van Leeuwen JP. Evidence for multiple peroxisome proliferator-activated receptor gamma transcripts in bone: fine-tuning by hormonal regulation and mRNA stability. *FEBS Lett* 2008;582:1618-1624.
45. Szanto A, Roszer T. Nuclear receptors in macrophages: a link between metabolism and inflammation. *FEBS Lett* 2008;582:106-116.
46. Lecka-Czernik B, Gubrij I, Moerman EJ, Kajkenova O, Lipschitz DA, Manolagas SC, Jilka RL. Inhibition of *Osf2/Cbfa1* expression and terminal osteoblast differentiation by *PPARgamma2*. *J Cell Biochem* 1999;74:357-371.
47. Omar OM, Lenneras ME, Suska F, Emanuelsson L, Hall JM, Palmquist A, Thomsen P. The correlation between gene expression of proinflammatory markers and bone formation during osseointegration with titanium implants. *Biomaterials* .
48. Niyibizi C, Eyre DR. Structural characteristics of cross-linking sites in type V collagen of bone. Chain specificities and heterotypic links to type I collagen. *Eur J Biochem* 1994;224:943-950.
49. Pornprasertsuk S, Duarte WR, Mochida Y, Yamauchi M. Lysyl hydroxylase-2b directs collagen cross-linking pathways in MC3T3-E1 cells. *J Bone Miner Res* 2004;19:1349-1355.
50. Yamauchi M, Shiiba M. Lysine hydroxylation and cross-linking of collagen. *Methods Mol Biol* 2008;446:95-108.
51. Mendonca DB, Miguez PA, Mendonca G, Yamauchi M, Aragao FJ, Cooper LF. Titanium surface topography affects collagen biosynthesis of adherent cells. *Bone* 2011;49:463-472.
52. Omar O, Lenneras M, Svensson S, Suska F, Emanuelsson L, Hall J, Nannmark U, Thomsen P. Integrin and chemokine receptor gene expression in implant-adherent cells during early osseointegration. *J Mater Sci Mater Med* ;21:969-80.
53. Kojima N, Ozawa S, Miyata Y, Hasegawa H, Tanaka Y, Ogawa T. High-throughput gene expression analysis in bone healing around titanium implants by DNA microarray. *Clin Oral Implants Res* 2008;19:173-81.
54. Ogawa T, Sukotjo C, Nishimura I. Modulated bone matrix-related gene expression is associated with differences in interfacial strength of different implant surface roughness. *J Prosthodont* 2002;11:241-7.
55. Nakamura H, Shim J, Butz F, Aita H, Gupta V, Ogawa T. Glycosaminoglycan degradation reduces mineralized tissue-titanium interfacial strength. *J Biomed Mater Res A* 2006;77:478-486.

56. Canalis E, Economides AN, Gazzerro E. Bone morphogenetic proteins, their antagonists, and the skeleton. *Endocr Rev* 2003;24:218-235.
57. De Ranieri A, Viridi AS, Kuroda S, Shott S, Dai Y, Sumner DR. Local application of rhTGF-beta2 modulates dynamic gene expression in a rat implant model. *Bone* 2005;36:931-40.
58. Bonewald LF, Mundy GR. Role of transforming growth factor-beta in bone remodeling. *Clin Orthop Relat Res* 1990;(250):261-276.
59. Hattersley G, Chambers TJ. Effects of transforming growth factor beta 1 on the regulation of osteoclastic development and function. *J Bone Miner Res* 1991;6:165-172.
60. Filvaroff E, Erlebacher A, Ye J, Gitelman SE, Lotz J, Heilman M, Derynck R. Inhibition of TGF-beta receptor signaling in osteoblasts leads to decreased bone remodeling and increased trabecular bone mass. *Development* 1999;126:4267-4279.
61. Kanczler JM, Oreffo RO. Osteogenesis and angiogenesis: the potential for engineering bone. *Eur Cell Mater* 2008;15:100-114.
62. Gittens SA, Uludag H. Growth factor delivery for bone tissue engineering. *J Drug Target* 2001;9:407-429.
63. Street J, Bao M, deGuzman L, Bunting S, Peale FV, Jr, Ferrara N, Steinmetz H, Hoeffel J, Cleland JL, Daugherty A, van Bruggen N, Redmond HP, Carano RA, Filvaroff EH. Vascular endothelial growth factor stimulates bone repair by promoting angiogenesis and bone turnover. *Proc Natl Acad Sci U S A* 2002;99:9656-9661.
64. Bouletreau PJ, Warren SM, Spector JA, Peled ZM, Gerrets RP, Greenwald JA, Longaker MT. Hypoxia and VEGF up-regulate BMP-2 mRNA and protein expression in microvascular endothelial cells: implications for fracture healing. *Plast Reconstr Surg* 2002;109:2384-2397.
65. Kunkel EJ, Campbell DJ, Butcher EC. Chemokines in lymphocyte trafficking and intestinal immunity. *Microcirculation* 2003;10:313-323.
66. Campbell DJ, Kim CH, Butcher EC. Chemokines in the systemic organization of immunity. *Immunol Rev* 2003;195:58-71.
67. Yasuda H, Shima N, Nakagawa N, Yamaguchi K, Kinosaki M, Mochizuki S, Tomoyasu A, Yano K, Goto M, Murakami A, Tsuda E, Morinaga T, Higashio K, Udagawa N, Takahashi N, Suda T. Osteoclast differentiation factor is a ligand for osteoprotegerin/osteoclastogenesis-inhibitory factor and is identical to TRANCE/RANKL. *Proc Natl Acad Sci U S A* 1998;95:3597-3602.
68. Tsuda E, Goto M, Mochizuki S, Yano K, Kobayashi F, Morinaga T, Higashio K. Isolation of a novel cytokine from human fibroblasts that specifically inhibits osteoclastogenesis. *Biochem Biophys Res Commun* 1997;234:137-142.
69. Yasuda H, Shima N, Nakagawa N, Mochizuki SI, Yano K, Fujise N, Sato Y, Goto M, Yamaguchi K, Kuriyama M, Kanno T, Murakami A, Tsuda E, Morinaga T, Higashio K. Identity of osteoclastogenesis inhibitory factor (OCIF) and osteoprotegerin (OPG): a mechanism by which OPG/OCIF inhibits osteoclastogenesis in vitro. *Endocrinology* 1998;139:1329-1337.
70. Pennypacker B, Shea M, Liu Q, Masarachia P, Saftig P, Rodan S, Rodan G, Kimmel D. Bone density, strength, and formation in adult cathepsin K (-/-) mice. *Bone* 2009;44:199-207.
71. Wilson SR, Peters C, Saftig P, Bromme D. Cathepsin K activity-dependent regulation of osteoclast actin ring formation and bone resorption. *J Biol Chem* 2009;284:2584-2592.
72. Engsig MT, Chen QJ, Vu TH, Pedersen AC, Therkildsen B, Lund LR, Henriksen K, Lenhard T, Foged NT, Werb Z, Delaisse JM. Matrix metalloproteinase 9 and vascular endothelial growth factor are essential for osteoclast recruitment into developing long bones. *J Cell Biol* 2000;151:879-889.

73. Krane SM, Inada M. Matrix metalloproteinases and bone. *Bone* 2008;43:7-18.
74. Hollberg K, Hultenby K, Hayman A, Cox T, Andersson G. Osteoclasts from mice deficient in tartrate-resistant acid phosphatase have altered ruffled borders and disturbed intracellular vesicular transport. *Exp Cell Res* 2002;279:227-238.
75. Blair HC. How the osteoclast degrades bone. *Bioessays* 1998;20:837-846.
76. Sly WS, Hu PY. Human carbonic anhydrases and carbonic anhydrase deficiencies. *Annu Rev Biochem* 1995;64:375-401.
77. Supanchart C, Kornak U. Ion channels and transporters in osteoclasts. *Arch Biochem Biophys* 2008;473:161-165.
78. Hattersley G, Chambers TJ. Calcitonin receptors as markers for osteoclastic differentiation: correlation between generation of bone-resorptive cells and cells that express calcitonin receptors in mouse bone marrow cultures. *Endocrinology* 1989;125:1606-1612.
79. Lee SK, Goldring SR, Lorenzo JA. Expression of the calcitonin receptor in bone marrow cell cultures and in bone: a specific marker of the differentiated osteoclast that is regulated by calcitonin. *Endocrinology* 1995;136:4572-4581.
80. Omar OM, Lenneras ME, Suska F, Emanuelsson L, Hall JM, Palmquist A, Thomsen P. The correlation between gene expression of proinflammatory markers and bone formation during osseointegration with titanium implants. *Biomaterials* 2011;32:374-386.
81. Monjo M, Lamolle SF, Lyngstadaas SP, Ronold HJ, Ellingsen JE. In vivo expression of osteogenic markers and bone mineral density at the surface of fluoride-modified titanium implants. *Biomaterials* 2008;29:3771-80.
82. Donos N, Retzepi M, Wall I, Hamlet S, Ivanovski S. In vivo gene expression profile of guided bone regeneration associated with a microrough titanium surface. *Clin Oral Implants Res* 2011;22:390-398.
83. Ivanovski S, Hamlet S, Salvi GE, Huynh-Ba G, Bosshardt DD, Lang NP, Donos N. Transcriptional profiling of osseointegration in humans. *Clin Oral Implants Res* 2011;22:373-381.
84. Eriksson C, Nygren H, Ohlson K. Implantation of hydrophilic and hydrophobic titanium discs in rat tibia: cellular reactions on the surfaces during the first 3 weeks in bone. *Biomaterials* 2004;25:4759-66.
85. Eriksson C, Broberg M, Nygren H, Oster L. Novel in vivo method for evaluation of healing around implants in bone. *Journal of Biomedical Materials Research* 2003;66A:662-668.
86. Kim YD, Kim SS, Hwang DS, Kim SG, Kwon YH, Shin SH, Kim UK, Kim JR, Chung IK. Effect of low-level laser treatment after installation of dental titanium implant-immunohistochemical study of RANKL, RANK, OPG: An experimental study in rats. *Lasers in surgery and medicine* 2007;39:441-450.
87. Liao H, Brandsten C, Lundmark C, Wurtz T, Li J. Responses of bone to titania-hydroxyapatite composite and nacreous implants: A preliminary comparison by in situ hybridization. *Journal of Materials Science: Materials in Medicine* 1997;8:823-827.
88. Ysander M, Branemark R, Olmarker K, Myers RR. Intramedullary osseointegration: Development of a rodent model and study of histology and neuropeptide changes around titanium implants. *Journal of Rehabilitation Research and Development* 2001;38:183-190.
89. Yamano S, Berley JA, Kuo WP, Gallucci GO, Weber HP, Sukotjo C. Effects of nicotine on gene expression and osseointegration in rats. *Clin Oral Implants Res* .
90. Ozawa S, Ogawa T, Iida K, Sukotjo C, Hasegawa H, Nishimura RD, Nishimura I. Ovariectomy hinders the early stage of bone-implant integration: histomorphometric, biomechanical, and molecular analyses. *Bone* 2002;30:137-43.

91. Vandamme K, Holy X, Bensidhoum M, Logeart-Avramoglou D, Naert I, Duyck J, Petite HX. Establishment of an in vivo model for molecular assessment of titanium implant osseointegration in compromised bone. *Tissue Eng Part C Methods* .
92. Karimbux NY, Sirakian A, Weber HP, Nishimura I. A new animal model for molecular biological analysis of the implant-tissue interface: spatial expression of type XII collagen mRNA around a titanium oral implant. *J Oral Implantol* 1995;21:107-13; discussion 114-5.
93. Petzold C, Rubert M, Lyngstadaas SP, Ellingsen JE, Monjo M. In vivo performance of titanium implants functionalized with eicosapentaenoic acid and UV irradiation. *J Biomed Mater Res A* .
94. Taxt-Lamolle SF, Rubert M, Haugen HJ, Lyngstadaas SP, Ellingsen JE, Monjo M. Controlled electro-implementation of fluoride in titanium implant surfaces enhances cortical bone formation and mineralization. *Acta Biomater* ;6:1025-32.
95. Roser K, Johansson CB, Donath K, Albrektsson T. A new approach to demonstrate cellular activity in bone formation adjacent to implants. *J Biomed Mater Res* 2000;51:280-91.
96. Colnot C, Romero DM, Huang S, Rahman J, Currey JA, Nanci A, Brunski JB, Helms JA. Molecular analysis of healing at a bone-implant interface. *J Dent Res* 2007;86:862-7.
97. Chikazu D, Tomizuka K, Ogasawara T, Saijo H, Koizumi T, Mori Y, Yonehara Y, Susami T, Takato T. Cyclooxygenase-2 activity is essential for the osseointegration of dental implants. *Int J Oral Maxillofac Surg* 2007;36:441-6.

Chapter 3

Comparative Molecular Assessment of Early Osseointegration in Implant-Adherent Cells: Rat model

Abstract:

Objective: to identify the early molecular processes involved in osseointegration associated with a micro roughened and nanosurface superimposed featured implants.

Materials and methods: Thirty-two titanium implants with surface topographies exhibiting a micro roughened (AT-II) and nanosurface superimposed featured implants (AT-I) were placed in the tibiae of 8 rats and subsequently harvested at 2 and 4 days after placement. Total RNA was isolated from cells adherent to retrieved implants. A whole genome microarray using the Affymetrix Rat gene 1.1 ST Array followed by validation of select genes through qRT-PCR was used to describe the gene expression profiles that were differentially regulated by the implant surfaces.

Results: Whilst significant differences at the gene level were not noted when comparing the two-implant surfaces at each time point, the microarray identified several genes that were differentially regulated at day 4 vs. day 2 for both implant surfaces. A total of 649 genes were differentially regulated at day4 vs. day2 in AT-I and 392 genes in AT-II implants. Functionally relevant categories related to ossification, skeletal system development, osteoblast differentiation, bone development, bone mineralization and biomineral tissue development were upregulated and more prominent at AT-I (day 4 vs. day2) compared to AT-II. Analysis of the downregulated gene lists (day 4 vs. day 2) with average fold change >2 (were not stastically significant) revealed the biological processes involved with the inflammatory/immune response gene expression. The

number of genes that were associated with the inflammatory/immune response category was greater for AT-I than AT-II.

Conclusions: The presence of nanosurface features modulated in vivo bone response. This work confirms previous evaluations and further implicates modulation of the inflammatory/immune responses as a factor affecting the accrual of bone mass shortly after implant placement.

Introduction:

The placement of endosseous implants is a common treatment option to treat edentulism. The success of dental implants is based on the concept of osseointegration introduced by Branemark[1]. Despite the high success rates achieved, implant failures that mandate implant removal do occur. Factors attributing to implant failures include local and systemic conditions such as reduced bone volume, reduced bone density, periodontitis, and impaired wound healing (e.g., diabetes, smoking, osteoporosis, radiation therapy, chemotherapy) [2-6]. Efforts to enhance osseointegration of dental implants allowing for faster prosthetic rehabilitation and improved success rates in clinically challenging situations, included modifications to the physical and chemical properties of the implants surfaces. It is well demonstrated that implants with moderately rough surfaces (average height deviation of 1-2 μ m) [7] enhance the rate and quality of osseointegration with greater bone-to-implant contact and higher resistance to torque removal[8-12].

In contrast to micron-features of alloplastic materials, bone is composed of constituent nanofeatures[13]. Nanostructured materials are those with features less than 100nm in at least one dimension[14]. Simulation of nanofeatures at implant surfaces has shown favorable bioactivities with titanium surfaces[15]. Enhanced in vivo bone responses to implants with nanofeatures compared to machined or micro roughened surfaces measured by histological and biomechanical means have been shown in several animal models (eg, rabbits, dogs, rats) [16-23]. The topography of titanium surface at the nanolevel has been reported to modulate differentiation, proliferation, and increase expression of osteogenic markers[17,24,25]. Yet, the exact role of nanosurface topography on the molecular events occurring early in the process of osseointegration remains poorly understood. Prior studies mainly focused on select target genes; typically markers for osteoblasts including *Cbfa1/Runx2* [26,27] , *Osterix (Osx)* [26-29] , *Osteocalcin (Ocn)* [30-34] , *Osteopontin (Opn)* [35-38] , *Collagen I* [39-42] and *Alkaline phosphatase (Alp)* [27,29,43,44] .

It is of interest to further investigate the overall gene expression profiles by implant adherent cells during the early phase of osseointegration. The advent of gene expression microarrays allows the rapid and high-throughput quantification of thousands of genes simultaneously [45]. Microarray analysis may unveil the regulation of individual genes that might not be identified otherwise. These molecular details may represent targets for future therapeutic improvement. Most recently, this approach has been applied in vitro in the analysis of MG63 osteoblastic- cell response to a nanoporous Ti6AL4V surface (produced by blasting with tricalcium

phosphate and light nitric acid treatment; nanoPORE, Out-Link, Sweden and Martina, Due Carrare, Padova, Italy) [46]. However, we recognize that the biological environment *in vivo* is very different from the *in vitro* conditions and contains a variety of cells that each can respond to the implant surface and produce several cytokines and growth factors influencing each other's behavior. Few whole genome-wide profiling studies have been reported using *in-vivo* models [47-49]. Profiles of gene expression of *in vivo* bone healing with or without titanium implants (osteotomy sites) were described in a rat model [48,50] at different time points with 1 week time point representing the earliest analysis[50]. Moreover, Donos et al [47] reported on the gene expression profiles associated with a moderately rough surface (SLA) compared to a chemically modified moderately rough surface (SLActive) in a human model. The microarray analysis was carried out at 4, 7 and 14 days post surgery.

Various methods have been developed in order to create a nanosurface. Typically applied techniques include lithography, ionic implantation, anodization, acid etching, alkali treatment, peroxidation and sol-gel deposition[15,51]. Recently, Johansson et al. [52], reported on a newly developed nanosurface (AT-I) produced by sequential chemical treatment with oxalic acid and hydrofluoric acid preceded by blasting with titanium oxide particles. These implants were tested in a rabbit model and compared with implants with micro-roughened surface (AT-II). The results demonstrated greater 2D bone-to-implant contact and 3D removal torque values for the nanosurface implants. The objective of the present study was to further investigate the effect of this newly developed nanosurface (AT-I) topography imposition on the whole genome expression profiles at early time points in the process of osseointegration using an *in-vivo* rat model and compare it to those of the micro-roughened surface (AT-II).

Materials and methods:

Implants:

Newly developed implant surfaces of commercially pure titanium grade IV screws (2.0mmx3.0mm) were used in this study. The test samples were manufactured per protocol described previously by Johansson et al, 2011[52]. Briefly, the samples were degreased, blasted with titanium oxide particles and rinsed in sterile water. These samples were then treated in a different sequential process resulting in two different surface structures. One sample group was treated in oxalic acid, named AT-II, while the other group was treated in oxalic acid and hydrofluoric acid sequentially (AT-I). All implants are washed by sterile water and beta-sterilized.

Surface characterization:

The implant surfaces were examined by a high-resolution scanning electron microscope [ESEM XL30, FEI Company, 5651 GG Eindhoven, the Netherlands]. The three-dimensional surface parameters were determined using optic interferometry (MicroXam, Phase-Shift, Tucson, AZ). Three specimens of each surface type was analyzed, and each specimen was analyzed in three areas. Errors of form were removed using a Gaussian filter size of 50x50mm. Surface roughness values were reported by the S_a and $S_{dr}\%$ values per the suggested guidelines by Wennerberg A & Albrektsson T for the topographic evaluation of implant surfaces. [53]

The S_a represents the average height of the analyzed area

The S_{dr} represents the developed interfacial area ratio %

The chemical nature of the surfaces was examined using X-ray photoelectron spectroscopy (XPS). A Quantum 2000 ESCA Scanning Microscope A Quantum 2000 ESCA Scanning Microscope (Physical Electronics, Chanhassen, MN, USA) with an X-ray source of monochromatic AlK α was used to obtain a spectrum for each surface. The mean numbers and standard deviation (SD) were deduced from measurements of three implants per group with two regions per implants resulting in n=6 per implant type. The wettability was measured by using the sessile drop technique on titanium coins with the AT-I and AT-II surfaces.

Model:

A rat tibia model of osseointegration was used [18,54]. All procedures were approved by the Institutional Animal Care and Use Committee at the University of North Carolina, Chapel Hill (IACUC ID: 10-127.0). Eight male Sprague Dawley rats (326-350 g) were purchased from Harlan laboratories and acclimated for 7 days prior to initiation of studies. Anesthesia was achieved using Ketamine/Xylazine (80-100mg/kg and 10 mg/kg respectively) along with supplemental local anesthesia (Lidocaine 2% with epinephrine (1:100,000)). The dorsal/medial aspect of the tibiae was identified, shaved, and disinfected using betadine and 70% ethanol scrub. Using aseptic technique, a full thickness myocutaneous flap was made and carefully retracted to reveal the medial aspect of the tibia bone. With sterilized stainless steel burs, two drill holes were created with copious irrigation. The drill holes were made approximately 5 mm apart. Two implants (cp titanium) were placed in each tibia to provide sufficient RNA for each experimental sample. For every time point (day 2 and 4), 4 rats were used. Each animal received two AT-I implants in one tibia and two AT-II implants in the contralateral

tibia (randomly distributed). The periosteum was adapted over the site using interrupted 4-0 chromic gut sutures for subcuticular closure. The skin was then closed using vicryl sutures. Animals were monitored continuously following surgery. Ambulation was the defined criteria for immediate recovery. A postoperative analgesic was provided for 48 hours after surgery, by means of subcutaneous ketoprofen injections (5mg/kg) once daily. At the time of sacrifice, each animal was placed in a CO₂—saturated chamber. Death was assured by thoracotomy and severance of the inferior vena cava for exsanguination.

RNA isolation:

At 2 and 4 days following surgery, animals were euthanized. Immediately thereafter, the tibia sites were isolated and the implant site was exposed using sterile technique and the entire tibias were harvested and the implants were explanted by fracture of the tibia. For evaluation of mRNA expression in cells adherent to explanted endosseous implant surfaces, the implants were rinsed in cold PBS immediately following retrieval and then placed into 1000 µl of Tri-reagent. Total RNA was isolated from the lysates using the standard Tri-reagent protocol and collected by ethanol precipitation. This was followed by purification using RNeasy MinElute Clean up kit (Qiagen, Valencia, CA, USA). RNA was assessed for quality and quantity using a bioanalyzer (Agilent, Santa Clara, CA, USA) and nanodrop ND-1000 spectrophotometer (Nanodrop, Wilmington, DE) respectively. Samples were processed and hybridized to the Affymetrix Rat gene 1.1 ST Array at the UNC core facility following the manufacturer's recommended protocols and reagents (Affymetrix, San Clara, CA). The Rat Gene 1.1 ST Array Plate interrogates more than 27,000 well-annotated genes with more than 720,000 distinct probes. The raw microarray data is available online at the NCBI-GEO (<http://www.ncbi.nlm.nih.gov/geo/>) database, accession number GSE35976.

Microarray data analysis:

Data analysis was completed using GeneSpring software v.11.5.1 (Agilent Technologies, Santa Clara, CA). 2-Way ANOVAs statistical analysis was applied to determine differentially expressed genes among the various parameters (implant surface type and time points). Further analysis included pairwise comparisons of each implant surface independently at the different time points (day4 vs. day 2). A p-value of 0.05 was used as the threshold for statistical significance. Exported lists included significant genes, fold changes and p-values for comparisons. These lists of genes were then condensed into organized classes of related biology using The GO Ontology Browser function in the GeneSpring. Significant GO P<0.05 was corrected for multiple sampling

using the method of Benjamini and the Hochberg false discovery rate method[55]. In addition, to focus on the major gene expression changes, we analyzed genes with over twofold-changed expression compared to control.

Real-time quantitative PCR:

Following microarray analysis, quantitative real-time PCR (qRT-PCR) was performed using the same RNA samples in order to validate expression patterns for select genes. We have selected the following genes for this RT-qPCR validation: highly upregulated genes (*Phex*, *Aspn*, *Satb2*), known osteoblast marker (*Bsp*), highly downregulated genes with greater than 2 fold change (*Il-1 β* , *Cxcl2*, *Ccl3* (all belonged to the inflammatory response). First strand cDNA was synthesized (Superscript III, Invitrogen) from total RNA (500 ng) in a standard 20- μ l reaction. Subsequently, equal volumes of cDNA were used to run real-time PCR reactions specific for mRNAs encoding the following markers: phosphate regulating endopeptidase homolog, X-linked (Assay ID: Rn00448130_m1), pannexin 3 (Assay ID: Rn01640170_m1), SATB homeobox 2 (Assay ID: Rn01438160_m1), Ibsp (Assay ID: Rn00561414_m1), interleukin 1 beta (Assay ID: Rn00580432_m1), chemokine (C-C motif) ligand 3 (Assay ID: Rn01464736_g1), chemokine (C-X-C motif) ligand 2 (Assay ID: Rn00586403_m1). Reactions were performed using TaqMan Universal PCR Master Mix and thermocycling in an ABI 7200 real-time thermocycler (Applied Biosystems, Foster City, CA). Relative mRNA abundance was determined by the $2^{-\Delta\Delta C_t}$ method and reported as -fold induction. GAPDH mRNA abundance was used for normalization[56]. Samples were run in triplicate and the average was used for further analysis. The data points analyzed were 2 and 4 days. The surface-matched Day2 was used as a calibrator.

Results:

Surface analysis:

SEM images (Figure1) revealed a micro-roughened surface for AT-II, whereas AT-I produced by the additional treatment of hydrofluoric acid is comprised of nanostructures superimposed on a moderately roughened surface. Measurements of surface parameters (Table 1) showed that the two surfaces examined have similar S_a values. XPS analysis (Table 2) showed a significantly higher carbon signal for the AT-II sample and presence of oxalate in the surface oxide for this sample. Both surfaces were hydrophobic (AT; a contact angle of 90-110°, AT-II; a contact angle of $\sim 90^\circ$).

Microarray data:

To gain insight into the mechanisms by which surface topography influences the process of

osseointegration, quadruplicate genome wide expression studies of implant adherent cells were performed as a function of time (t=2,4 days) with either micro (AT-II) or nanosurface topology implants (AT-I).

2-Way ANOVA was applied to determine differentially expressed genes among the various parameters (implant surface type and time points). No genes were identified (p -value <0.05) to be different when comparing the 2 implants surfaces at each time point. Further analysis included pairwise comparisons of each implant surface independently at the different time points (day 4 vs. day2) to allow understanding of the early molecular events occurring at either surface (AT-I, AT-II). 649 genes were found to be differentially expressed (p -value ≤ 0.05) at AT-I; of these, 601 were upregulated, and 48 were downregulated. On the other hand, 392 genes were found to be differentially expressed ($p \leq 0.05$) at AT-II; of these, 294 were upregulated and 98 were downregulated (Table 3). The identity of the top 35 genes differentially expressed at the two implants surfaces (day 4 vs. day 2; p -value <0.05) is shown in tables 4 and 5. Another table (table 6) was created to include list of top 25 differentially expressed genes (p -value ≤ 0.05) at AT-I (Day 4 vs. day2) with their fold regulation in AT-I, AT-II. Nevertheless, the downregulated subset of genes that reached statistical significance (p -value <0.05) did not include any with fold regulation more than 2. The top 25-downregulated genes at AT-I and AT-II are listed in tables 7 and 8.

Validation of Affymetrix microarray data by qRT-PCR

The abundance of selected gene transcripts was analyzed on each implant surface at the different time points using RT-qPCR. Table 9 summarizes results obtained with the two techniques for the selected genes (*Aspn*, *Phex*, *Satb2*, *Bsp*, *Cxcl2*, *Ccl3*, *Il-1 β*). The results were expressed as mean fold change. Results obtained from RT-qPCR were in full concordance with those from microarray, validating our microarray results.

Identification of significant gene ontologies associated with the different implant surfaces

GO analysis was carried out on the differentially regulated genes between day 4 and day 2 (fold change ≥ 2 ; $p \leq 0.05$) at both implants surfaces. These sets of genes comprised only upregulated genes and did not include downregulated genes. As mentioned earlier, the downregulated subset of genes that reached statistical significance included only genes with less than 2 fold downregulation. To focus on the major changes that might have been caused by reduced expression, another analysis was carried out on the downregulated genes

with more than 2 fold (p-value>0.05).

GO terms upregulated at AT-I, AT-II (day 4 compared with day 2)

The gene functional annotation identified at AT-I consisted of a large variety of processes. 80 terms satisfied $p \leq 0.05$. Functionally relevant categories relevant to ossification, skeletal system development, skeletal system morphogenesis, osteoblast differentiation, bone development, bone mineralization and biomineral tissue development were clearly demonstrated at AT-I. Fourteen genes associated with ossification were differentially upregulated ($P \leq 0.05$) at AT-I. The increased expression of ossification genes at the AT-I surface is consistent with the notion that there is an active and accelerated bone formation at this time point (Day4). These genes included *Fgfr2* (4.55 fold), *Ostn* (2.23 fold), *Dmp1* (9.67 fold), *Bmp3* (8.25 fold), *Aspn* (14.61 fold), *Coll1a1* (5.91 fold), *Mef2c* (2.03 fold), *Coll1a2* (2.3 fold), *Dlx5* (3.86 fold), *Ptn* (2.63 fold), *Sp7* (3.55 fold), *Pth1r* (5.88 fold), *Runx2* (2.33 fold) and *Satb2* (9.15 fold). This list also demonstrates the representation associated to extracellular matrix, developmental processes, cell adhesion, collagen fibril organization and regulation of cell proliferation. Interestingly, there was a representation of neurogenesis and axonogenesis.

Nevertheless, 70 GO terms satisfied the p-value cut off 0.05 in AT-II. Several functionally GO categories were over-represented in the list of genes that were up regulated at AT-II, including the category of extracellular matrix, cell adhesion and collagen fibril organization. Likewise to AT-I, neurogenesis was also prominent at AT-II. Significantly, the category related to bone was limited to ossification and skeletal system development. Bone biomineralization and biomineral tissue development were not identified by this GO analysis at AT-II surface. The counts of genes involved in both categories in AT-II were less than those in AT-I; with skeletal development count limited to 7 genes in AT-II opposed to 15 genes in AT-I and ossification count limited to 3 in AT-II opposed to 14 in AT-I. Furthermore, our results identify higher p-values for both ossification ($p=0.0025$) and skeletal system development ($p=0.00122$) in AT-II in comparison with the p-values for these categories in AT-I (ossification; $p\text{-value}=8.66\text{E-}09$, skeletal system development; $p\text{-value}=1.01\text{E-}07$). The p-value for each GO term reflects the enrichment in frequency of that GO term in the entity list, which further emphasizes the presence of enhanced bone response in AT-I at this early stage of osseointegration (Day4).

GO terms downregulated at AT-I, AT-II (day 4 compared with day 2)

Further functional annotation analysis of the downregulated lists of AT-I and AT-II highlighted several categories in this domain. 205 terms satisfied $p \leq 0.05$ in AT-I, with only 21 terms in AT-II. Table 12 outlines the top 25 GO terms in AT-I and table 13 outlines the 21 terms that met the eligibility criteria in AT-II.

An overrepresentation of functional annotations associated with inflammatory response, immune response and chemotaxis were essentially demonstrated by both surfaces. However, examination of the number of genes associated with each GO term in both lists show that AT-I is by far associated with a higher number of genes in each functional GO term. This implies that AT-I surface might have a role in rapidly downregulating a wide range of genes associated with the inflammatory and immune response processes in the early days following implant placement. This is also highlighted when we examine the list of genes downregulated at both surfaces (Tables 7 and 8) with further more downregulation of several inflammatory genes at AT-I. We recognize that these lists of genes did not reach statistical significance. However, this could be due to the proximity of the two data points analyzed.

Discussion:

This study describes the detailed genetic responses to a micro-roughened (AT-II) and nanostructured (AT-I) implant surfaces in a rat tibia model. With the advent of molecular biology techniques, comparative analysis of gene expression of a large number of genes spanning a significant fraction of the genome using microarrays and not only a few selected activities is possible. This also allows interrogation of broad biological processes as well as individual genes. This analysis effectively reveals the early cellular and molecular mechanisms that drive the process of osseointegration at both surfaces using the Affymetrix Rat gene 1.1 ST Array. The transcriptional analysis described in this study reports the gene expression profiles associated with osseointegration at days 2 and 4 following implant placement. The choice of time points was taken to detect very early molecular events.

Whilst significant differences at the gene level were not noted when comparing the two-implant surfaces at each time point, the general trend was striking. Pairwise comparisons of each implant surface at the two time points (day 4 vs. day 2) allowed us to further comprehend the initial wound healing process associated with

each implant surface. 649 genes were found to be differentially expressed at AT-I and 392 genes were found to be differentially expressed at AT-II. The gene expression profile in AT-I at day 4 is characteristic of induced bone formation with the over-representation of the functional biological processes related to ossification, skeletal system development, osteoblast differentiation and biomineral formation with greater number of genes that were up-regulated in each category in response to the AT-I surface compared with the AT-II surface. Hence, more rapid bone formation is expected with AT-I surface. This is in agreement with published histological and biomechanical data comparing these two implant surfaces at 6 weeks in a rabbit model showing greater implant-bone contact and higher torque removal values for AT-I surface compared with AT-II surface [52]. The genes associated with skeletogenesis at AT-I included *Fgfr2*, *Ostn*, *Dmp1*, *Bmp3*, *Aspn*, *Col11a1*, *Mef2c*, *Col11a2*, *Dlx5*, *Ptn*, *Sp7*, *Pth1r*, *Runx2*, *Satb2*, *Shox2*, *Papss2*, *Pdgfra*, *Gli3*, *Mmp2*, *Tbx15*, *Ryk*, *Vdr* and *Phex*. Implants placed in the jaws often penetrate the bone marrow cavity coming in direct contact with several different cell types including hematopoietic cells, fibroblasts, vascular pericytes and those with an osteogenic capacity (including osteoblasts and MSCs), which was definitely the case in our rat tibia model. The potential of a surface to elicit osseointegration is dependent on its ability to induce the differentiation of pluripotent mesenchymal stem cells along the osteoblast cell lineage and stimulate the secretion of a calcified matrix by these osteoblasts [57]. This is orchestrated by several transcriptional factors, among which is RUNX2, OSX and SATB2 which regulate the expression of several bone matrix extracellular protein genes that encode for bone sialoprotein, osteocalcin and collagen type I [58-61]. Modulation of *Runx2* and *Osx* expression by the presence of nanosurface features on implant surfaces topography has been observed by several investigations [18,24,26]. Recent evidence showed that SATB2 is a downstream of OSX. *Satb2* knock out mice exhibit multiple craniofacial defects including a significant truncation of the mandible, a shortening of the oral maxillofacial bones, and defects in osteoblast differentiation [61]. The potential role of *SATB2* in osseointegration has been observed in a recent microarray data demonstrating its differential upregulation (2.5 fold) on a chemically modified surface (SLActive) between day 4 and day 14 [49] in a human model. Other genes in our data lists associated with skeletogenesis that were also upregulated in the aforementioned microarray data included COL11A1, COL11A2, PHEX, DLX5, SP7, PTHR1, PTN and PDGFRA. The precise role of each of these genes in the modulation of osseointegration requires further investigation.

Furthermore, day 4 demonstrated the representation associated to extracellular matrix, cell adhesion,

collagen fibril organization and regulation of cell proliferation in both surfaces.

We realize that the process of osseointegration may be affected by regulation of other cells resident in the blood clot and bone marrow. Analysis of implants adherent gene expression profiles that were downregulated at day 4 suggested a decline in the inflammatory/immune responses. Even though this subset of genes did not reach statistical significance; which could be due to the proximity of the two data points analyzed, its relevance is very critical. Indeed, AT-I was by far associated with greater number of genes associated with inflammatory/immune responses that were downregulated. Furthermore, this is highlighted with further more downregulation of several inflammatory associated genes at AT-I (Tables 7 and 8). The role of implant surface topography and/or chemistry on modulating the inflammatory/immune response has been suggested by several studies. An in vivo study using the rat tibia model demonstrated a higher expression of *Tnf- α* (after 6 and 28 days) and *Il-1 β* (6, 14 and 28 days) on machined surfaces compared to the oxidized implants[62]. Furthermore, an in vitro investigation using RAW264.7 cells grown on a nanoscale calcium phosphate coated titanium implants elicited a gene expression profile with marked downregulation of several pro-inflammatory cytokines (*Tnf- α* , *Il-1 β* , *Il-1 δ*), chemokines (*Ccl2*, *Ccl3*, *Ccl5*, *Ccl8*, *Ccl11*, *Ccl12*) and the chemokine receptors *Ccr1* and *Xcr1*[63]. On the other hand, the effect of chemical modification of titanium implants on macrophage cytokine gene expression has been reported; hydrophilic implant surfaces (SLActive) resulted in a significant downregulation of key pro-inflammatory cytokines *Tnf- α* , *Il-1 α* , *Il-1 β* and the chemokine *Ccl-2* in RAW 264.7 cells 24 hours post seeding compared with either smooth polished or sandblasted acid-etched (SLA) surfaces [64].

These surface specific responses suggest that the presence of nanotopographic cues on the titanium surface topography may modulate the various implant adherent cells resulting in unique differential phenotypes affecting inflammatory, mesenchymal stem cells, and osteoblastic cells. These biological advantages acquired by the imposition of nano-features through triggering of gene expression crucial for osteoblast differentiation, skeletal development and the rapid decline in inflammatory related processes in nanosurface adherent cells may provide a cardinal role into how we can make more bone faster. However, the present study did not segregate potential effects of surface chemistry.

Conclusion:

The present study investigated experimental surfaces with either nanosurface vs. a moderately rough surface in a rat tibia model at early implantation times. Here, initial efforts were deployed to unravel the molecular mechanism early in the process of osseointegration associated with micro-roughened and nanosurface dental implants. The nanosurface modulates earlier and higher bone repair response as revealed by the recruited expression of gene involvements in the processes related to skeletal development, ossification and osteoblast differentiation. A potential role of the nanosurface in downregulating the inflammatory/immune responses at a faster rate than a micro-roughened surface is implicated. Comprehensive understanding of the complex biological events occurring the bone implant interface will ultimately lead to improve biologically driven strategies for improved osseointegration. In this study distinct biochemical responses that underlie the process of osseointegration to the nanosurface were revealed, which could not have been observed through the use of selected gene studies or through in vitro exams. Further detailed studies using additional points may verify the significance of the results obtained. In addition, complementary in vitro and in vivo studies (using genetically modified animals) are required to identify the biological roles of the isolated gene transcripts.

Figure 1. Scanning electron microscopic (SEM) evaluation of tested implant surfaces (a) AT-I surface blasted with TiO₂ particles and sequentially treated in oxalic and hydrofluoric acid (b) AT-II surface blasted with TiO₂ particles and treated in oxalic acid at 5000X magnification (c) AT-I and (d) AT-II at 50000X. Note that AT-I surface is randomly covered with topography features of approximately 100nm.

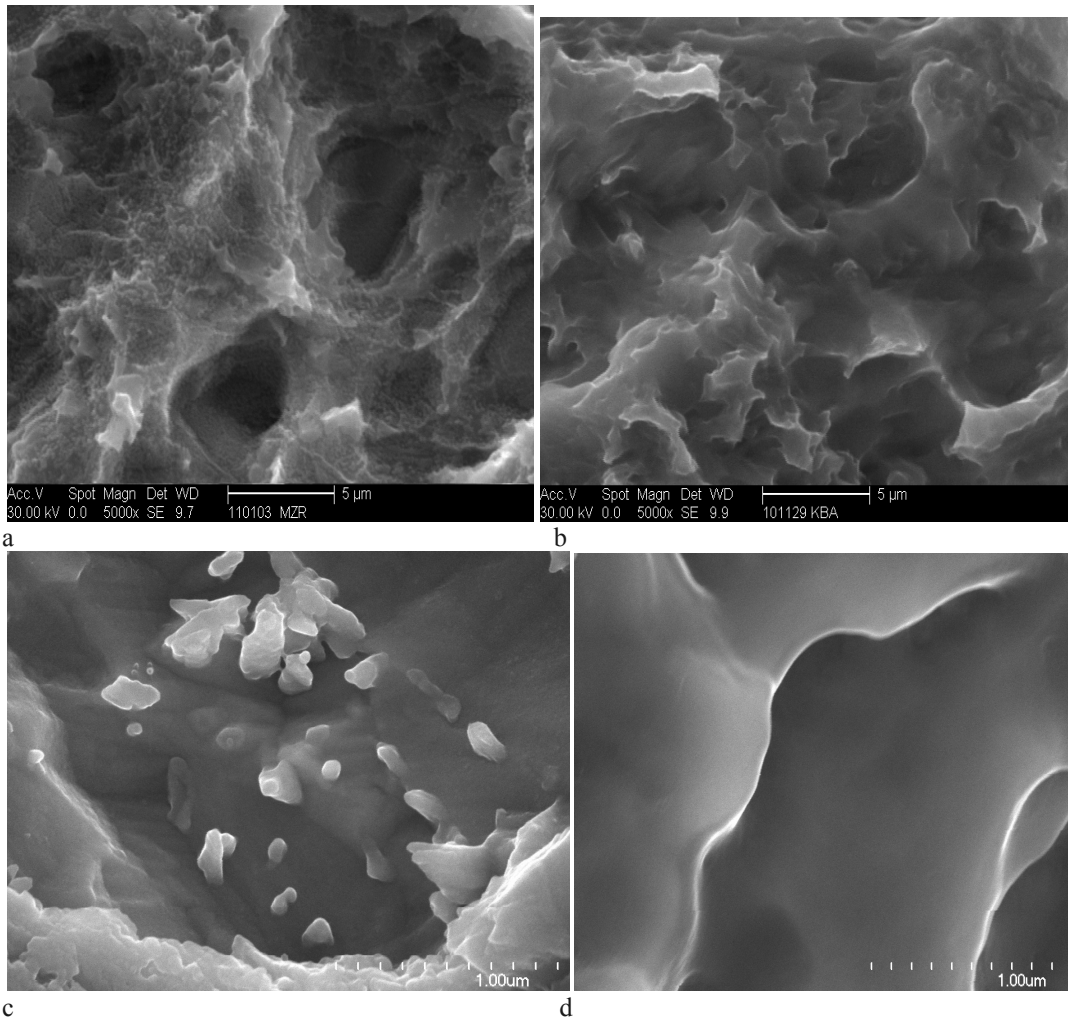


Table 1:
Surface roughness values as determined by optical interferometry ((MicroXam, PhaseShift).

Sample	S _a (μm)	S _{dr} (%)
AT-I	1.50 (0.15)	45.52 (8.98)
AT-II	1.58 (0.16)	66.01 (10.43)

The mean numbers and standard deviation (SD) are deduced from measurements of three implants per group with three regions per implant type (n=27).

Table 2:Quantitative chemical surface composition (atomic percentage) as determined by X-ray photoelectron spectroscopy (Quantum 2000ESCA Scanning Microscope, Physical Electronics)

Surface type	C1s	N1s	O1s	Ti2p	Si2p	F1s
AT-I	24.48 (5.36)	1.06 (0.59)	52.31 (3.72)	20.88 (3.47)	0.50 (1.11)	0.31(0.79)
AT-II	30.41 (7.66)	1.40 (0.62)	48.62 (5.02)	19.36 (3.56)	0.13 (0.2)	-----

The mean numbers and standard deviation (SD) are deduced from measurements of three implants per group with two regions per implants resulting in n=6 per implant type.

Table 3. Number of genes differentially expressed (Day 4 vs. Day 2)

Comparison	Differentially expressed genes *	Downregulated genes*	Upregulated genes*	Upregulated genes with FC >2	Downregulated genes with FC >2
AT-I	649	48	601	419	93
AT-II	392	98	294	314	19

* Upregulated (>1.1) and downregulated (<1.1) genes with p-value <0.05. FC; fold change

Table 4.: List of the top 35 differentially regulated genes at AT-I (Day4 vs. Day2). P-value <0.05.

Transcripts Cluster Id	Gene symbol	Gene description	Fold change	P-value
10916247	Panx3	pannexin 3	14.85	0.016
10797660	Aspn	asporin	14.61	0.018
10933664	Phex	phosphate regulating endopeptidase homolog, X-linked	13.14	0.015
10797657	Omd	osteomodulin	10.70	0.020
10744687	Slc13a5	solute carrier family 13 (sodium-dependent citrate transporter), member 5	10.15	0.018
10810817	Smpd3	sphingomyelin phosphodiesterase 3, neutral	9.89	0.022
10775375	Dmp1	dentin matrix acidic phosphoprotein 1	9.67	0.016
10928191	Satb2	SATB homeobox 2	9.15	0.023
10775573	Bmp3	bone morphogenetic protein 3	8.25	0.043
10867761	Mmp16	matrix metalloproteinase 16	7.00	0.022
10726676	Ifitm5	interferon induced transmembrane protein 5	6.65	0.016
10853963	Ptprz1	protein tyrosine phosphatase, receptor-type, Z polypeptide 1	6.60	0.020
10729377	Mamdc2	MAM domain containing 2	6.36	0.015
10895075	Dcn	decorin	6.26	0.044
10809540	Mmp2	matrix metalloproteinase 2	6.18	0.036
10869616	Ptprd	protein tyrosine phosphatase, receptor type, D	6.14	0.015
10818502	Col11a1	collagen, type XI, alpha 1	5.91	0.018
10883212	Cgrefl	cell growth regulator with EF hand domain 1	5.90	0.034
10920524	Pth1r	parathyroid hormone 1 receptor	5.88	0.039
10811248	Adamts18	ADAM metalloproteinase with thrombospondin type 1 motif, 18	5.52	0.029
10896263	Cthrc1	collagen triple helix repeat containing 1	5.43	0.048
10834982	Cercam	cerebral endothelial cell adhesion molecule	5.23	0.015
10738177	Fkbp10	FK506 binding protein 10	5.22	0.023
10803323	Cdh2	cadherin 2	5.22	0.016
10890951	Slc8a3	solute carrier family 8 (sodium/calcium exchanger), member 3	5.02	0.015
10744939	Serpinf1	serine (or cysteine) peptidase inhibitor, clade F, member 1	5.00	0.038
10759177	Tmem119	transmembrane protein 119	4.96	0.023
10815679	Mme	membrane metallo endopeptidase	4.85	0.023
10733258	Adamts2	ADAM metalloproteinase with thrombospondin type 1 motif, 2	4.80	0.022
10847474	Creb3l1	cAMP responsive element binding protein 3-like 1	4.76	0.023
10764050	Fmod	fibromodulin	4.76	0.022
10846340	Fkbp7	FK506 binding protein 7	4.70	0.034
10729667	Dkk1	dickkopf homolog 1 (<i>Xenopus laevis</i>)	4.69	0.039
10842500	RGD1562846	similar to Docking protein 5 (Downstream of tyrosine kinase 5) (Protein dok-5)	4.63	0.050

Table 5. List of the top 35 differentially regulated genes at AT-II (day4 vs. day2). P-value ≤0.05.

Transcripts Cluster Id	Gene symbol	Gene description	Fold change	P-value
10933664	Phex	phosphate regulating endopeptidase homolog, X-linked	10.90	0.037
10775375	Dmp1	dentin matrix acidic phosphoprotein 1	9.74	0.036
10744687	Slc13a5	solute carrier family 13 (sodium-dependent citrate transporter), member 5	7.87	0.046
10928191	Satb2	SATB homeobox 2	7.22	0.045
10761446	LOC687426	similar to G protein-coupled receptor 133	6.65	0.031
10853963	Ptprz1	protein tyrosine phosphatase, receptor-type, Z polypeptide 1	6.02	0.037
10726676	Ifitm5	interferon induced transmembrane protein 5	5.84	0.032
10818502	Col11a1	collagen, type XI, alpha 1	5.64	0.047
10817583	Itga10	integrin, alpha 10	5.60	0.031
10764050	Fmod	fibromodulin	5.38	0.032
10871775	Rhbdl2	rhomboid, veinlet-like 2 (Drosophila)	5.30	0.031
10809540	Mmp2	matrix metalloproteinase 2	5.24	0.049
10729667	Dkk1	dickkopf homolog 1 (Xenopus laevis)	5.23	0.031
10883212	Cgref1	cell growth regulator with EF hand domain 1	4.98	0.049
10739455	Gprc5c	G protein-coupled receptor, family C, group 5, member C	4.76	0.031
10890951	Slc8a3	solute carrier family 8 (sodium/calcium exchanger), member 3	4.71	0.031
10869616	Ptprd	protein tyrosine phosphatase, receptor type, D	4.67	0.037
10715416	Loxl4	lysyl oxidase-like 4	4.50	0.032
10915131	Fat3	FAT tumor suppressor homolog 3 (Drosophila)	4.39	0.041
10847474	Creb311	cAMP responsive element binding protein 3-like 1	4.38	0.032
10759177	Tmem119	transmembrane protein 119	4.37	0.039
10733258	Adamts2	ADAM metalloproteinase with thrombospondin type 1 motif, 2	4.33	0.034
10773435	Cpz	carboxypeptidase Z	4.30	0.034
10744939	Serpinf1	serine (or cysteine) peptidase inhibitor, clade F, member 1	4.23	0.046
10742766	Slc36a2	solute carrier family 36 (proton/amino acid symporter), member 2	4.20	0.032
10726620	Sprn	shadow of prion protein homolog (zebrafish)	4.16	0.041
10895075	Dcn	decorin	4.06	0.044
10855348	Zfp862	zinc finger protein 862	3.91	0.034
10752695	Robo2	roundabout, axon guidance receptor, homolog 2 (Drosophila)	3.89	0.037
10846340	Fkbp7	FK506 binding protein 7	3.88	0.046
10739449	Gprc5c	G protein-coupled receptor, family C, group 5, member C	3.85	0.039
10860499	Sema3d	sema domain, immunoglobulin domain (Ig), short basic domain, secreted, (semaphorin) 3D	3.70	0.031
10715667	Kazald1	Kazal-type serine peptidase inhibitor domain 1	3.67	0.034
10866535	Rerg	RAS-like, estrogen-regulated, growth-inhibitor	3.65	0.031

Table 6. List of top 25 differentially expressed genes at AT-I (Day 4 vs. day2) with their fold regulation in AT-I, AT-II.

Gene symbol	Gene description	Fold change ([ATI-Day4] vs [ATI-Day2])	Fold change ([ATII-Day4] vs [ATII-Day2])
Panx3	pannexin 3	14.85*	10.79
Aspn	asporin	14.61*	6.66
Phex	phosphate regulating endopeptidase homolog, X-linked	13.14*	10.90*
Bglap	bone gamma-carboxyglutamate (gla) protein	12.66	10.05
Omd	osteomodulin	10.70*	7.11
Slc13a5	solute carrier family 13 (sodium-dependent citrate transporter), member 5	10.15*	7.87*
Smpd3	sphingomyelin phosphodiesterase 3, neutral	9.89*	6.85
Dmp1	dentin matrix acidic phosphoprotein 1	9.67*	9.74*
Satb2	SATB homeobox 2	9.15*	7.22*
Bmp3	bone morphogenetic protein 3	8.25*	5.93
Mmp16	matrix metalloproteinase 16	7.00*	5.42
Ibsp	integrin-binding sialoprotein	6.94	4.91
Ifitm5	interferon induced transmembrane protein 5	6.65*	5.84*
Ptprz1	protein tyrosine phosphatase, receptor-type, Z polypeptide 1	6.60*	6.02*
Mamdc2	MAM domain containing 2	6.36*	5.36
Dcn	decorin	6.26*	4.06*
Mmp2	matrix metalloproteinase 2	6.18*	5.24*
Ptprd	protein tyrosine phosphatase, receptor type, D	6.14*	4.67*
Col11a1	collagen, type XI, alpha 1	5.91*	5.64*
Cgref1	cell growth regulator with EF hand domain 1	5.90*	4.98*
Pth1r	parathyroid hormone 1 receptor	5.88*	4.46
Adams18	ADAM metalloproteinase with thrombospondin type 1 motif, 18	5.52*	5.03
Cthre1	collagen triple helix repeat containing 1	5.43*	4.09
Cercam	cerebral endothelial cell adhesion molecule	5.23*	4.49

*P-value <0.05.

Table 7. Top 25 downregulated genes at AT-I.

Gene symbol	Gene description	Fold change ([AT-I-Day4] vs. [AT-I-Day2])
Cxcl2	chemokine (C-X-C motif) ligand 2	-9.74
Niacr1	niacin receptor 1	-5.88
Irg1	immunoresponsive 1 homolog (mouse)	-5.33
Car4	carbonic anhydrase 4	-5.06
Nos2	nitric oxide synthase 2, inducible	-4.90
Ccl3	chemokine (C-C motif) ligand 3	-4.72
Il1b	interleukin 1 beta	-4.56
Cxcl1	chemokine (C-X-C motif) ligand 1 (melanoma growth stimulating activity, alpha)	-4.29
Olr1	oxidized low density lipoprotein (lectin-like) receptor 1	-4.29
Il1a	interleukin 1 alpha	-3.73
G0s2	G0/G1switch 2	-3.72
Isg15	ISG15 ubiquitin-like modifier	-3.64
Ptgs2	prostaglandin-endoperoxide synthase 2	-3.46
Il6	interleukin 6	-3.21
Il23a	Interleukin 23, alpha subunit p19	-3.17
Ifit3	interferon-induced protein with tetratricopeptide repeats 3	-3.14
Upp1	uridine phosphorylase 1	-3.13
Cxcl3	chemokine (C-X-C motif) ligand 3	-3.10
Clec4e	C-type lectin domain family 4, member e	-3.09
Rab20	RAB20, member RAS oncogene family	-3.07
Ier3	immediate early response 3	-2.96
Cd274	CD274 molecule	-2.81
Osm	oncostatin M	-2.74
Slpi	secretory leukocyte peptidase inhibitor	-2.73
Il1rn	interleukin 1 receptor antagonist	-2.64

Table 8. Top 25 downregulated genes at AT-II.

Gene symbol	Gene description	Fold change ([ATII-Day4] vs. [ATII- Day2])
Cxcl2	chemokine (C-X-C motif) ligand 2	-3.22
Niacr1	niacin receptor 1	-3.08
Il6	interleukin 6	-2.87
Olr1	oxidized low density lipoprotein (lectin-like) receptor 1	-2.47
Upp1	uridine phosphorylase 1	-2.24
Ass1	argininosuccinate synthetase 1	-2.20
Rab20	RAB20, member RAS oncogene family	-2.20
Irg1	immunoresponsive 1 homolog (mouse)	-2.15
Il1b	interleukin 1 beta	-2.13
Fam111a	family with sequence similarity 111, member A	-2.12
G0s2	G0/G1 switch 2	-2.10
Far2	fatty acyl CoA reductase 2	-2.09
Clec4e	C-type lectin domain family 4, member e	-2.07
Prtn3	proteinase 3	-2.06
Plekhb1	pleckstrin homology domain containing, family B (eectins) member 1	-2.05
Ms4a3	membrane-spanning 4-domains, subfamily A, member 3	-2.03
Fetub	fetuin B	-1.97
RGD1565374	similar to hypothetical protein LOC199675	-1.96
Slpi	secretory leukocyte peptidase inhibitor	-1.94
Car4	carbonic anhydrase 4	-1.93
Cxcl3	chemokine (C-X-C motif) ligand 3	-1.87
Mx2	myxovirus (influenza virus) resistance 2	-1.86
Tspo	translocator protein	-1.82
Nos2	nitric oxide synthase 2, inducible	-1.82
Il1r2	interleukin 1 receptor, type II	-1.81

Table 9. The validation of the array data was carried out by qRT-PCR of select number of transcripts for equal number of AT-I and AT-II samples (n=3).

Gene symbol	Gene description	Affymetrix fold change AT-I (day 4 vs. day 2)	qRT-PCR fold change AT-I (day 4 vs. day 2)	Affymetrix fold change AT-II (day 4 vs. day 2)	qRT-PCR fold change AT-II(day 4 vs. day 2)
Panx3	pannexin 3	14.85*	16.95	10.79	10.18
Phex	phosphate regulating endopeptidase homolog, X-linked	13.14*	14.31	10.90*	10.74
Satb2	SATB homeobox 2	9.15*	10.05	7.22*	7.25
Ibsp	integrin-binding sialoprotein	6.94	7.99	4.91	5.73
Cxcl2	chemokine (C-X-C motif) ligand 2	-9.74	-10.4	-3.22	- 3.7
Ccl3	chemokine (C-C motif) ligand 3	-4.72	-4.93	-1.71	- 2.02
Il1b	interleukin 1 beta	-4.56	-4.17	-2.13	-2.17

Table 10. Top 60 GO terms for differentially regulated genes at AT-I (Day 4 vs Day2). 80 terms satisfied $p < 0.05$

GO ACCESSION	GO Term	Corrected p-value	Count in Selection
GO:0031012	extracellular matrix	5.39E-12	24
GO:0007275	multicellular organismal development	4.90E-10	46
GO:0032502	developmental process	1.35E-09	50
GO:0044421	extracellular region part	8.66E-09	24
GO:0001503	ossification	8.66E-09	14
GO:0048856	anatomical structure development	1.73E-08	41
GO:0007155	cell adhesion	1.73E-08	25
GO:0022610	biological adhesion	1.73E-08	25
GO:0048731	system development	2.15E-08	38
GO:0005576	extracellular region	9.42E-08	42
GO:0001501	skeletal system development	1.01E-07	15
GO:0005578	proteinaceous extracellular matrix	1.18E-07	14
GO:0048513	organ development	5.24E-07	28
GO:0009653	anatomical structure morphogenesis	1.50E-06	23
GO:0048705	skeletal system morphogenesis	8.29E-06	6
GO:0002062	chondrocyte differentiation	2.37E-05	7
GO:0009887	organ morphogenesis	3.24E-05	10
GO:0031175	neuron projection development	7.56E-05	14
GO:0048812	neuron projection morphogenesis	7.56E-05	12
GO:0007409	axonogenesis	8.38E-05	11
GO:0007410			
GO:0000904	cell morphogenesis involved in differentiation	8.56E-05	12
GO:0048666	neuron development	9.23E-05	14
GO:0048468	cell development	1.02E-04	19
GO:0030030	cell projection organization	1.53E-04	14
GO:0048667	cell morphogenesis involved in neuron differentiation	2.46E-04	11
GO:0048858	cell projection morphogenesis	2.54E-04	12
GO:0007399	nervous system development	2.71E-04	19
GO:0048699	generation of neurons	2.71E-04	14
GO:0032990	cell part morphogenesis	2.71E-04	12
GO:0007156	homophilic cell adhesion	2.71E-04	10
GO:0009888	tissue development	2.88E-04	13
GO:0022008	neurogenesis	3.56E-04	14
GO:0004222	metalloendopeptidase activity	4.03E-04	10
GO:0030154	cell differentiation	4.43E-04	27
GO:0051216	cartilage development	5.73E-04	9
GO:0005886	plasma membrane	6.57E-04	50
GO:0005904			
GO:0000902	cell morphogenesis	6.57E-04	13
GO:0007148			
GO:0045790			
GO:0045791			
GO:0048869	cellular developmental process	8.35E-04	27
GO:0030182	neuron differentiation	8.75E-04	14
GO:0001649	osteoblast differentiation	9.74E-04	5
GO:0071944	cell periphery	0.001	50
GO:0032989	cellular component morphogenesis	0.002	13
GO:0016337	cell-cell adhesion	0.002	11
GO:0005509	calcium ion binding	0.003	20

GO:0035107	appendage morphogenesis	0.003	7
GO:0035108	limb morphogenesis	0.003	7
GO:0030199	collagen fibril organization	0.003	5
GO:0048736	appendage development	0.004	7
GO:0060173	limb development	0.004	7
GO:0008237	metallopeptidase activity	0.004	11
GO:0043062	extracellular structure organization	0.005	8
GO:0005913	cell-cell adherens junction	0.005	6
GO:0060348	bone development	0.006	2
GO:0030198	extracellular matrix organization	0.007	8
GO:0030326	embryonic limb morphogenesis	0.007	7
GO:0035113	embryonic appendage morphogenesis	0.007	7
GO:0030282	bone mineralization	0.009	4
GO:0031214	biomineral tissue development	0.009	5
GO:0042127	regulation of cell proliferation	0.011	13
GO:0004714	transmembrane receptor protein tyrosine kinase activity	0.014	2

Table 11. Top 60 GO terms for the differentially regulated genes at AT-II satisfying the criteria of fold upregulation >2 and p-value <0.05. 70 terms satisfying the p-value cut off of 0.05

GO ACCESSION	GO Term	Corrected p-value	Count in Selection
GO:0031012	extracellular matrix	3.92E-10	18
GO:0005576	extracellular region	3.78E-07	32
GO:0005578	proteinaceous extracellular matrix	3.78E-07	11
GO:0044421	extracellular region part	6.84E-07	18
GO:0007155	cell adhesion	7.27E-07	19
GO:0022610	biological adhesion	7.27E-07	19
GO:0032502	developmental process	2.98E-05	25
GO:0048856	anatomical structure development	5.09E-05	21
GO:0007275	multicellular organismal development	6.86E-05	25
GO:0030030	cell projection organization	6.86E-05	11
GO:0048731	system development	1.69E-04	21
GO:0048699	generation of neurons	2.17E-04	12
GO:0031175	neuron projection development	4.09E-04	11
GO:0048468	cell development	5.76E-04	12
GO:0022008	neurogenesis	6.87E-04	12
GO:0000904	cell morphogenesis involved in differentiation	7.09E-04	9
GO:0030198	extracellular matrix organization	7.14E-04	8
GO:0022603	regulation of anatomical structure morphogenesis	7.75E-04	2
GO:0048666	neuron development	7.82E-04	11
GO:0007156	homophilic cell adhesion	8.56E-04	8
GO:0048812	neuron projection morphogenesis	8.56E-04	9
GO:0008237	metallopeptidase activity	8.84E-04	10
GO:0004222	metalloendopeptidase activity	0.001	8
GO:0001501	skeletal system development	0.001	7
GO:0043062	extracellular structure organization	0.001	8
GO:0007409	axonogenesis	0.001	8
GO:0007410			
GO:0009653	anatomical structure morphogenesis	0.001	11
GO:0000902	cell morphogenesis	0.002	10
GO:0007148			
GO:0045790			
GO:0045791			
GO:0048858	cell projection morphogenesis	0.002	9
GO:0032990	cell part morphogenesis	0.002	9
GO:0001503	ossification	0.003	3
GO:0030182	neuron differentiation	0.003	11
GO:0005886	plasma membrane	0.003	35
GO:0005904			
GO:0048667	cell morphogenesis involved in neuron differentiation	0.003	8
GO:0032989	cellular component morphogenesis	0.004	10
GO:0007399	nervous system development	0.005	15
GO:0071944	cell periphery	0.005	35
GO:0045595	regulation of cell differentiation	0.005	3
GO:0016043	cellular component organization	0.006	20
GO:0008046	axon guidance receptor activity	0.006	3
GO:0060284	regulation of cell development	0.009	2
GO:0021891	olfactory bulb interneuron development	0.009	2
GO:0030154	cell differentiation	0.009	15
GO:0030199	collagen fibril organization	0.010	4

GO:0021889	olfactory bulb interneuron differentiation	0.013	2
GO:0048513	organ development	0.013	14
GO:0048869	cellular developmental process	0.013	15
GO:0071840	cellular component organization or biogenesis	0.013	20
GO:0002062	chondrocyte differentiation	0.014	3
GO:2000026	regulation of multicellular organismal development	0.015	2
GO:0005592	collagen type XI	0.017	2
GO:0050925	negative regulation of negative chemotaxis	0.017	2
GO:0009887	organ morphogenesis	0.018	4
GO:0016337	cell-cell adhesion	0.021	8
GO:0051128	regulation of cellular component organization	0.023	2
GO:0019838	growth factor binding	0.030	1
GO:0050793	regulation of developmental process	0.030	3
GO:0009888	tissue development	0.032	5
GO:0009880	embryonic pattern specification	0.038	2
GO:0010453	regulation of cell fate commitment	0.038	1

Table 12. Top 25 GO terms for downregulated genes at AT-I (Day 4 vs Day 2). 205 terms satisfied $p < 0.05$ and fold downregulation > 2 .

GO ACCESSION	GO Term	Corrected p-value	Count in Selection
GO:0006954	inflammatory response	1.79E-14	17
GO:0005126	cytokine receptor binding	1.81E-12	10
GO:0006952 GO:0002217 GO:0042829	defense response	1.81E-12	19
GO:0005125	cytokine activity	3.36E-12	13
GO:0009611 GO:0002245	response to wounding	4.65E-12	18
GO:0009607	response to biotic stimulus	8.17E-12	15
GO:0006955	immune response	8.61E-11	16
GO:0006950	response to stress	9.78E-11	23
GO:0002376	immune system process	2.06E-10	18
GO:0051707 GO:0009613 GO:0042828	response to other organism	1.56E-09	14
GO:0051704 GO:0051706	multi-organism process	3.37E-09	14
GO:0009617 GO:0009618 GO:0009680	response to bacterium	1.50E-08	12
GO:0032496	response to lipopolysaccharide	2.85E-08	10
GO:0002237	response to molecule of bacterial origin	4.57E-08	10
GO:0008009	chemokine activity	4.57E-08	7
GO:0042379	chemokine receptor binding	5.14E-08	7
GO:0042493 GO:0017035	response to drug	8.89E-08	14
GO:0009605	response to external stimulus	1.26E-07	13
GO:0030593	neutrophil chemotaxis	1.33E-07	6
GO:0050896 GO:0051869	response to stimulus	1.58E-07	35
GO:0051384	response to glucocorticoid stimulus	2.02E-07	9
GO:0031960	response to corticosteroid stimulus	3.71E-07	9
GO:0050900	leukocyte migration	8.66E-07	7
GO:0030595	leukocyte chemotaxis	2.32E-06	6
GO:0060326	cell chemotaxis	4.96E-06	6

Table 13. GO terms related to downregulated genes at AT-II. 21 terms satisfied $p < 0.05$ and fold downregulation > 2 .

GO ACCESSION	GO Term	corrected p-value	Count in Selection
GO:0001780	neutrophil homeostasis	0.008	2
GO:0001781	neutrophil apoptosis	0.004	2
GO:0002237	response to molecule of bacterial origin	0.013	4
GO:0002262	myeloid cell homeostasis	0.016	2
GO:0002376	immune system process	0.016	6
GO:0002526	acute inflammatory response	0.016	2
GO:0005125	cytokine activity	0.047	2
GO:0006952 GO:0002217 GO:0042829	defense response	0.014	5
GO:0006953	acute-phase response	0.004	2
GO:0006954	inflammatory response	0.003	5
GO:0006955	immune response	0.013	5
GO:0009611 GO:0002245	response to wounding	0.016	5
GO:0009617 GO:0009618 GO:0009680	response to bacterium	0.024	4
GO:0010574	regulation of vascular endothelial growth factor production	0.016	1
GO:0030593	neutrophil chemotaxis	0.047	2
GO:0032496	response to lipopolysaccharide	0.012	4
GO:0032755	positive regulation of interleukin-6 production	0.047	2
GO:0033028	myeloid cell apoptosis	0.005	2
GO:0045429	positive regulation of nitric oxide biosynthetic process	0.047	2
GO:0050995	negative regulation of lipid catabolic process	0.016	2
GO:0051707 GO:0009613 GO:0042828	response to other organism	0.047	4

References

1. BRANEMARK PI. Vital microscopy of bone marrow in rabbit. *Scand J Clin Lab Invest* 1959;11 Supp 38:1-82.
2. Alsaadi G, Quirynen M, Komarek A, van Steenberghe D. Impact of local and systemic factors on the incidence of oral implant failures, up to abutment connection. *J Clin Periodontol* 2007;34:610-617.
3. Anner R, Grossmann Y, Anner Y, Levin L. Smoking, diabetes mellitus, periodontitis, and supportive periodontal treatment as factors associated with dental implant survival: a long-term retrospective evaluation of patients followed for up to 10 years. *Implant Dent* 2010;19:57-64.
4. Nevins ML, Karimbux NY, Weber HP, Giannobile WV, Fiorellini JP. Wound healing around endosseous implants in experimental diabetes. *Int J Oral Maxillofac Implants* 1998;13:620-629.
5. Takeshita F, Murai K, Iyama S, Ayukawa Y, Suetsugu T. Uncontrolled diabetes hinders bone formation around titanium implants in rat tibiae. A light and fluorescence microscopy, and image processing study. *J Periodontol* 1998;69:314-320.
6. van Steenberghe D, Jacobs R, Desnyder M, Maffei G, Quirynen M. The relative impact of local and endogenous patient-related factors on implant failure up to the abutment stage. *Clin Oral Implants Res* 2002;13:617-622.
7. Wennerberg A, Albrektsson T. On implant surfaces: a review of current knowledge and opinions. *Int J Oral Maxillofac Implants* 2010;25:63-74.
8. Cochran DL, Schenk RK, Lussi A, Higginbottom FL, Buser D. Bone response to unloaded and loaded titanium implants with a sandblasted and acid-etched surface: a histometric study in the canine mandible. *J Biomed Mater Res* 1998;40:1-11.
9. Wennerberg A, Albrektsson T, Andersson B, Krol JJ. A histomorphometric and removal torque study of screw-shaped titanium implants with three different surface topographies. *Clin Oral Implants Res* 1995;6:24-30.
10. Wennerberg A, Hallgren C, Johansson C, Danelli S. A histomorphometric evaluation of screw-shaped implants each prepared with two surface roughnesses. *Clin Oral Implants Res* 1998;9:11-19.
11. Buser D, Schenk RK, Steinemann S, Fiorellini JP, Fox CH, Stich H. Influence of surface characteristics on bone integration of titanium implants. A histomorphometric study in miniature pigs. *J Biomed Mater Res* 1991;25:889-902.
12. Gotfredsen K, Wennerberg A, Johansson C, Skovgaard LT, Hjorting-Hansen E. Anchorage of TiO₂-blasted, HA-coated, and machined implants: an experimental study with rabbits. *J Biomed Mater Res* 1995;29:1223-1231.
13. Bozec L, Horton MA. Skeletal tissues as nanomaterials. *J Mater Sci Mater Med* 2006;17:1043-1048.
14. Balasundaram G, Webster TJ. Nanotechnology and biomaterials for orthopedic medical applications. *Nanomedicine (Lond)* 2006;1:169-176.
15. Mendonca G, Mendonca DB, Aragao FJ, Cooper LF. Advancing dental implant surface technology--from micron- to nanotopography. *Biomaterials* 2008;29:3822-3835.
16. Li Y, Zou S, Wang D, Feng G, Bao C, Hu J. The effect of hydrofluoric acid treatment on titanium implant osseointegration in ovariectomized rats. *Biomaterials* 2010;31:3266-3273.
17. Monjo M, Lamolle SF, Lyngstadaas SP, Ronold HJ, Ellingsen JE. In vivo expression of osteogenic markers and bone mineral density at the surface of fluoride-modified titanium implants. *Biomaterials* 2008;29:3771-3780.

18. Guo J, Padilla RJ, Ambrose W, De Kok IJ, Cooper LF. The effect of hydrofluoric acid treatment of TiO₂ grit blasted titanium implants on adherent osteoblast gene expression in vitro and in vivo. *Biomaterials* 2007;28:5418-5425.
19. Kubo K, Tsukimura N, Iwasa F, Ueno T, Saruwatari L, Aita H, Chiou WA, Ogawa T. Cellular behavior on TiO₂ nanonodular structures in a micro-to-nanoscale hierarchy model. *Biomaterials* 2009;30:5319-5329.
20. Mendonca G, Mendonca DB, Simoes LG, Araujo AL, Leite ER, Duarte WR, Cooper LF, Aragao FJ. Nanostructured alumina-coated implant surface: effect on osteoblast-related gene expression and bone-to-implant contact in vivo. *Int J Oral Maxillofac Implants* 2009;24:205-215.
21. Meirelles L, Arvidsson A, Andersson M, Kjellin P, Albrektsson T, Wennerberg A. Nano hydroxyapatite structures influence early bone formation. *J Biomed Mater Res A* 2008;87:299-307.
22. Ellingsen JE, Johansson CB, Wennerberg A, Holmen A. Improved retention and bone-to-implant contact with fluoride-modified titanium implants. *Int J Oral Maxillofac Implants* 2004;19:659-666.
23. Berglundh T, Abrahamsson I, Albohy JP, Lindhe J. Bone healing at implants with a fluoride-modified surface: an experimental study in dogs. *Clin Oral Implants Res* 2007;18:147-152.
24. Mendonca G, Mendonca DB, Simoes LG, Araujo AL, Leite ER, Duarte WR, Aragao FJ, Cooper LF. The effects of implant surface nanoscale features on osteoblast-specific gene expression. *Biomaterials* 2009;30:4053-4062.
25. de Oliveira PT, Nanci A. Nanotexturing of titanium-based surfaces upregulates expression of bone sialoprotein and osteopontin by cultured osteogenic cells. *Biomaterials* 2004;25:403-413.
26. Valencia S, Gretzer C, Cooper LF. Surface nanofeature effects on titanium-adherent human mesenchymal stem cells. *Int J Oral Maxillofac Implants* 2009;24:38-46.
27. Mendonca G, Mendonca DB, Aragao FJ, Cooper LF. The combination of micron and nanotopography by H₂SO₄/H₂O₂ treatment and its effects on osteoblast-specific gene expression of hMSCs. *J Biomed Mater Res A* ;94:169-79.
28. Guo J, Padilla RJ, Ambrose W, De Kok IJ, Cooper LF. The effect of hydrofluoric acid treatment of TiO₂ grit blasted titanium implants on adherent osteoblast gene expression in vitro and in vivo. *Biomaterials* 2007;28:5418-25.
29. Mendonca G, Mendonca DB, Simoes LG, Araujo AL, Leite ER, Duarte WR, Aragao FJ, Cooper LF. The effects of implant surface nanoscale features on osteoblast-specific gene expression. *Biomaterials* 2009;30:4053-62.
30. Annunziata M, Oliva A, Buosciolo A, Giordano M, Guida A, Guida L. Bone marrow mesenchymal stem cell response to nano-structured oxidized and turned titanium surfaces. *Clin Oral Implants Res* 2011.
31. Brammer KS, Choi C, Frandsen CJ, Oh S, Johnston G, Jin S. Comparative cell behavior on carbon-coated TiO₂ nanotube surfaces for osteoblasts vs. osteo-progenitor cells. *Acta Biomater* 2011;7:2697-2703.
32. Dalby MJ, McCloy D, Robertson M, Wilkinson CD, Oreffo RO. Osteoprogenitor response to defined topographies with nanoscale depths. *Biomaterials* 2006;27:1306-1315.
33. Dimitrievska S, Bureau MN, Antoniou J, Mwale F, Petit A, Lima RS, Marple BR. Titania-hydroxyapatite nanocomposite coatings support human mesenchymal stem cells osteogenic differentiation. *J Biomed Mater Res A* 2011;98:576-588.
34. Gittens RA, McLachlan T, Olivares-Navarrete R, Cai Y, Berner S, Tannenbaum R, Schwartz Z, Sandhage KH, Boyan BD. The effects of combined micron-/submicron-scale surface roughness and nanoscale features on cell proliferation and differentiation. *Biomaterials* 2011;32:3395-3403.

35. Oh S, Brammer KS, Li YS, Teng D, Engler AJ, Chien S, Jin S. Stem cell fate dictated solely by altered nanotube dimension. *Proc Natl Acad Sci U S A* 2009;106:2130-5.
36. Sima LE, Stan GE, Morosanu CO, Melinescu A, Ianculescu A, Melinte R, Neamtu J, Petrescu SM. Differentiation of mesenchymal stem cells onto highly adherent radio frequency-sputtered carbonated hydroxylapatite thin films. *J Biomed Mater Res A* 2010;95:1203-1214.
37. Sugita Y, Ishizaki K, Iwasa F, Ueno T, Minamikawa H, Yamada M, Suzuki T, Ogawa T. Effects of pico-to-nanometer-thin TiO₂ coating on the biological properties of microroughened titanium. *Biomaterials* 2011.
38. Yu WQ, Jiang XQ, Xu L, Zhao YF, Zhang FQ, Cao X. Osteogenic gene expression of canine bone marrow stromal cell and bacterial adhesion on titanium with different nanotubes. *J Biomed Mater Res B Appl Biomater* 2011;99:207-216.
39. Bigi A, Nicoli-Aldini N, Bracci B, Zavan B, Boanini E, Sbaiz F, Panzavolta S, Zorzato G, Giardino R, Facchini A, Abatangelo G, Cortivo R. In vitro culture of mesenchymal cells onto nanocrystalline hydroxyapatite-coated Ti13Nb13Zr alloy. *J Biomed Mater Res A* 2007;82:213-21.
40. Guida L, Annunziata M, Rocci A, Contaldo M, Rullo R, Oliva A. Biological response of human bone marrow mesenchymal stem cells to fluoride-modified titanium surfaces. *Clin Oral Implants Res* 2010;21:1234-1241.
41. Gurzawska K, Svava R, Syberg S, Yihua Y, Haugshoj KB, Damager I, Ulvskov P, Christensen LH, Gotfredsen K, Jorgensen NR. Effect of nanocoating with rhamnogalacturonan-I on surface properties and osteoblasts response. *J Biomed Mater Res A* 2012;100:654-664.
42. Han P, Ji WP, Zhao CL, Zhang XN, Jiang Y. Improved osteoblast proliferation, differentiation and mineralization on nanophase Ti6Al4V. *Chin Med J (Engl)* 2011;124:273-279.
43. Menon D, Divyarani VV, Lakshmanan VK, Anitha VC, Koyakutty M, Nair SV. Osteointegration of titanium implant is sensitive to specific nanostructure morphology. *Acta Biomater* 2012.
44. Mozumder MS, Zhu J, Perinpanayagam H. TiO₂ -enriched polymeric powder coatings support human mesenchymal cell spreading and osteogenic differentiation. *Biomed Mater* 2011;6:035009.
45. Schena M, Shalon D, Davis RW, Brown PO. Quantitative monitoring of gene expression patterns with a complementary DNA microarray. *Science* 1995;270:467-470.
46. Carinci F, Pezzetti F, Volinia S, Francioso F, Arcelli D, Marchesini J, Caramelli E, Piattelli A. Analysis of MG63 osteoblastic-cell response to a new nanoporous implant surface by means of a microarray technology. *Clin Oral Implants Res* 2004;15:180-186.
47. Donos N, Hamlet S, Lang NP, Salvi GE, Huynh-Ba G, Bosshardt DD, Ivanovski S. Gene expression profile of osseointegration of a hydrophilic compared with a hydrophobic microrough implant surface. *Clin Oral Implants Res* 2011;22:365-372.
48. Mengatto CM, Mussano F, Honda Y, Colwell CS, Nishimura I. Circadian rhythm and cartilage extracellular matrix genes in osseointegration: a genome-wide screening of implant failure by vitamin D deficiency. *PLoS One* 2011;6:e15848.
49. Ivanovski S, Hamlet S, Salvi GE, Huynh-Ba G, Bosshardt DD, Lang NP, Donos N. Transcriptional profiling of osseointegration in humans. *Clin Oral Implants Res* 2011;22:373-381.
50. Kojima N, Ozawa S, Miyata Y, Hasegawa H, Tanaka Y, Ogawa T. High-throughput gene expression analysis in bone healing around titanium implants by DNA microarray. *Clin Oral Implants Res* 2008;19:173-81.
51. Lavenus S, Louarn G, Layrolle P. Nanotechnology and dental implants. *Int J Biomater* 2010;2010:915327.

52. Johansson CB, Gretzer C, Jimbo R, Mattisson I, Ahlberg E. Enhanced implant integration with hierarchically structured implants: a pilot study in rabbits. *Clin Oral Implants Res* 2011.
53. Wennerberg A, Albrektsson T. Suggested guidelines for the topographic evaluation of implant surfaces. *Int J Oral Maxillofac Implants* 2000;15:331-344.
54. Masuda T, Salvi GE, Offenbacher S, Felton DA, Cooper LF. Cell and matrix reactions at titanium implants in surgically prepared rat tibiae. *Int J Oral Maxillofac Implants* 1997;12:472-485.
55. Benjamini Y, Drai D, Elmer G, Kafkafi N, Golani I. Controlling the false discovery rate in behavior genetics research. *Behav Brain Res* 2001;125:279-284.
56. Livak KJ, Schmittgen TD. Analysis of relative gene expression data using real-time quantitative PCR and the 2(-Delta Delta C(T)) Method. *Methods* 2001;25:402-408.
57. Albrektsson T, Johansson C. Osteoinduction, osteoconduction and osseointegration. *Eur Spine J* 2001;10 Suppl 2:S96-101.
58. Ducy P, Starbuck M, Priemel M, Shen J, Pinero G, Geoffroy V, Amling M, Karsenty G. A *Cbfa1*-dependent genetic pathway controls bone formation beyond embryonic development. *Genes Dev* 1999;13:1025-1036.
59. Harada H, Tagashira S, Fujiwara M, Ogawa S, Katsumata T, Yamaguchi A, Komori T, Nakatsuka M. *Cbfa1* isoforms exert functional differences in osteoblast differentiation. *J Biol Chem* 1999;274:6972-6978.
60. Tang W, Li Y, Osimiri L, Zhang C. Osteoblast-specific transcription factor Osterix (*Osx*) is an upstream regulator of *Satb2* during bone formation. *J Biol Chem* 2011;286:32995-33002.
61. Dobreva G, Chahrouh M, Dautzenberg M, Chirivella L, Kanzler B, Farinas I, Karsenty G, Grosschedl R. *SATB2* is a multifunctional determinant of craniofacial patterning and osteoblast differentiation. *Cell* 2006;125:971-986.
62. Omar OM, Lenneras ME, Suska F, Emanuelsson L, Hall JM, Palmquist A, Thomsen P. The correlation between gene expression of proinflammatory markers and bone formation during osseointegration with titanium implants. *Biomaterials* 2011;32:374-386.
63. Hamlet S, Ivanovski S. Inflammatory cytokine response to titanium chemical composition and nanoscale calcium phosphate surface modification. *Acta Biomater* 2011;7:2345-2353.
64. Hamlet S, Alfarsi M, George R, Ivanovski S. The effect of hydrophilic titanium surface modification on macrophage inflammatory cytokine gene expression. *Clin Oral Implants Res* 2011.

Chapter 4

Early molecular assessment of osseointegration in humans

Abstract:

Objective: To determine the early temporal wide genome transcription regulation by the surface topography at the bone-implant interface of implants bearing micro-roughened or superimposed nanosurface topology.

Materials and methods: Four commercially pure titanium implants (2.2 x5.0mm) with either a moderately roughened surface (TiOblast) or super-imposed nanoscale topography (Osseospeed) were placed (n=2/surface) in edentulous sites of eleven systemically healthy subjects and subsequently removed after 3 and 7 days. Total RNA was isolated from cells adherent to retrieved implants. A whole genome microarray using the Affymetrix Human gene 1.1 ST Array was used to describe the gene expression profiles that were differentially regulated by the implant surfaces.

Results: There were no significant differences when comparing the two-implant surfaces at each time point. However, the microarray identified several genes that were differentially regulated at day 7 vs. day 3 for both implant surfaces. Functionally relevant categories related to the extracellular matrix, collagen fibril organization and angiogenesis were upregulated at both surfaces (day7 vs. day3). Abundant upregulation of several differential markers of alternative activated macrophages was observed (eg. *MRC1*, *MSR1*, *MS444A*, *SLC38A6* and *CCL18*). The biological processes involved with the inflammatory/immune response gene expression were concomitantly downregulated.

Conclusions: Gene regulation implicating collagen fibrillogenesis and extracellular matrix organization as well as the inflammatory/immune responses involving the alternative activated pathway are observed in implant adherent cells at early (3-7 days) after implantation. These gene expression events may indicate an important role for surface in modulating collagen fibrillogenesis as well as immunomodulation that play pivotal roles in altering bone accrual and biomechanical physical properties of the implant-bone interface.

Introduction:

Dental implants are of therapeutic benefit in the pursuit of alloplastic tooth replacement. The success of contemporary dental implants is largely attributed to the process of osseointegration. Osseointegration is a term defined as the direct structural and functional combination between the bone and the implant at the level of light microscopy [1]. The formed bone tissue microstructure is predominantly affected by the remodeling processes occurring in the early phase of peri-implant healing at the level of the bone-implant interface [2-4]. The implant surface serves as an intricate signaling cue for the attached cells playing an important role in altering the rate and quality of osseointegration [5-8]. The different physico/chemical features of the implant surface influence the biomolecular and cellular interactions with the implant [9-15]. Roughened surfaces enhance focal adhesion formation [16], promote cell commitment to the osteoblastic lineage and support greater expression of phenotype specific markers [17-19]. These changes result in greater bone formation evidenced by in-vivo histomorphometric and removal torque studies with improved bone anchorage of the roughened titanium implants than smoother surfaces [7,20]. In the dynamic research field of implants, a multitude of biomaterial modification approaches with nanoscale features have been pursued [21]. Various reports support that embellishment of the micron-rough surface with nanoscale features further enhances osteoblast differentiation [9,22-24], which could also promote stability and increase interfacial biomechanical locking with bone [25-28].

In contrast to the direct bone to implant contact representing osseointegration, fibrous encapsulation of implants leading to their failures remains a clinical challenge in situations where there is lack of primary implant stability, poor bone quality, or patients with compromised healing capacity such as those with a history of head and neck irradiation, uncontrolled diabetes, chronic periodontitis, smoking, etc.[29-31]. Fibrous encapsulation represents a repair mechanism of tissue directed by the cellular responses to the implanted device environment.

A comprehensive understanding of the molecular and cellular processes relevant to peri-implant healing is critical for achieving therapeutically relevant targets to positively influence implant osseointegration. Research devoted to deciphering the molecular mechanisms controlling implant-bone interface development is mostly interrogated through in vitro investigation in cell culture. A systematic review revealed approximately 90% of these studies focused on osteoblastic cell model able to differentiate under culture stimulation [32]. Key

observations indicated that adhesion to surfaces of increased topographic magnitude results in increased osteoinductive and bone matrix specific gene expression. Achieving optimum peri-implant healing requires an orchestration of the complex biological and molecular events of cell migration, proliferation, extracellular matrix (ECM) deposition, angiogenesis and remodeling. Apposition of a mature mineralized bone matrix is dependent on pivotal events of the early healing cascade. For example, the quality of the bone-implant interface may be determined by the hierarchical micro-architecture of its ECM constituents in which collagen plays a central role [33]. A recent in vitro investigation described the differential regulation of collagen biosynthesis in cells adherent to smooth and rough titanium surfaces [34]. This revealed greater collagen biosynthesis and enhanced expression of several collagen-modifying genes including prolyl hydroxylases, lysyl oxidases and lysyl hydroxylases within cells adherent to the roughened titanium substrates. Information about the role of the aforementioned genes and other potential collagen modifying genes in modulating implant integration in in-vivo models is still missing.

Additionally, among the many factors contributing to non-healing is impairment in the production of cytokines by local inflammatory cells and fibroblasts and reduced angiogenesis. Implant adherent macrophages and multinuclear cells are detected prior to bone formation at the surfaces of different materials inserted in bone [35]. However, their role in osseointegration remains poorly defined. Recent evidence suggests a positive influence of macrophages during bone healing in fracture models. Alexander et al [36] demonstrated that depletion of macrophages in Mafia transgenic mice is associated with significantly suppressed collagen type I bone matrix deposition and mineralization during bone healing in vivo in a tibia fracture model.

While in vitro studies can be a valuable tool and provide important insights into the biological mechanisms underlying osseointegration, they do not fully recapitulate the complex in-vivo microenvironment [37,38]. Various animal models have been used previously to evaluate the early molecular events at the implant surface interface. Most studies employed either qRT-PCR or immunohistochemistry [39]. However, these studies are limited in the number of genes that could be identified due to the non-global nature of these approaches. A recent investigation evaluated early molecular events (day4 vs day2) occurring at either a moderately roughened surface (AT-II) or a moderately roughened surface with super-imposed nanofeatures (AT-I) in a rat model using Affymetrix array [40]. Functionally relevant categories related to ossification, skeletal system development, osteoblast differentiation, bone development, bone mineralization and biomineral tissue development were

upregulated and more prominent with at AT-I (day 4 vs. day2) compared to AT-II. However, the bone turnover and resorption in a rat is several times faster than in a human [41]. In contrast to the rat model where early signs of new bone formation appear within 7 days after implantation and complete bone formation around a moderately roughened implant is achieved in 28 days [42- 44], osseointegration in human bone occurs at a slower pace and is achieved later [45]. Still, these timelines are significantly affected by the implant surface topography [46]. Understanding the kinetics of early phases of healing in human in vivo models of osseointegration should be more fully investigated. The aim of this study is to determine the early temporal molecular events associated with osseointegration in a human model in the implant adherent cells by assessing the whole genome expression profile at days 3 and 7 following the insertion of either a micro-roughened implant (TiOblast) or a moderately roughened with superimposed nanofeatures (Osseospeed).

Materials and methods:

Preparation of the model implants:

Forty-four screw-shaped mini-implants (2.2 x5.0 mm) were manufactured by AstraTech Dental (AstraTech, Molndal, Sweden) from grade IV commercially pure titanium. One sample group (n=22) was grit blasted with 75µm particles TiO₂ (AstraTech AB TiOblast™), while the other group (n=22) was blasted with TiO₂ particles in a similar manner and further subjected to HF immersion treatment according to Osseospeed manufacturing procedure (AstraTech AB Osseospeed™). All samples were washed by sterile water and beta-sterilized according to standard protocols for manufacture of dental implants.

Previous studies on surface roughness, expressed in S_a-values according to the methods described by Wennerberg et al. [47] reported S_a-values ~ 1-1.2 µm for TiOblast implants (TiO-moderately roughened) and 1.4-1.5 µm for the Osseospeed implants (OS). HF immersion produces discrete 50-200 nm nanofeatures on the OS surface (moderately roughened with superimposed nanofeatures). In addition, XPS analysis studies identified the presence of fluoride at approximately 1.0 % on the OS surface but not on the TiO surface [22,48].

Subjects' inclusion

The study protocol was approved by the Institutional Review Board (IRB) at University of North Carolina at Chapel Hill (IRB protocol #10-1963).

Eleven systemically healthy individuals who were either partially or completely edentulous were included in this study. The absence of at least 2 teeth, with adequate bone volume to allow placement of four mini-implants without impingement on vital anatomical structures (sinuses, nerves and adjacent teeth) and an edentulous period of at least 6 months were defined criteria for enrollment. Patients who were smokers, or with any systemic condition that could affect bone healing such as uncontrolled diabetes, history of radiotherapy in the head and neck region, taking corticosteroids or bisphosphonates, etc, were excluded. Included were 9 females and 2 males between the ages 47-69 with a mean age of 60.2.

Surgery:

Prior to surgery, informed written consents to participate in this study were obtained. Panoramic x-rays were made to assess the height of the alveolar bone as well as proximity to vital structures in the edentulous planned surgical sites. The radiographs were also screened for any pathology.

Following anesthesia, two separate crestal incisions approximately 6mm in length were made and full thickness mucoperiosteal flaps were raised. Each subject received two TiO and two OS implants. Two osteotomies were prepared per site to allow placement of one implant of each surface (1 TiO and 1 OS). This paired surgical design permitted the retrieval of the first 2 implants (1 of each surface) at the earlier time point without disturbing the healing of the other 2 implants. Drilling was completed using a 2.0 mm twist osteotomy drill under profuse irrigation with sterile saline. Single use osteotomy drills were used on each subject. All implants were placed by a self-tapping procedure and primary stability at the time of implant placement was insured. A submerged implant installation technique was used and the mucosal tissues were closed primarily with 4-0 chromic gut sutures.

Implants retrieval:

At 3 and 7 days following surgery, one surgical site was chosen at random, re-entered and the paired (One TiO and one OS) implants were removed by reverse threading. The implants were immediately rinsed in cold PBS and then placed into 1000 µl of Tri-reagent (Invitrogen, Carlsbad, CA). Cell lysates were snap frozen, and stored at -80°C until further use. Tissues were again reapproximated and closed with 4.0 chromic gut sutures.

RNA isolation and microarray hybridization:

Total RNA was isolated from the lysates using the standard Tri-reagent protocol and collected by ethanol precipitation. This was followed by purification using RNeasy MinElute Clean up kit (Qiagen, Valencia, CA, USA). RNA was assessed for quality and quantity using a bioanalyzer (Agilent, Santa Clara, CA, USA) and nanodrop ND-1000 spectrophotometer (Nanodrop, Wilmington, DE) respectively. Samples were processed and hybridized to the Affymetrix Human Gene 1.1 ST Array at the UNC core facility following the manufacturer's recommended protocol and reagents (Affymetrix, Santa Clara, CA). The Human Gene 1.1 ST Array Plate interrogates more than 27,000 well-annotated genes. The raw microarray data is available online at the NCBI-GEO (<http://www.ncbi.nlm.nih.gov/geo/>) database, accession number GSE41446.

Microarray data analysis:

Data analysis was completed using GeneSpring software v.12.0 (Agilent Technologies, Santa Clara, CA). 2-Way ANOVAs statistical analysis was applied to determine differentially expressed genes among the various parameters (implant surface type and time points). Further analysis included pairwise comparisons of each implant surface independently at the different time points (day 7 vs. day 3). A p-value of 0.05 was set as the threshold for statistical significance. Exported gene lists included significant genes; fold changes and p-values for comparisons. These lists of genes were then condensed into organized classes of related biology using the GO Ontology Browser function in the GeneSpring. Significant GO ($p < 0.05$) was corrected for multiple sampling using the method of Benjamini and the Hochberg false discovery rate method [49].

Results:

Microarray

2-Way ANOVA was applied to determine differentially expressed genes among the various parameters (implant surface type and time points). No genes were identified ($p\text{-value} < 0.05$) to be significantly different when comparing the 2 implants surfaces at each time point. Next, pairwise comparisons were made to determine the time-course dependent effects on gene expression profiles at either surface (TiO, OS) independently (day 7 vs. day3). 6450 genes were found to be differentially expressed (Fold change (FC) > 1.1 ; $p\text{-value} \leq 0.05$) at OS; of these, 2495 were upregulated, and 3955 were downregulated. On the other hand, 13,292 genes were found to be differentially expressed (FC > 1.1 ; $p \leq 0.05$) at TiO; of these, 3262 were

upregulated and 10,030 were downregulated (Table 1). The identity of the top 35 genes differentially upregulated at OS implants surfaces (day 7 vs. day 3; p-value<0.05) with their fold regulation in OS and TiO is shown in table 2. Another table (table 3) was created to include list of top 35 differentially downregulated genes (p-value≤0.05) at Osseospeed (Day 7 vs. day3) with their fold regulation in OS and TiO.

Identification of significant gene ontologies associated with the different implant surfaces

GO analysis was used to identify functional categories overrepresented in the gene lists of the differentially upregulated and downregulated genes between day 7 and day 3 (fold change ≥2; p ≤0.05) independently at both implants surfaces.

GO terms upregulated at Osseospeed and TiOblast (day 7 compared with day 3)

The gene functional annotation identified at OS and TiO consisted of a large variety of processes. 97 terms satisfied p≤0.05 at OS and 216 terms satisfied p≤0.05 at TiO. Table 4 outlines the top 30 GO terms for both surfaces. Functionally relevant categories relevant to the extracellular region and matrix, collagen fibril organization and blood vessel development were clearly demonstrated at both surfaces. Gene lists of differentially expressed genes relevant to the extracellular matrix category, collagen fibril organization, ossification and blood vessel development are represented in Table 5.

In this study, a high number of genes encoding ECM components were upregulated including several collagens (*COL1A1*, *COL1A2*, *COL3A1*, *COL6A1*, *COL6A3*, *COL12A1*), glycoproteins (*SPARC*, *ECM1*, *CHI3L1*, *IBSP*, *GPNMB*), and proteoglycans (*DCN*, *BGN*, *LUM*, *GPC4*). Increased levels of several genes involved in collagen biosynthesis, processing and post-translational modifications including *PLOD1*, *PLOD2*, *PLOD3* and *LOX* were also identified. Differential upregulation of heat shock protein 47 (*HSP47*) and (procollagen C-endopeptidase enhancer) *PCOLCE* was also evident. In addition, we observed an upregulation of several matrix metalloproteinases (MMPs) including *MMP2*, *MMP7*, *MMP8*, *MMP9*, *MMP12*, *MMP13* and *MMP14*. Upregulation of *TIMP2*, *TIMP3* and *A2M* was also identified. Furthermore, several phenotypical markers characteristic of osteoclast/bone resorption activity including cathepsin K (*CTSK*), acid phosphatase 5, tartrate resistant (*ACP5*) were increased at both surfaces.

In addition, when we analyzed the lists of the differentially upregulated genes on both surfaces, we identified a number of genes (table 6) that have been associated with the alternatively activated macrophage (M2) including the membrane receptors mannose receptor, C type 1 (*MRC1*), macrophage scavenger receptor 1 (*MSR1*), membrane-spanning 4-domains, subfamily A member 4 (*MS444A*), the solute carrier family 38, member 6 (*SLC38A6*), and the chemokines *CCL18*, *CCL22*.

GO terms downregulated at Osseospeed, TiOBlast (day 7 compared with day 3)

Further functional annotation analysis of the differentially downregulated genes at both surfaces highlighted several categories in this domain. 97 terms satisfied $p \leq 0.05$ in both surfaces. The functional categories differentially regulated were the same for both surfaces. Table 7 outlines the top 30 terms. An overrepresentation of functional annotations associated with chemotaxis, immune response and inflammatory response was demonstrated. Involved were several chemokines (*CCL3*, *CCL4*, *CXCL1*, *CXCL2*, *CXCL5*, *CCL20*), interleukins along with their associated receptors and kinases (*IRAK2*, *IL1RAP*, *IL1B*, *IL1A*, *IL8*), defensins (*DEFA3|DEFA1|DEFA1B*, *DEFB4A*), *TREM1* and prostaglandin-endoperoxide synthase 2 (*PTGS2*).

Discussion:

This study evaluated the global transcription regulation in implant adherent cells to either micro-roughened (TiO) or nanostructured (OS) titanium implants at an early phase of osseointegration (day 3 and 7) in human. Comparative analysis of gene expression profiles at these early time points did not reveal significant differences between both surfaces. To further comprehend the early molecular events determining the process of osseointegration, analysis of the time course dependent changes (day 7 vs. day 3) on each surface was performed. 6450 genes were found to be differentially expressed at OS and 13,292 genes were found to be differentially expressed at TiO. A large number of genes upregulated at this early phase of osseointegration were related to the extracellular matrix and collagen fibril organization. The expression of several collagen encoding mRNAs including *COL1A1*, *COL1A2*, *COL3A1*, *COL6A1*, *COL6A2* and *COL12A1* was increased. Collagens comprise 90% of the organic content of bone [50]. Type I collagen constitutes the major type of collagen in bone [51]. Essential to collagen integrity and bone mechanical strength is regulation of fibrillogenesis by providing specific molecular bridges between collagen fibrils and other matrix components [52]. Type III and type XII collagen modulates the size of type I collagen and play a role in collagen fibril

formation [53,54]. Dysregulation of proper fibrillogenesis can ultimately affect bone strength and biomechanical properties. For instance, *Col12a1*^{-/-} mice exhibits skeletal abnormalities including shorter, more slender long bones with decreased mechanical strength [54]. HSP47 is the molecular chaperone that assists in the folding and/or assembly of procollagen [55,56] and it was also upregulated. It is essential for the maturation of collagen. Fibrils of type I collagen secreted from *hsp47*^{-/-} cells are abnormally thin and are more sensitive to protease digestion [57]. Collagens types I to III are secreted as procollagen precursors containing N and C propeptides that are cleaved to yield mature triple helical monomers that associate into fibrils. BMP1, also known as procollagen C proteinase, and related metalloproteinases cleave the C propeptides [58]. Attenuated BMP1 function compromises osteogenesis leading to bone fragility due to improper collagen fibrils maturation [59]. The activity of BMP1 is potentiated by a secreted glycoprotein, designated the procollagen C-endopeptidase enhancer [*PCOLCE*/procollagen C-proteinase enhancer (PCPE)] [60]. An increased expression of *PCOLCE* was identified in the implant adherent cells implicating the role of collagen maturation in achieving implant integration. Other non-collagenous proteins involved in ECM assembly and cell matrix interaction were also differentially upregulated including various proteoglycans (eg. *DCN*, *BGN*, *LUM*, *GPC4*) and glycoproteins (e.g. *SPARC*, *ECM1*, *IBSP*). Several of the ECM related proteins differentially expressed are known to play a direct role in bone formation; lumican [61], SPARC [62], ECM protein1 [63,64], periostin [65], biglycan [66], decorin [67] and IBSP [68]. Decorin, biglycan and lumican are secreted extracellular small leucine-rich proteoglycans (SLRPs) that modulate collagen matrix assembly and regulate fibrillogenesis [66,67]. An earlier report demonstrated the role of proteoglycans in the establishment of a bone-titanium integration where the addition of GAG degradation enzymes significantly reduced the interfacial strength of the titanium and the mineralized osteoblastic tissue culture [69]. Enhanced expression of several genes involved in the posttranslational modification of collagen was also observed. Included were the Lysyl hydroxylases (*PLOD1*, *PLOD2*, *PLOD3*) and the Lysyl oxidase (*LOX*). These genes encode for proteins involved in catalyzing the hydroxylation and the oxidative deamination of specific lysine and/or hydroxylysine residues in collagen respectively [70-73]. These posttranslational modifications greatly influence the pattern of collagen cross-linking. The organization, density and the amount of cross-linking of collagen determine the mechanical strength and ultimately, hierarchical tissue organization. In addition, the type and quantity of cross-linking are crucial for proper mineralization [74,75]. This study highlights the role of various ECM related genes during

implant healing that might be crucial in the biological and biomechanical establishment of the bone-implant interface. These not only provide the structural support and the scaffold for mineralization, but also contain reservoirs of cell signaling motifs that may guide subsequent cellular adhesion and behavior [16].

In addition, increased expression of various MMPs (*MMP7*, *MMP8*, *MMP9*, *MMP13*, *MMP14*) occurred. MMPs are zinc-dependent endoproteases, which have the capacity to degrade a variety of extracellular components. They are also involved in bone resorption and remodeling by osteoclasts [76]. Establishment of osseointegration is a dynamic process; where there is a delicate interplay between bone resorption in contact regions and bone formation in contact free regions [77]. Several genes implicated with the osteoclastogenic bone resorption were upregulated including *CATK* and *ACP5*. Recent histological data in human implicated a potential role of osteoclasts in modulating the process of osseointegration, where no new bone formation was observed in areas with no prior resorptive processes visible [78,79]. The recruitment and invasion of cells during vasculogenesis also involve proteolytic activities and degradation of the extracellular matrix [80]. This interrelationship is highlighted by gene deletions in mice demonstrating the essential role of MMPs in the onset of angiogenesis in the fracture healing and bone formation [81-83]. Indeed, our bioinformatics analysis revealed an overrepresentation of the functional biological processes related to blood vessel development in cells adherent to the implant surface. The development of an elaborate vascular network maybe an important step for bone regeneration and successful integration of implants leading to turnover of necrotic bone that develops after implant placement. Precise regulation of MMP activity is crucial for preventing excessive ECM degradation that can hinder the formation of a functional bone-implant interface. Here, the array data identified differential expression of specific tissue inhibitors of metalloproteinases (TIMP2 and TIMP3) as well as the more broad-spectrum tissue inhibitor (A2M), which suggests the presence of tight mechanisms associated with the early remodeling processes. In contrast to most MMPs, MMP-12 (macrophage metalloelastase) which has potent extracellular remodeling properties [84], has also been shown to cleave and inactivate human ELR+CXC chemokines consistent with a role in controlling the duration of the inflammatory cellular infiltrate of PMNs [85]. MMP-12 is mainly expressed by macrophages [86] and its activity is one of the mechanisms to dampen inflammation and promote resolution.

The osseointegration process is a consequence for the coordinated interplay of several cell types. Implant adherent macrophages and multinuclear cells are detected prior to bone formation at the surfaces of different

materials inserted in bone [35]. While macrophages have an established role in wound healing through the activity of secreted cytokine, their potential influence of macrophages in modulating implant-tissue integration has been briefly described. A previous in vivo report demonstrated the preferential accumulation of macrophages on rough implant surfaces, which was associated with more rapid bone-like tissue production [87]. Furthermore, Cooper and coworkers established utilizing the murine macrophage cell line the influence of surface roughness on BMP2 expression, which directly affects osteoblasts cell maturation and bone formation [88-90]. In cell culture model, Hamlet et al suggested the potential role for downregulation of a macrophage's pro-inflammatory phenotype including cytokines and chemokines (eg. *Tnf α* , *Ccl2*, *Ccl5 Il-1 β* , *Ill1 α*) adjacent to nanoscale CaP-modified implants and chemically modified SLActive surfaces as a mechanism for the clinically proven superior osseointegration associated with these surface modifications [91,92]. Similarly in a human model, Bryington et al[48] demonstrated the influence of the presence of nanofeatures (OS) in mediating an immunomodulatory effect on macrophages by enhanced expression of IL-9 (a Th2-associated cytokine that reduces monocyte oxidative burst and TNF- α release) [93]) and IL-22 compared with micro-roughened surfaces (TiO).

The dynamic changes in the presence of polarized macrophages with pro-inflammatory (M1) and anti-inflammatory (M2) properties may affect the early healing processes to achieve implant-tissue integration. The classical 'M1' activation of monocytes (eg. LPS- Th1 cytokines-INF γ , IL-1B) leads to the production of the pro-inflammatory cytokines such as IL-1 β , IL-6 and TNF- α , whereas the alternative 'M2' macrophage activation (IL-4 activated or IL-13 activated-Th2 cytokines) exhibits an anti-inflammatory profile with the expression of IL-10. M2 macrophages are able to phagocytose without oxidant production [94] and their activation is associated with immunoregulation, matrix deposition and remodeling [95,96]. Omar et al [97] revealed surface specific signaling of human monocytes resulting in significantly greater expression of BMP2 and RUNX2 of hMSCs cultured with conditioned media at oxidized surfaces compared with machined surfaces. They implicated a role for classical activation of monocytes (LPS activation) with osteoblast differentiation of hMSCs. Their in vivo analysis of LPS coated implants demonstrated an important role for signaling of osteoclasts but involving the classically activated monocytes. How alternatively activated macrophages are engaged was not directly considered in this previous study. In the present report, however, abundant upregulation of genes related to acquisition of M2 properties [98,99] [100] was identified. The data set included

the membrane receptors mannose receptor, C type 1 (*MRC1*), macrophage scavenger receptor 1 (*MSR1*), membrane-spanning 4-domains, subfamily A member 4 (*MS444A*), the solute carrier family 38, member 6 (*SLC38A6*), and the chemokines (*CCL18*, *CCL22*). Indirect and direct co-cultures of either M1 or M2 polarized human monocytes with hMSCs revealed their differential effects on the growth of hMSCs [101] where M2 macrophages and their associated cytokines supported the growth and proliferation of hMSCs, while M1 macrophages and their associated cytokines were detrimental to the growth and survival of hMSC. Hence, the type of macrophage cells (M2 vs. M1) may potentially impact the early process of osseointegration by harnessing the host tissue response towards enhanced survival and function of hMSCs repair cells. M2 macrophages release various chemokines including CCL18 [102], CCL22 [103], the anti-inflammatory IL-10 and TGF β -1. CCL18 was suggested to play a role at the resolution stage of the inflammatory process as it upregulates IL-10, known for its capacity to inhibit production of Th1 cytokines. CCL18 can also induce an M2 spectrum macrophage phenotype even in the absence of IL-4 [104]. CCL18 activated macrophages can remove cellular debris and apoptotic cells in the absence of a respiratory burst. The development of the bone-implant interface requires the colonization of the implant surface with MSCs/osteoprogenitors cells and their subsequent proliferation and differentiation. Homing of MSCs to the implant site is essential. CCL22 is amongst the chemokines that serve as a migratory cue that drive transendothelial migration of MSCs [105]. Consistent with the notion where M2 activation stands at the cross road between inflammation and resolution, our array data identified downregulation of several chemokines (*CCL3*, *CCL4*, *CXCL1*, *CXCL2*, *CXCL5*, *CCL20*), interleukins along with their associated receptors and kinases (*IRAK2*, *IL1RAP*, *IL1B*, *IL1A*, *IL8*), defensins (*DEFA3|DEFA1|DEFA1B*, *DEFB4A*), *TREM1* and prostaglandin-endoperoxide synthase 2 (*PTGS2*) [106-109]. Meanwhile, we also identified the differential upregulation of Chitinase 3-like 1 (*CHI3LI*), also known as YKL-40. YKL-40 inhibits cellular responses induced by IL-1 and TNF- α [110] suggesting that the induction of YKL-40 feeds back to control local tissue responses. While a general picture of selection of M2 macrophages and diminished inflammation emerges in the context of the bone forming events at endosseous implants, further characterization of the roles of M2 macrophage is required.

Histomorphometric data using several animal models [26,111] demonstrates differential bone formation at the two surfaces annotated here (OS > TiO). Analysis of differential gene expression at this early time failed to identify significant differences between both surfaces. Moreover, upregulation of osteoblast differentiation

transcription factors was not demonstrated. In contrast, Bryington et al [48] were able to demonstrate a differential upregulation of OSX, a key transcription factor for osteoblast differentiation on the nanoscale featured implants compared with the microtopography TiOblast surface. A possible factor contributing to this difference is the age of the population included. In our study, the mean age was 60 years old as opposed to 36 year old in Bryington et al study. MSCs are susceptible to age-related changes. MSCs from older donors have an overall decline in their differentiation potential [112-114]. This implicates that modulation of osteogenic gene expression might have been delayed in our aging population. Hence, further investigations using later time periods may be needed to identify key elements essential for modulating the osteoblast differentiation. In support of this speculation, a previous study [115] using a trephine model of the peri-implant tissue in the retromolar area has identified sequential inflammatory (days 4), angiogenic (days 7) and osteogenic (days 14) responses involved in the process of osseointegration. These repair responses were evaluated with SLA, SLActive implants. In addition, while this study incorporated the use of Affymetrix microarray, Bryington et al [48] utilized qRT-PCR to identify differential gene expression in implant adherent cells. Differences in the sensitivity of the platforms used for assessing mRNA gene expression might have contributed to the differences in the results obtained [116].

Our explanted model with implant adherent cells provides important information critical to driving the process of osseointegration at the implant-bone interface. One limitation to this approach is the scarcity of the RNA quantity on human explanted implants in this population that did not allow further validation of our microarray data using qRT-PCR.

Conclusions:

The present study investigated the global transcription regulation in implant adherent cells adherent to either a nanosurface or a moderately rough surface in a human model at early implantation times. In this study, novel biomolecular and cellular responses that underlie the process of osseointegration at this early phase were revealed. These genes exert a multitude of functions including ECM matrix organization, immune modulation, angiogenesis and skeletal remodeling. Numerous genes associated with the fibrillogenesis and cross-linking of the collagen matrix were identified. In addition, key markers for the alternatively activated ‘M2’ macrophage

were revealed. Further characterization of the roles of the genes identified is crucial to identifying potential targets for improving osseointegration.

Table 1: Number of genes differentially expressed (Day 7 vs. Day 3)

Comparison	Differentially expressed genes *	Upregulated genes*	Downregulated genes*	Differentially expressed (FC>2)
OS	6450	2495	3955	163
TiO	13292	3262	10,030	269

* Upregulated (>1.1) and downregulated (<1.1) genes with p-value <0.05. FC; fold change

Table 2: List of top 35 differentially upregulated genes at OS (Day 7 vs. day3) with their fold regulation and p-value in OS and TiO.

Gene symbol	Gene description	FC ([OS-Day7] vs [OS-Day3])	p-value	FC ([TiO-Day7] vs [TiO-Day3])	p-value
CTSK	cathepsin K	8.21	0.008	8.66	0.002
MMP12	matrix metalloproteinase 12 (macrophage elastase)	8.10	0.015	11.73	0.003
MMP9	matrix metalloproteinase 9 (gelatinase B, 92kDa gelatinase, 92kDa type IV collagenase)	7.03	0.008	9.14	0.002
MMP7	matrix metalloproteinase 7 (matrilysin, uterine)	6.91	0.014	9.73	0.004
TCTEX1D2 TM4SF19/// TM4SF19	Tctex1 domain containing 2 transmembrane 4 L six family member 19/// transmembrane 4 L six family member 19	5.67	0.011	7.53	0.002
CHI3L1	chitinase 3-like 1 (cartilage glycoprotein-39)	4.92	0.013	8.72	0.003
LUM	lumican	4.84	0.019	5.53	0.002
COL6A3	collagen, type VI, alpha 3	4.50	0.013	4.79	0.002
COL3A1	collagen, type III, alpha 1	4.50	0.014	4.84	0.002
POSTN	periostin, osteoblast specific factor	4.47	0.014	4.13	0.003
COL1A1	collagen, type I, alpha 1	4.44	0.014	4.68	0.002
DCN	decorin	3.94	0.019	4.16	0.003
CHIT1	chitinase 1 (chitotriosidase)	3.87	0.033	7.50	0.007
ACP5	acid phosphatase 5, tartrate resistant	3.81	0.010	4.32	0.004
GM2A	GM2 ganglioside activator	3.77	0.013	4.86	0.002
PNLIP COL1A2/// COL1A2	pancreatic lipase collagen, type I, alpha 2/// collagen, type I, alpha 2	3.75	0.015	3.73	0.002
COL12A1	collagen, type XII, alpha 1	3.41	0.015	3.16	0.003
TPM2	tropomyosin 2 (beta)	3.40	0.008	2.95	0.002
SPARC	secreted protein, acidic, cysteine-rich (osteonectin)	3.35	0.014	4.21	0.002
BGN	biglycan	3.29	0.016	4.20	0.002
LPL	lipoprotein lipase	3.17	0.026	3.48	0.008
GPNMB	glycoprotein (transmembrane) nmb	3.07	0.021	3.77	0.003
MSR1	macrophage scavenger receptor 1	3.05	0.022	2.78	0.006
C1QB	complement component 1, q subcomponent, B chain	3.04	0.016	3.49	0.004
MMP13	matrix metalloproteinase 13 (collagenase 3)	3.03	0.026	2.43	0.010
COL6A1	collagen, type VI, alpha 1	3.00	0.013	3.01	0.002
CDR1 YTHD C2	cerebellar degeneration-related protein 1, 34kDa YTH domain containing 2	2.98	0.016	2.82	0.005
HIST1H3B	histone cluster 1, H3b	2.93	0.014	2.84	0.004
C1QC	complement component 1, q subcomponent, C chain	2.87	0.023	1.55	NS
LIPA	lipase A, lysosomal acid, cholesterol esterase	2.84	0.024	2.68	NS
CCL22	chemokine (C-C motif) ligand 22	2.82	0.020	5.76	0.006
BIRC5 EPR1	baculoviral IAP repeat-containing 5 effector cell peptidase receptor 1 (non-protein)	2.70	0.013	2.05	0.008

	coding)				
CCL18	chemokine (C-C motif) ligand 18 (pulmonary and activation-regulated)	2.70	0.027	2.56	0.005
CKB	creatine kinase, brain	2.67	0.025	2.17	0.017
ATP1B1 NME7	ATPase, Na ⁺ /K ⁺ transporting, beta 1 polypeptide non-metastatic cells 7, protein expressed in (nucleoside-diphosphate kinase)	2.67	0.018	2.50	0.007

Table 3: List of top 35 differentially downregulated genes at OS (Day 7 vs. day3) with their fold regulation and p-value in OS and TiO.

Gene symbol	Gene description	FC ([OS-Day7] vs [OS-Day3])	p-value	FC ([TiO-Day7] vs [TiO-Day3])	p-value
DEFA3 DEFA1 DEFA1B	defensin, alpha 3, neutrophil-specific defensin, alpha 1 defensin, alpha 1B	-3.03	0.016	-2.80	0.014
SPRR2A SPRR2B	small proline-rich protein 2A small proline-rich protein 2B	-2.90	0.040	-3.00	0.014
SPRR2E	small proline-rich protein 2E	-2.75	0.037	-2.87	0.018
IL1B	interleukin 1, beta	-2.60	0.019	-3.58	0.008
KRT6C KRT6B KRT6A	keratin 6C keratin 6B keratin 6A	-2.58	0.038	-2.27	0.017
ALOX5AP	arachidonate 5-lipoxygenase-activating protein	-2.35	0.021	-3.00	0.005
CXCL1	chemokine (C-X-C motif) ligand 1 (melanoma growth stimulating activity, alpha)	-2.24	0.022	-2.80	0.013
LIPN	lipase, family member N	-2.23	0.036	-2.20	0.048
S100A2	S100 calcium binding protein A2	-2.19	0.039	-2.41	0.025
PTGS2	prostaglandin-endoperoxide synthase 2 (prostaglandin G/H synthase and cyclooxygenase)	-2.18	0.045	-2.20	NS
CYTIP	cytohesin 1 interacting protein	-2.16	0.021	-4.67	NS
TMEM154	transmembrane protein 154	-2.15	0.022	-2.06	0.045
CSF3R	colony stimulating factor 3 receptor (granulocyte)	-2.12	0.032	-2.25	0.009
IL1A	interleukin 1, alpha	-2.11	0.033	-2.92	0.009
RGS2	regulator of G-protein signaling 2, 24kDa	-2.11	0.022	-2.00	NS
MIR222	microRNA 222	-2.06	0.027	-1.67	0.009
RNU11	RNA, U11 small nuclear	-2.02	0.025	-2.23	0.031
SPRR1B	small proline-rich protein 1B (cornifin)	-1.99	0.039	-1.94	0.016
NCF1 NCF1C NCF1B	neutrophil cytosolic factor 1 neutrophil cytosolic factor 1C pseudogene neutrophil cytosolic factor 1B pseudogene	-1.98	0.034	-1.95	0.020
GPR97	G protein-coupled receptor 97	-1.98	0.029	-2.49	0.023
SPRR2D SPRR2B SPRR2B SPRR2F SPRR2D SPRR2A SPRR2B SPRR2B	small proline-rich protein 2D small proline-rich protein 2B small proline-rich protein 2B small proline-rich protein 2F small proline-rich protein 2D small proline-rich protein 2A small proline-rich protein 2B small proline-rich protein 2B	-1.97	0.041	-2.07	0.022
FPR1	formyl peptide receptor 1	-1.96	0.031	-2.04	0.030
IER3	immediate early response 3	-1.96	0.029	-2.27	0.030
IL1R2	interleukin 1 receptor, type II	-1.96	0.039	-1.74	ns
FOS	FBJ murine osteosarcoma viral oncogene homolog	-1.96	0.012	-1.22	0.038
SORL1	sortilin-related receptor, L(DLR class) A repeats-containing	-1.95	0.034	-1.71	0.020
IL1RAP	interleukin 1 receptor accessory protein	-1.92	0.036	-2.29	0.015
KCNJ15	potassium inwardly-rectifying channel,	-1.90	0.023	-2.00	0.021

	subfamily J, member 15				
TREM1	triggering receptor expressed on myeloid cells 1	-1.89	0.037	-2.59	0.017
DUSP1	dual specificity phosphatase 1	-1.87	0.020	-1.58	ns
ZFP36	zinc finger protein 36, C3H type, homolog (mouse)	-1.87	0.032	-1.99	ns
MIR223	microRNA 223	-1.85	0.030	-1.79	ns

Table 4: Top 30 GO terms for differentially upregulated genes at both surfaces (Day 7 vs. Day3). 98 terms satisfied $p < 0.05$ at OS; 216 terms satisfied $p < 0.05$ at TiO.

GO Term - OS	p-value (OS)	Count in Selection (OS)	GO Term - TiO	p-value (TiO)	Count in Selection (TiO)
extracellular region part	3.59E-20	47	extracellular region part	2.89E-15	49
proteinaceous extracellular matrix	2.47E-16	27	proteinaceous extracellular matrix	1.61E-13	28
extracellular matrix	2.47E-16	28	extracellular matrix	1.61E-13	29
extracellular region	2.67E-14	57	extracellular region	4.79E-10	62
extracellular space	2.66E-10	30	extracellular space	7.65E-08	32
Extracellular matrix organization	2.66E-10	14	cytoplasmic part	7.65E-08	103
extracellular structure organization	2.66E-10	14	extracellular matrix part	8.92E-08	14
extracellular matrix part	8.31E-10	14	localization	1.05E-06	72
collagen fibril organization	3.59E-08	8	melanosome	2.17E-06	12
collagen	8.29E-07	8	pigment granule	2.17E-06	12
collagen metabolic process	9.39E-06	7	collagen fibril organization	1.82E-05	7
multicellular organismal macromolecule metabolic process	1.62E-05	7	establishment of localization	2.89E-05	63
multicellular organismal process	4.21E-05	66	cell surface	3.00E-05	18
multicellular organismal metabolic process	4.21E-05	7	mitochondrial inner membrane	3.65E-05	18
fatty acid binding	4.25E-05	6	transport	3.93E-05	62
pattern binding	1.09E-04	11	mitochondrial membrane	4.23E-05	21
polysaccharide binding	1.09E-04	11	mitochondrial envelope	8.55E-05	21
lipid binding	1.81E-04	17	organelle inner membrane	8.68E-05	18
tissue remodeling	3.31E-04	7	anatomical structure development	8.68E-05	59
cellular component organization	5.38E-04	43	regulation of plasma lipoprotein particle levels	8.68E-05	7
monocarboxylic acid binding	7.23E-04	6	multicellular organismal process	8.83E-05	83
platelet-derived growth factor binding	0.0018	4	blood vessel development	8.94E-05	15
carbohydrate binding	0.0018	14	vasculature development	1.21E-04	15
cellular component organization or biogenesis	0.0019	43	collagen	1.30E-04	7
extracellular matrix binding	0.0021	5	extracellular matrix organization	1.79E-04	10
fibrillar collagen	0.0021	4	extracellular structure organization	1.79E-04	10
ossification	0.0026	8	system development	2.20E-04	52
blood vessel development	0.0026	11	mitochondrial membrane part	2.29E-04	11
glycosaminoglycan	0.0026	9	mitochondrial part	2.37E-04	24

glycosaminoglycan binding	0.0026	9	mitochondrial part	2.37E-04	24
collagen biosynthetic	0.0026	3	cholesterol transport	2.48E-04	7

Table 5: list of differentially expressed genes in the functional categories related to ECM and collagen fibril organization, blood vessel development, ossification and osteoclastogenesis.

Extracellular matrix and collagen fibril organization					
Gene description	Gene symbol	FC [OS-D7 vs OS-D3]	p-value	FC [TiO-D7 vs TiO-D3]	p-value
periostin, osteoblast specific factor	POSTN	4.47	0.014	4.13	0.003
chitinase 3-like 1 (cartilage glycoprotein-39)	CHI3L1	4.92	0.013	8.72	0.003
collagen, type I, alpha 1	COL1A1	4.44	0.014	4.68	0.002
pancreatic lipase collagen, type I, alpha 2///collagen, type I, alpha 2	PNLIP COL1A2///COL1A2	3.75	0.015	3.73	0.002
collagen, type III, alpha 1	COL3A1	4.50	0.014	4.84	0.002
collagen, type VI, alpha 1	COL6A1	3.00	0.013	3.01	0.002
collagen, type VI, alpha 3	COL6A3	4.50	0.013	4.80	0.002
collagen, type XII, alpha 1	COL12A1	3.41	0.015	3.16	0.003
coiled-coil domain containing 80	CCDC80	2.19	0.027	1.90	0.011
decorin	DCN	3.94	0.019	4.16	0.003
extracellular matrix protein 1	ECM1	2.01	0.011	1.86	0.003
glypican 4	GPC4	1.89	0.024	2.60	0.006
annexin A2	ANXA2	2.18	0.015	2.34	0.003
tenascin C	TNC	2.05	0.028	2.38	0.005
lectin, galactoside-binding, soluble, 1	LGALS1	1.90	0.013	2.02	0.002
lysyl oxidase	LOX	2.07	0.027	1.87	0.020
procollagen-lysine 1, 2-oxoglutarate 5-dioxygenase 1	PLOD1	1.77	0.013	1.90	0.002
procollagen-lysine, 2-oxoglutarate 5-dioxygenase 2	PLOD2	2.22	0.018	1.75	0.032
procollagen-lysine, 2-oxoglutarate 5-dioxygenase 3	PLOD3	1.45	0.021	1.53	0.006
lipoprotein lipase	LPL	3.17	0.026	3.48	0.008
lumican	LUM	4.84	0.019	5.53	0.002
matrix metalloproteinase 2 (gelatinase A, 72kDa gelatinase, 72kDa type IV collagenase)	MMP2	1.87	0.029	1.81	0.008
matrix metalloproteinase 7 (matrilysin, uterine)	MMP7	6.91	0.014	9.73	0.004
matrix metalloproteinase 8 (neutrophil collagenase)	MMP8	2.46	0.018	3.24	0.008
matrix metalloproteinase 9 (gelatinase B, 92kDa gelatinase, 92kDa type IV collagenase)	MMP9	7.03	0.008	9.14	0.002
matrix metalloproteinase 12 (macrophage elastase)	MMP12	8.10	0.015	11.73	0.003
matrix metalloproteinase 13 (collagenase 3)	MMP13	3.03	0.026	2.43	0.011

matrix metallopeptidase 14 (membrane-inserted)	MMP14	2.35	0.013	2.51	0.002
	CD248	2.20	0.019	2.03	0.010
biglycan	BGN	3.29	0.016	4.20	0.002
solute carrier family 1 (glial high affinity glutamate transporter), member 3	SLC1A3	1.75	0.028	2.16	0.008
secreted protein, acidic, cysteine-rich (osteonectin)	SPARC	3.35	0.014	4.21	0.002
transforming growth factor, beta-induced, 68kDa	TGFBI	2.05	0.018	1.78	0.005
TIMP metallopeptidase inhibitor 2	TIMP2	2.09	0.013	2.11	0.002
TIMP metallopeptidase inhibitor 3	TIMP3	2.58	0.013	2.62	0.005
alpha-2-macroglobulin	A2M	2.49	0.020	2.87	0.006
calreticulin	CALR	1.72	0.024	2.02	0.005
procollagen C-endopeptidase enhancer	PCOLCE	2.50	0.017	2.12	0.006
serpin peptidase inhibitor, clade H (heat shock protein 47), member 1, (collagen binding protein 1)	SERPINH1	2.12	0.015	1.98	0.005
Ossification					
glycoprotein (transmembrane) nmb	GPNMB	3.07	0.021	3.77	0.003
collagen, type I, alpha 1	COL1A1	4.44	0.014	4.68	0.002
extracellular matrix protein 1	ECM1	2.01	0.011	1.86	0.003
integrin-binding sialoprotein	IBSP	2.00	0.034	1.96	0.023
ectonucleotide pyrophosphatase/phosphodiesterase 1	ENPP1	2.13	0.037	1.94	0.006
Osteoclast-related genes					
cathepsin K	CTSK	8.21	0.008	8.66	0.002
acid phosphatase 5, tartrate resistant	ACP5	3.81	0.009	4.32	0.004
matrix metallopeptidase 9 (gelatinase B, 92kDa gelatinase, 92kDa type IV collagenase)	MMP9	7.03	0.008	9.14	0.002
matrix metallopeptidase 14 (membrane-inserted)	Mmp14	2.35	0.013	2.51	0.002
integrin, alpha V (vitronectin receptor, alpha polypeptide, antigen CD51)		1.99	0.016	2.03	0.003
integrin, beta 3 (platelet glycoprotein IIIa, antigen CD61)	ITGB3	1.83	0.047	1.84	0.017
Blood vessel development					
collagen, type I, alpha 1	COL1A1	4.44	0.014	4.68	0.002
pancreatic lipase collagen, type I, alpha 2///collagen, type I, alpha 2	PNLIP COL1A2///COL1A2	3.75	0.015	3.73	0.002
collagen, type III, alpha 1	COL3A1	4.50	0.014	4.84	0.002
endothelial PAS domain protein 1	EPAS1	2.01	0.015	2.09	6.43E-04
annexin A2	ANXA2	2.18	0.020	2.34	0.003
apolipoprotein E high mobility group AT-hook	APOE HMGA1 //HMGA1	1.92 ⁵	0.017	2.08	0.007

apolipoprotein E high mobility group AT-hook 1///high mobility group AT-hook 1	APOE HMGA1 ///HMGA1	1.92	0.017	2.08	0.007
apolipoprotein E high mobility group AT-hook 1	APOE HMGA1	2.33	0.020	2.65	0.005
interleukin 18 (interferon-gamma-inducing factor)	IL18	2.04	0.013	2.27	0.004
integrin, alpha V (vitronectin receptor, alpha polypeptide, antigen CD51)	ITGAV	1.99	0.016	2.03	0.003
lysyl oxidase	LOX	2.07	0.030	1.87	0.020
matrix metalloproteinase 14 (membrane-inserted)	MMP14	2.35	0.013	2.51	0.002
myosin IE	MYO1E	2.05	0.023	2.15	0.009
ATP synthase, H+ transporting, mitochondrial F1 complex, beta polypeptide	ATP5B	1.82	0.018	2.34	0.004
tumor necrosis factor receptor superfamily member 12A	TNFRSF12A	1.89	0.015	2.28	0.004

Table 6: list of genes differentially expressed relevant to alternative activation of macrophages pathway (M2)

Gene description	Gene symbol	FC [OS D7 vs D3]	p-value	FC [TiO D7 vs D3]	p-value
mannose receptor, C type 1 mannose receptor, C type 1-like 1	MRC1 MRC1L1	1.79	0.025	1.54	0.017
macrophage scavenger receptor 1	MSR1	3.05	0.022	2.78	0.006
membrane-spanning 4-domains, subfamily A, member 4	MS4A4A	2.05	0.019	1.99	0.009
chemokine (C-C motif) ligand 22	CCL22	2.82	0.020	5.76	0.006
chemokine (C-C motif) ligand 18 (pulmonary and activation-regulated)	CCL18	2.70	0.027	2.56	0.005
solute carrier family 38, member 6	SLC38A6	2.14	0.022053376	2.78	0.002
transforming growth factor, beta-induced, 68kDa	TGFBI	2.05	0.018	1.78	0.005

Table 7: Top 30 downregulated genes at both surfaces.

GO ID	GO Term	P-value	Count in Selection
5051	chemotaxis	5.80E-16	20
19177	taxis	5.80E-16	20
5637	chemokine activity	4.18E-13	11
19226	chemokine receptor binding	7.63E-13	11
19080	response to chemical stimulus	1.06E-12	37
18862	locomotion	5.74E-12	21
3707	cytokine activity	1.16E-11	15
5065	immune response	1.18E-11	23
6918	response to external stimulus	1.55E-11	22
6924	response to wounding	3.60E-11	20
3708	cytokine receptor binding	5.20E-11	14
5062	defense response	5.20E-11	22
5064	inflammatory response	7.49E-11	16
1699	immune system process	7.77E-11	26
5061	response to stress	9.72E-11	33
1024	G-protein coupled receptor binding	4.83E-09	11
6920	response to biotic stimulus	2.38E-08	15
3985	extracellular space	8.88E-08	19
26637	response to other organism	8.88E-08	14
3949	extracellular region	1.69E-06	29
21158	extracellular region part	1.72E-06	20
12798	keratinocyte differentiation	4.11E-06	7
30186	cellular response to chemical stimulus	5.23E-06	15
6928	response to bacterium	6.52E-06	10
7201	epidermal cell differentiation	6.71E-06	7
13861	keratinization	9.03E-06	6
25864	response to stimulus	9.61E-06	48
26635	multi-organism process	9.75E-06	17
7176	tissue development	2.13E-05	16
18995	regulation of cell proliferation	2.13E-05	17

References:

1. BRANEMARK PI. Vital microscopy of bone marrow in rabbit. *Scand J Clin Lab Invest* 1959;11 Supp 38:1-82.
2. Ogawa T, Sukotjo C, Nishimura I. Modulated bone matrix-related gene expression is associated with differences in interfacial strength of different implant surface roughness. *J Prosthodont* 2002;11:241-7.
3. Schwartz Z, Lohmann CH, Oefinger J, Bonewald LF, Dean DD, Boyan BD. Implant surface characteristics modulate differentiation behavior of cells in the osteoblastic lineage. *Adv Dent Res* 1999;13:38-48.
4. Cooper LF. Biologic determinants of bone formation for osseointegration: clues for future clinical improvements. *J Prosthet Dent* 1998;80:439-449.
5. Cooper LF, Deporter D, Wennerberg A, Hammerle C. What physical and/or biochemical characteristics of roughened endosseous implant surfaces particularly enhance their bone-implant contact capability? *Int J Oral Maxillofac Implants* 2005;20:307-312.
6. Schwarz F, Wieland M, Schwartz Z, Zhao G, Rupp F, Geis-Gerstorfer J, Schedle A, Brogгинi N, Bornstein MM, Buser D, Ferguson SJ, Becker J, Boyan BD, Cochran DL. Potential of chemically modified hydrophilic surface characteristics to support tissue integration of titanium dental implants. *J Biomed Mater Res B Appl Biomater* 2009;88:544-57.
7. Buser D, Schenk RK, Steinemann S, Fiorellini JP, Fox CH, Stich H. Influence of surface characteristics on bone integration of titanium implants. A histomorphometric study in miniature pigs. *J Biomed Mater Res* 1991;25:889-902.
8. Abrahamsson I, Berglundh T, Linder E, Lang NP, Lindhe J. Early bone formation adjacent to rough and turned endosseous implant surfaces. An experimental study in the dog. *Clin Oral Implants Res* 2004;15:381-392.
9. Mendonca G, Mendonca DB, Aragao FJ, Cooper LF. The combination of micron and nanotopography by H₂SO₄/H₂O₂ treatment and its effects on osteoblast-specific gene expression of hMSCs. *J Biomed Mater Res A* ;94:169-79.
10. Guo J, Padilla RJ, Ambrose W, De Kok IJ, Cooper LF. The effect of hydrofluoric acid treatment of TiO₂ grit blasted titanium implants on adherent osteoblast gene expression in vitro and in vivo. *Biomaterials* 2007;28:5418-25.
11. Olivares-Navarrete R, Hyzy SL, Hutton DL, Dunn GR, Appert C, Boyan BD, Schwartz Z. Role of non-canonical Wnt signaling in osteoblast maturation on microstructured titanium surfaces. *Acta Biomater* 2011;7:2740-2750.
12. Wall I, Donos N, Carlqvist K, Jones F, Brett P. Modified titanium surfaces promote accelerated osteogenic differentiation of mesenchymal stromal cells in vitro. *Bone* 2009;45:17-26.
13. Olivares-Navarrete R, Raz P, Zhao G, Chen J, Wieland M, Cochran DL, Chaudhri RA, Ornoy A, Boyan BD, Schwartz Z. Integrin alpha2beta1 plays a critical role in osteoblast response to micron-scale surface structure and surface energy of titanium substrates. *Proc Natl Acad Sci U S A* 2008;105:15767-72.
14. Isa ZM, Schneider GB, Zaharias R, Seabold D, Stanford CM. Effects of fluoride-modified titanium surfaces on osteoblast proliferation and gene expression. *Int J Oral Maxillofac Implants* 2006;21:203-11.
15. Zhao G, Schwartz Z, Wieland M, Rupp F, Geis-Gerstorfer J, Cochran DL, Boyan BD. High surface energy enhances cell response to titanium substrate microstructure. *J Biomed Mater Res A* 2005;74:49-58.
16. Stevens MM, George JH. Exploring and engineering the cell surface interface. *Science* 2005;310:1135-1138.

17. Schneider GB, Zaharias R, Seabold D, Keller J, Stanford C. Differentiation of preosteoblasts is affected by implant surface microtopographies. *J Biomed Mater Res A* 2004;69:462-8.
18. Passeri G, Cacchioli A, Ravanetti F, Galli C, Elezi E, Macaluso GM. Adhesion pattern and growth of primary human osteoblastic cells on five commercially available titanium surfaces. *Clin Oral Implants Res* ;21:756-65.
19. Zhao G, Zinger O, Schwartz Z, Wieland M, Landolt D, Boyan BD. Osteoblast-like cells are sensitive to submicron-scale surface structure. *Clin Oral Implants Res* 2006;17:258-64.
20. Shalabi MM, Gortemaker A, Van't Hof MA, Jansen JA, Creugers NH. Implant surface roughness and bone healing: a systematic review. *J Dent Res* 2006;85:496-500.
21. Mendonca G, Mendonca DB, Aragao FJ, Cooper LF. Advancing dental implant surface technology--from micron- to nanotopography. *Biomaterials* 2008;29:3822-3835.
22. Valencia S, Gretzer C, Cooper LF. Surface nanofeature effects on titanium-adherent human mesenchymal stem cells. *Int J Oral Maxillofac Implants* 2009;24:38-46.
23. Cooper LF, Zhou Y, Takebe J, Guo J, Abron A, Holmen A, Ellingsen JE. Fluoride modification effects on osteoblast behavior and bone formation at TiO₂ grit-blasted c.p. titanium endosseous implants. *Biomaterials* 2006;27:926-936.
24. Dalby MJ, Gadegaard N, Curtis AS, Oreffo RO. Nanotopographical control of human osteoprogenitor differentiation. *Curr Stem Cell Res Ther* 2007;2:129-38.
25. Ellingsen JE, Johansson CB, Wennerberg A, Holmen A. Improved retention and bone-to-implant contact with fluoride-modified titanium implants. *Int J Oral Maxillofac Implants* 2004;19:659-666.
26. Berglundh T, Abrahamsson I, Albouy JP, Lindhe J. Bone healing at implants with a fluoride-modified surface: an experimental study in dogs. *Clin Oral Implants Res* 2007;18:147-152.
27. Meirelles L, Currie F, Jacobsson M, Albrektsson T, Wennerberg A. The effect of chemical and nanotopographical modifications on the early stages of osseointegration. *Int J Oral Maxillofac Implants* 2008;23:641-647.
28. Johansson CB, Gretzer C, Jimbo R, Mattisson I, Ahlberg E. Enhanced implant integration with hierarchically structured implants: a pilot study in rabbits. *Clin Oral Implants Res* 2011.
29. Mancha de la Plata M, Gias LN, Diez PM, Munoz-Guerra M, Gonzalez-Garcia R, Lee GY, Castrejon-Castrejon S, Rodriguez-Campo FJ. Osseointegrated implant rehabilitation of irradiated oral cancer patients. *J Oral Maxillofac Surg* 2012;70:1052-1063.
30. Liddel G, Klineberg I. Patient-related risk factors for implant therapy. A critique of pertinent literature. *Aust Dent J* 2011;56:417-26.
31. Moy PK, Medina D, Shetty V, Aghaloo TL. Dental implant failure rates and associated risk factors. *Int J Oral Maxillofac Implants* 2005;20:569-577.
32. Thalji G, Cooper LF. Molecular Assessment of Osseointegration In Vitro: A review of the current literature. *Oral and Craniofacial Tissue Engineering*. 2012; 2: 221–249.
33. Tzaphlidou M. The role of collagen in bone structure: an image processing approach. *Micron* 2005;36:593-601.
34. Mendonca DB, Miguez PA, Mendonca G, Yamauchi M, Aragao FJ, Cooper LF. Titanium surface topography affects collagen biosynthesis of adherent cells. *Bone* 2011;49:463-472.

35. Larsson C, Esposito M, Liao H, Thomsen P. The titanium-bone interface in vivo. In: Brunette DM, Tengvall P, Textor M, Thomsen P, editors, *Titanium in medicine*, Basel: Springer Verlag, 2001, chapter 18.
36. Alexander KA, Chang MK, Maylin ER, Kohler T, Muller R, Wu AC, Van Rooijen N, Sweet MJ, Hume DA, Raggatt LJ, Pettit AR. Osteal macrophages promote in vivo intramembranous bone healing in a mouse tibial injury model. *J Bone Miner Res* 2011;26:1517-1532.
37. Davies JE. In vitro modeling of the bone/implant interface. *Anat Rec* 1996;245:426-445.
38. Cooper LF, Masuda T, Yliheikkila PK, Felton DA. Generalizations regarding the process and phenomenon of osseointegration. Part II. In vitro studies. *Int J Oral Maxillofac Implants* 1998;13:163-74.
39. Thalji G, Cooper LF. Molecular Assessment of Osseointegration In Vivo: A review of the current literature. *Oral and Craniofacial Tissue Engineering*. 2012; 2: 9–22.
40. Thalji G, Gretzer C, Cooper LF. Comparative molecular assessment of early osseointegration in implant-adherent cells. *Bone* 2012.
41. Ballo AM, Broke J. Evaluation of implant osseointegration in small laboratory animals. In: Ballo AM, editor. *Implant Dentistry Research Guide: Basic, Translation, and Clinical Research*. Hauppauge, NY, Nova Publishers; 2012:151-176.
42. Masuda T, Salvi GE, Offenbacher S, Felton DA, Cooper LF. Cell and matrix reactions at titanium implants in surgically prepared rat tibiae. *Int J Oral Maxillofac Implants* 1997;12:472-485.
43. Futami T, Fujii N, Ohnishi H, Taguchi N, Kusakari H, Ohshima H, Maeda T. Tissue response to titanium implants in the rat maxilla: ultrastructural and histochemical observations of the bone-titanium interface. *J Periodontol* 2000;71:287-298.
44. Murai K, Takeshita F, Ayukawa Y, Kiyoshima T, Suetsugu T, Tanaka T. Light and electron microscopic studies of bone-titanium interface in the tibiae of young and mature rats. *J Biomed Mater Res* 1996;30:523-533.
45. Branemark PI. Osseointegration and its experimental background. *J Prosthet Dent* 1983;50:399-410.
46. Wennerberg A, Albrektsson T. On implant surfaces: a review of current knowledge and opinions. *Int J Oral Maxillofac Implants* 2010;25:63-74.
47. Wennerberg A, Albrektsson T. Suggested guidelines for the topographic evaluation of implant surfaces. *Int J Oral Maxillofac Implants* 2000;15:331-344.
48. Bryington M, Mendonca G, Nares S, Cooper LF. Osteoblastic and cytokine gene expression of implant adherent cells in human. *Clin Oral Implants Res* 2012. Accepted for publication.
49. Benjamini Y, Drai D, Elmer G, Kafkafi N, Golani I. Controlling the false discovery rate in behavior genetics research. *Behav Brain Res* 2001;125:279-284.
50. Eriksen EF, Charles P, Melsen F, Mosekilde L, Risteli L, Risteli J. Serum markers of type I collagen formation and degradation in metabolic bone disease: correlation with bone histomorphometry. *J Bone Miner Res* 1993;8:127-132.
51. Keene DR, Sakai LY, Burgeson RE. Human bone contains type III collagen, type VI collagen, and fibrillin: type III collagen is present on specific fibers that may mediate attachment of tendons, ligaments, and periosteum to calcified bone cortex. *J Histochem Cytochem* 1991;39:59-69.
52. Gordon MK, Hahn RA. Collagens. *Cell Tissue Res* 2010;339:247-257.
53. Kadler KE, Hojima Y, Prockop DJ. Collagen fibrils in vitro grow from pointed tips in the C- to N-terminal direction. *Biochem J* 1990;268:339-343.

54. Izu Y, Sun M, Zwolanek D, Veit G, Williams V, Cha B, Jepsen KJ, Koch M, Birk DE. Type XII collagen regulates osteoblast polarity and communication during bone formation. *J Cell Biol* 2011;193:1115-1130.
55. Lamande SR, Bateman JF. Procollagen folding and assembly: the role of endoplasmic reticulum enzymes and molecular chaperones. *Semin Cell Dev Biol* 1999;10:455-464.
56. Hendershot LM, Bulleid NJ. Protein-specific chaperones: the role of hsp47 begins to gel. *Curr Biol* 2000;10:R912-5.
57. Ishida Y, Kubota H, Yamamoto A, Kitamura A, Bachinger HP, Nagata K. Type I collagen in Hsp47-null cells is aggregated in endoplasmic reticulum and deficient in N-propeptide processing and fibrillogenesis. *Mol Biol Cell* 2006;17:2346-2355.
58. Kessler E, Takahara K, Biniaminov L, Brusel M, Greenspan DS. Bone morphogenetic protein-1: the type I procollagen C-proteinase. *Science* 1996;271:360-362.
59. Asharani PV, Keupp K, Semler O, Wang W, Li Y, Thiele H, Yigit G, Pohl E, Becker J, Frommolt P, Sonntag C, Altmüller J, Zimmermann K, Greenspan DS, Akarsu NA, Netzer C, Schonau E, Wirth R, Hammerschmidt M, Nurnberg P, Wollnik B, Carney TJ. Attenuated BMP1 function compromises osteogenesis, leading to bone fragility in humans and zebrafish. *Am J Hum Genet* 2012;90:661-674.
60. Steiglitz BM, Keene DR, Greenspan DS. PCOLCE2 encodes a functional procollagen C-proteinase enhancer (PCPE2) that is a collagen-binding protein differing in distribution of expression and post-translational modification from the previously described PCPE1. *J Biol Chem* 2002;277:49820-49830.
61. Raouf A, Ganss B, McMahon C, Vary C, Roughley PJ, Seth A. Lumican is a major proteoglycan component of the bone matrix. *Matrix Biol* 2002;21:361-367.
62. Delany AM, Hankenson KD. Thrombospondin-2 and SPARC/osteonectin are critical regulators of bone remodeling. *J Cell Commun Signal* 2009;3:227-238.
63. Deckers MM, Smits P, Karperien M, Ni J, Tylzanowski P, Feng P, Parmelee D, Zhang J, Bouffard E, Gentz R, Lowik CW, Merregaert J. Recombinant human extracellular matrix protein 1 inhibits alkaline phosphatase activity and mineralization of mouse embryonic metatarsals in vitro. *Bone* 2001;28:14-20.
64. Mongiat M, Fu J, Oldershaw R, Greenhalgh R, Gown AM, Iozzo RV. Perlecan protein core interacts with extracellular matrix protein 1 (ECM1), a glycoprotein involved in bone formation and angiogenesis. *J Biol Chem* 2003;278:17491-17499.
65. Bonnet N, Conway SJ, Ferrari SL. Regulation of beta catenin signaling and parathyroid hormone anabolic effects in bone by the matricellular protein periostin. *Proc Natl Acad Sci U S A* 2012;109:15048-15053.
66. Parisuthiman D, Mochida Y, Duarte WR, Yamauchi M. Biglycan modulates osteoblast differentiation and matrix mineralization. *J Bone Miner Res* 2005;20:1878-1886.
67. Mochida Y, Parisuthiman D, Pornprasertsuk-Damrongsri S, Atsawasuwana P, Sricholpech M, Boskey AL, Yamauchi M. Decorin modulates collagen matrix assembly and mineralization. *Matrix Biol* 2009;28:44-52.
68. Gordon JA, Tye CE, Sampaio AV, Underhill TM, Hunter GK, Goldberg HA. Bone sialoprotein expression enhances osteoblast differentiation and matrix mineralization in vitro. *Bone* 2007;41:462-473.
69. Nakamura H, Shim J, Butz F, Aita H, Gupta V, Ogawa T. Glycosaminoglycan degradation reduces mineralized tissue-titanium interfacial strength. *J Biomed Mater Res A* 2006;77:478-486.
70. Pornprasertsuk S, Duarte WR, Mochida Y, Yamauchi M. Lysyl hydroxylase-2b directs collagen cross-linking pathways in MC3T3-E1 cells. *J Bone Miner Res* 2004;19:1349-1355.
71. Wang X, Li X, Bank RA, Agrawal CM. Effects of collagen unwinding and cleavage on the mechanical integrity of the collagen network in bone. *Calcif Tissue Int* 2002;71:186-192.

72. Atsawasuwan P, Mochida Y, Parisuthiman D, Yamauchi M. Expression of lysyl oxidase isoforms in MC3T3-E1 osteoblastic cells. *Biochem Biophys Res Commun* 2005;327:1042-1046.
73. Kaku M, Mochida Y, Atsawasuwan P, Parisuthiman D, Yamauchi M. Post-translational modifications of collagen upon BMP-induced osteoblast differentiation. *Biochem Biophys Res Commun* 2007;359:463-468.
74. Yamauchi M, Katz EP. The post-translational chemistry and molecular packing of mineralizing tendon collagens. *Connect Tissue Res* 1993;29:81-98.
75. Pornprasertsuk S, Duarte WR, Mochida Y, Yamauchi M. Overexpression of lysyl hydroxylase-2b leads to defective collagen fibrillogenesis and matrix mineralization. *J Bone Miner Res* 2005;20:81-87.
76. Krane SM, Inada M. Matrix metalloproteinases and bone. *Bone* 2008;43:7-18.
77. Berglundh T, Abrahamsson I, Lang NP, Lindhe J. De novo alveolar bone formation adjacent to endosseous implants. *Clin Oral Implants Res* 2003;14:251-262.
78. Bosshardt DD, Salvi GE, Huynh-Ba G, Ivanovski S, Donos N, Lang NP. The role of bone debris in early healing adjacent to hydrophilic and hydrophobic implant surfaces in man. *Clin Oral Implants Res* 2011;22:357-364.
79. Lang NP, Salvi GE, Huynh-Ba G, Ivanovski S, Donos N, Bosshardt DD. Early osseointegration to hydrophilic and hydrophobic implant surfaces in humans. *Clin Oral Implants Res* 2011;22:349-356.
80. van Hinsbergh VW, Engelse MA, Quax PH. Pericellular proteases in angiogenesis and vasculogenesis. *Arterioscler Thromb Vasc Biol* 2006;26:716-728.
81. Holmbeck K, Bianco P, Caterina J, Yamada S, Kromer M, Kuznetsov SA, Mankani M, Robey PG, Poole AR, Pidoux I, Ward JM, Birkedal-Hansen H. MT1-MMP-deficient mice develop dwarfism, osteopenia, arthritis, and connective tissue disease due to inadequate collagen turnover. *Cell* 1999;99:81-92.
82. Vu TH, Shipley JM, Bergers G, Berger JE, Helms JA, Hanahan D, Shapiro SD, Senior RM, Werb Z. MMP-9/gelatinase B is a key regulator of growth plate angiogenesis and apoptosis of hypertrophic chondrocytes. *Cell* 1998;93:411-422.
83. Colnot C, Thompson Z, Micalau T, Werb Z, Helms JA. Altered fracture repair in the absence of MMP9. *Development* 2003;130:4123-4133.
84. Gronski TJ, Jr, Martin RL, Kobayashi DK, Walsh BC, Holman MC, Huber M, Van Wart HE, Shapiro SD. Hydrolysis of a broad spectrum of extracellular matrix proteins by human macrophage elastase. *J Biol Chem* 1997;272:12189-12194.
85. Dean RA, Cox JH, Bellac CL, Doucet A, Starr AE, Overall CM. Macrophage-specific metalloelastase (MMP-12) truncates and inactivates ELR+ CXC chemokines and generates CCL2, -7, -8, and -13 antagonists: potential role of the macrophage in terminating polymorphonuclear leukocyte influx. *Blood* 2008;112:3455-3464.
86. Shapiro SD, Kobayashi DK, Ley TJ. Cloning and characterization of a unique elastolytic metalloproteinase produced by human alveolar macrophages. *J Biol Chem* 1993;268:23824-23829.
87. Chehroudi B, Ghrebi S, Murakami H, Waterfield JD, Owen G, Brunette DM. Bone formation on rough, but not polished, subcutaneously implanted Ti surfaces is preceded by macrophage accumulation. *J Biomed Mater Res A* 2010;93:724-737.
88. Takebe J, Champagne CM, Offenbacher S, Ishibashi K, Cooper LF. Titanium surface topography alters cell shape and modulates bone morphogenetic protein 2 expression in the J774A.1 macrophage cell line. *J Biomed Mater Res A* 2003;64:207-16.

89. Tan KS, Qian L, Rosado R, Flood PM, Cooper LF. The role of titanium surface topography on J774A.1 macrophage inflammatory cytokines and nitric oxide production. *Biomaterials* 2006;27:5170-7.
90. Takebe J, Ito S, Champagne CM, Cooper LF, Ishibashi K. Anodic oxidation and hydrothermal treatment of commercially pure titanium surfaces increases expression of bone morphogenetic protein-2 in the adherent macrophage cell line J774A.1. *J Biomed Mater Res A* 2007;80:711-718.
91. Hamlet S, Ivanovski S. Inflammatory cytokine response to titanium chemical composition and nanoscale calcium phosphate surface modification. *Acta Biomater* 2011;7:2345-2353.
92. Hamlet S, Alfarsi M, George R, Ivanovski S. The effect of hydrophilic titanium surface modification on macrophage inflammatory cytokine gene expression. *Clin Oral Implants Res* 2012;23:584-590.
93. Pilette C, Ouadrhiri Y, Van Snick J, Renauld JC, Staquet P, Vaerman JP, Sibille Y. Oxidative burst in lipopolysaccharide-activated human alveolar macrophages is inhibited by interleukin-9. *Eur Respir J* 2002;20:1198-1205.
94. Gordon S, Martinez FO. Alternative activation of macrophages: mechanism and functions. *Immunity* 2010;32:593-604.
95. Brunelli S, Rovere-Querini P. The immune system and the repair of skeletal muscle. *Pharmacol Res* 2008;58:117-121.
96. Martinez FO, Gordon S, Locati M, Mantovani A. Transcriptional profiling of the human monocyte-to-macrophage differentiation and polarization: new molecules and patterns of gene expression. *J Immunol* 2006;177:7303-7311.
97. Omar OM, Graneli C, Ekstrom K, Karlsson C, Johansson A, Lausmaa J, Wexell CL, Thomsen P. The stimulation of an osteogenic response by classical monocyte activation. *Biomaterials* 2011.
98. Stein M, Keshav S, Harris N, Gordon S. Interleukin 4 potently enhances murine macrophage mannose receptor activity: a marker of alternative immunologic macrophage activation. *J Exp Med* 1992;176:287-292.
99. Cornicelli JA, Butteiger D, Rateri DL, Welch K, Daugherty A. Interleukin-4 augments acetylated LDL-induced cholesterol esterification in macrophages. *J Lipid Res* 2000;41:376-383.
100. Martinez FO, Gordon S, Locati M, Mantovani A. Transcriptional profiling of the human monocyte-to-macrophage differentiation and polarization: new molecules and patterns of gene expression. *J Immunol* 2006;177:7303-7311.
101. Freytes DO, Kang JW, Marcos I, Vunjak-Novakovic G. Macrophages modulate the viability and growth of human mesenchymal stem cells. *J Cell Biochem* 2012.
102. Kodelja V, Muller C, Politz O, Hakij N, Orfanos CE, Goerdts S. Alternative macrophage activation-associated CC-chemokine-1, a novel structural homologue of macrophage inflammatory protein-1 alpha with a Th2-associated expression pattern. *J Immunol* 1998;160:1411-1418.
103. Andrew DP, Chang MS, McNinch J, Wathen ST, Rihaneck M, Tseng J, Spellberg JP, Elias CG, 3rd. STCP-1 (MDC) CC chemokine acts specifically on chronically activated Th2 lymphocytes and is produced by monocytes on stimulation with Th2 cytokines IL-4 and IL-13. *J Immunol* 1998;161:5027-5038.
104. Schraufstatter IU, Zhao M, Khaldoyanidi SK, Discipio RG. The chemokine CCL18 causes maturation of cultured monocytes to macrophages in the M2 spectrum. *Immunology* 2012;135:287-298.
105. Smith H, Whittall C, Weksler B, Middleton J. Chemokines stimulate bidirectional migration of human mesenchymal stem cells across bone marrow endothelial cells. *Stem Cells Dev* 2012;21:476-486.
106. Carr MW, Roth SJ, Luther E, Rose SS, Springer TA. Monocyte chemoattractant protein 1 acts as a T-lymphocyte chemoattractant. *Proc Natl Acad Sci U S A* 1994;91:3652-3656.

107. Xue ML, Thakur A, Cole N, Lloyd A, Stapleton F, Wakefield D, Willcox MD. A critical role for CCL2 and CCL3 chemokines in the regulation of polymorphonuclear neutrophils recruitment during corneal infection in mice. *Immunol Cell Biol* 2007;85:525-531.
108. Moser B, Clark-Lewis I, Zwahlen R, Baggiolini M. Neutrophil-activating properties of the melanoma growth-stimulatory activity. *J Exp Med* 1990;171:1797-1802.
109. Bonato CF, do-Amaral CC, Belini L, Salzedas LM, Oliveira SH. Hypertension favors the inflammatory process in rats with experimentally induced periodontitis. *J Periodontal Res* 2012;47:783-792.
110. Ling H, Recklies AD. The chitinase 3-like protein human cartilage glycoprotein 39 inhibits cellular responses to the inflammatory cytokines interleukin-1 and tumour necrosis factor-alpha. *Biochem J* 2004;380:651-659.
111. Cooper LF, Zhou Y, Takebe J, Guo J, Abron A, Holmen A, Ellingsen JE. Fluoride modification effects on osteoblast behavior and bone formation at TiO₂ grit-blasted c.p. titanium endosseous implants. *Biomaterials* 2006;27:926-36.
112. Tokalov SV, Gruner S, Schindler S, Wolf G, Baumann M, Abolmaali N. Age-related changes in the frequency of mesenchymal stem cells in the bone marrow of rats. *Stem Cells Dev* 2007;16:439-446.
113. Pandey AC, Semon JA, Kaushal D, O'Sullivan RP, Glowacki J, Gimble JM, Bunnell BA. MicroRNA profiling reveals age-dependent differential expression of nuclear factor kappaB and mitogen-activated protein kinase in adipose and bone marrow-derived human mesenchymal stem cells. *Stem Cell Res Ther* 2011;2:49.
114. Zhou S, Greenberger JS, Epperly MW, Goff JP, Adler C, Leboff MS, Glowacki J. Age-related intrinsic changes in human bone-marrow-derived mesenchymal stem cells and their differentiation to osteoblasts. *Aging Cell* 2008;7:335-343.
115. Ivanovski S, Hamlet S, Salvi GE, Huynh-Ba G, Bosshardt DD, Lang NP, Donos N. Transcriptional profiling of osseointegration in humans. *Clin Oral Implants Res* 2011;22:373-381.
116. Patterson TA, Lobenhofer EK, Fulmer-Smentek SB, Collins PJ, Chu TM, Bao W, Fang H, Kawasaki ES, Hager J, Tikhonova IR, Walker SJ, Zhang L, Hurban P, de Longueville F, Fuscoe JC, Tong W, Shi L, Wolfinger RD. Performance comparison of one-color and two-color platforms within the MicroArray Quality Control (MAQC) project. *Nat Biotechnol.* 2006 Sep;24(9):1140-5